

Statistical Analysis of Early Spectra in Type II and IIb Supernovae

Maider González-Bañuelos,^{1,2*} , Claudia P. Gutiérrez,^{2,1} , Lluís Galbany^{1,2} , and Santiago González-Gaitán^{3,4} 

¹ Institute of Space Sciences (ICE, CSIC), Campus UAB, Carrer de Can Magrans, s/n, E-08193 Barcelona, Spain.

² Institut d'Estudis Espacials de Catalunya (IEEC), 08860 Castelldefels (Barcelona), Spain

³ Instituto de Astrofísica e Ciências do Espaço, Faculdade de Ciências, Universidade de Lisboa, Ed. C8, Campo Grande, 1749-016 Lisbon, Portugal

⁴ European Southern Observatory, Alonso de Córdova 3107, Casilla 19, Santiago, Chile

ABSTRACT

We present a comprehensive analysis of the early spectra of type II and type IIb supernovae (SNe) to explore their diversity and distinguishable characteristics. Using 866 publicly available spectra from 393 SNe, 407 from type IIb SNe (SNe IIb) and 459 from type II SNe (SNe II), we analysed H α and He I 5876 Å at early phases (< 40 days from the explosion) to identify possible differences between these two SN types. By comparing the pseudo-equivalent width (pEW) and full width at half maximum (FWHM), we find that the strength of the absorption component of H α and He I lines serves as a quantitative discriminator, with SNe IIb exhibiting stronger lines at all times. The most significant differences emerge within the first 10–20 days. To assess the statistical significance of these differences, we apply statistical methods and machine-learning techniques. Population density evolution reveals a clear distinction in both pEW and FWHM. Quadratic Discriminant Analysis (QDA) confirms distinct evolutionary patterns, particularly in pEW, while FWHM variations are less pronounced. A combination of t-distributed Stochastic Neighbour Embedding (t-SNE) and Linear Discriminant Analysis (LDA) effectively separates the two SN types. Additionally, a Random Forest Classifier (RFC) demonstrates the robustness of pEW and FWHM as classification criteria, allowing for accurate classification of newly observed SNe II and IIb based on computed classification probabilities. Applying our method to low-resolution spectra obtained from the Zwicky Transient Facility Bright Transient, a magnitude-limited survey, we identified 34 misclassified SNe. This revision increases the estimated fraction of SNe IIb from 4.0% to 7.26%. This finding suggests that misclassification significantly impacts the estimated core-collapse SN rate. Our approach enhances classification accuracy and provides a valuable tool for future supernova studies.

Key words. supernovae: general,

1. Introduction

Core collapse supernovae (CCSNe) are those explosive phenomena associated with the death of massive stars ($> 8M_{\odot}$). When they reach the end of the nuclear fusion in hydrostatic burning, with no heavier elements to be synthesised, the core collapses as it can no longer be stabilised, causing supernovae (SNe; [Janka et al. 2007](#)). Among CCSNe, many subtypes have been established based on the different features shown in their spectra, which are determined by the composition of the exploding progenitor star. The main characteristic of the CCSNe spectral classification is the amount of retained hydrogen or helium. Those that have retained a significant fraction of their H envelope, i.e. H-rich CCSNe, are classified as type II (SNe II) and are characterised by strong Balmer lines in the spectra ([Minkowski 1979](#)). Moreover, SNe that have suffered a loss of their envelope before the explosion and thus have little or no hydrogen are known as Stripped-Envelope SNe (SESNe). SESNe that are hydrogen-poor (but still present) are classified as type IIb SNe (SNe IIb; [Filippenko et al. 1993](#)), having stripped part of its outermost hydrogen envelope in the star's last stages before the explosion. Those SESNe that are H-deficient but He-rich are classified as type Ib SNe (SNe Ib), exhibiting spectra dominated by He features. Notably, SNe IIb are considered to be transitional objects between SNe II and SNe Ib. In early phases, their spectra are dominated by Balmer P-Cygni lines, resembling those of SNe

II. However, as time passes, the H signatures disappear, and the He lines gradually dominate the spectra, comparable to SNe Ib. Finally, the H- and He-deficient are type Ic SNe (SNe Ic). Thus, the mass loss drives the following spectroscopic sequence as it increases: II → IIb → Ib → Ic ([Gal-Yam 2016](#); [Shivvers et al. 2017](#)).

Historically, SNe II are sub-classified based on the light curve (LC) shape. Type IIP SNe (SNe IIP) exhibit a plateau right after the maximum peak, while type IIL SNe (SNe IIL) show a fast decline after the peak ([Barbon et al. 1979](#)). However, recent works (e.g. [Anderson et al. 2014](#); [Sanders et al. 2015](#); [González-Gaitán et al. 2015](#); [Galbany et al. 2016](#)) have revealed that the observational properties of SNe IIP and IIL form a continuum rather than distinct groups, suggesting they represent a single population.

In addition to the general classification of SNe II, two further subclasses have been identified: SNe IIn (defined spectroscopically) and 1987A-like events (defined photometrically). SNe IIn are characterised by long-lasting narrow H emission lines ([Schlegel 1990](#)) attributed to interaction with the circumstellar medium (CSM). On the other hand, the 1987A-like events are distinguished by long-rising LCs, similar to those observed in SN 1987A ([Taddia et al. 2012](#); [Pastorello et al. 2012](#); [Taddia et al. 2016](#)).

The LC of H-poor SNe IIb is characterised by a bell shape similar to those observed in other SESNe. Their main peak is generally attributed to the powering by radioactive decay of ^{56}Ni

* E-mail: mgonzalez@ice.csic.es

(Shigeyama et al. 1994; Woosley et al. 1994; Bersten et al. 2012). Photometric studies of SNe IIb have revealed that some objects exhibit double-peaked LC, with an initial peak before the main one powered by ^{56}Ni . This initial peak has been suggested to be related to the cooling phase, a consequence of the cooling of the progenitor's envelope after the shock breaks out from the surface. That cooling phase will last longer or shorter depending on the size of the progenitor, although it also depends on its density distribution (Rabinak & Waxman 2011; Bersten et al. 2012; Nakar & Piro 2014; Morales-Garoffolo et al. 2015; Sapir & Waxman 2017).

Pre-explosion imaging at the sites of SN II explosions has identified Red Supergiant (RSG) stars with masses in the range of $8\text{--}18 M_{\odot}$ as their progenitors (Van Dyk et al. 2003; Smartt et al. 2004, 2009). For SNe IIb, the direct detection of the progenitor of SN 1993J (Maund et al. 2004) and SN 2011dh (Folatelli et al. 2014a; Maund 2019) suggests that some of these objects arise from stars in binary systems. Moreover, the detection of the possible companion stars for SN 1993J (Maund et al. 2004) and SN 2001ig (Ryder et al. 2018) further supports the binary scenario.

Given the striking similarities in the early-phase spectra of SNe II and IIb, it is plausible to suggest that their progenitors form a continuum of decreasing hydrogen envelope mass (e.g. Hiramatsu et al. 2021a; Dessart et al. 2024). However, recent studies have found a discontinuity in the observational properties of their LCs. For instance, Arcavi et al. (2012) analysed the LC morphology of SNe II and identified three distinct classes: IIP, IIL and IIb, which were interpreted as different progenitor populations. Faran et al. (2014) found that fast-declining SNe II (SNe IIL) appear to be photometrically related to SNe IIb. In contrast, Pessi et al. (2019) found a gap in the observed properties of SNe II and IIb, concluding that they represent two distinct families rather than a continuous sequence.

From a theoretical perspective, the radiative transfer calculations of massive stars in binary systems with different initial orbital periods presented by Dessart et al. (2024) show how varying degrees of hydrogen envelope stripping can produce the observed diversity in CCSNe explosions, forming a continuum in the V-band LC morphology based on the orbital separation (i.e. retained hydrogen mass). This study also reveals distinctions in the H α and helium lines features associated with different progenitor models, offering critical insights into the physical processes that drive the observed diversity among SNe II and IIb.

Previous studies on SNe II and IIb have focused on their observed photometric properties, leaving their spectral distinctions less explored. In this work, we present the first comprehensive analysis comparing and characterising the early spectra of these two SN classes. Drawing on methodologies from prior studies, such as those by Liu et al. (2016); Shivers et al. (2019) and Holmbo et al. (2023) for SESNe or Gutiérrez et al. (2017) and de Jaeger et al. (2019) for SNe II, we systematically examine the spectral features for each SN type. Additionally, this study introduces a novel classification method that exploits subtle differences in the spectral properties to distinguish between SNe II and IIb. Our results demonstrate that these differences are reliable diagnostic tools. They help reduce misclassifications and enable a more accurate categorisation of SNe II and IIb.

The paper is organised as follows. Section 2 describes the data sample and measurements. Sections 3 and 4 provide the analysis and results. Section 5 presents the discussion, while Section 6 lists the conclusions.

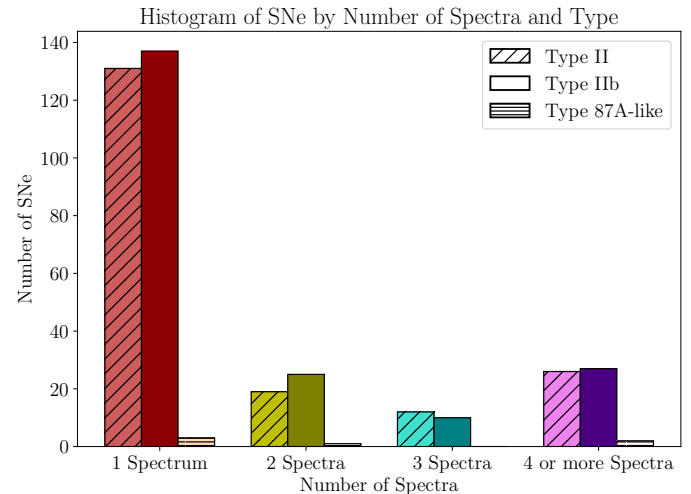


Fig. 1. Histogram of the number of spectra per SN. In total, our sample is composed of 866 spectra for 393 SNe.

2. Data sample and spectral measurements

2.1. Sample

The sample analysed in this study includes all available SN IIb spectra in the WISEREP¹ (Yaron & Gal-Yam 2012) repository. We retrieved these data using the WISEREP_API² tool. To ensure a comparable sample, and considering that SNe IIb are less abundant than SNe II ($\sim 10\%$ of the CCSNe vs $\sim 70\%$ of the CCSNe; Shivers et al. 2017), we selected a similar number of H-rich events. Our goal is not to recover the intrinsic population rates of these two SN types, but rather to investigate whether they can be reliably distinguished based on their spectral features, despite their similarities at early phases. To this end, we constructed balanced spectral samples for both types, allowing our method to focus on identifying the main features without being biased by the larger occurrence of SNe II. Therefore, our dataset consists of 449 low-redshift ($z < 0.12$) SNe observed between 1986 and 2024, comprising 222 SNe II (including 5 of the 1987A-like objects) and 227 SNe IIb. Given that we want to study the possible differences between SNe II and IIb at early phases, some additional cuts were applied. First, we only included spectra obtained within the first 40 days post-explosion (see Section 2.2). Second, since our line measurements were performed manually using a semi-interactive code (see Section 2.3), we assessed the quality of the spectra, retaining only those with a sufficient resolution (R) to perform reliable analysis. These are spectra with $R \geq 300$, where the spectral resolution is defined as $R = \lambda/\Delta\lambda$. Thus, we excluded the Spectral Energy Distribution Machine (SEDM) spectra ($R \approx 100$; Blagorodnova et al. 2018). Given the larger number of available SNe II, we prioritised selecting those with well-constrained explosion dates. However, to test the robustness of our method under less optimal conditions, we also included a subset of approximately 15 SNe with lower-quality spectral and photometric data.

After applying these cuts, our final dataset contained 393 SNe, represented by 866 spectra: 407 of SN IIb, 438 of SNe II, and 21 of SNe 1987A-like. Among the SNe in our sample, 55 have four or more spectra, 22 have three, and 42 have two, while 271 have only one spectrum. Figure 1 presents the histogram of

¹ <https://wiserep.weizmann.ac.il/>

² https://github.com/temuller/wiserep_api

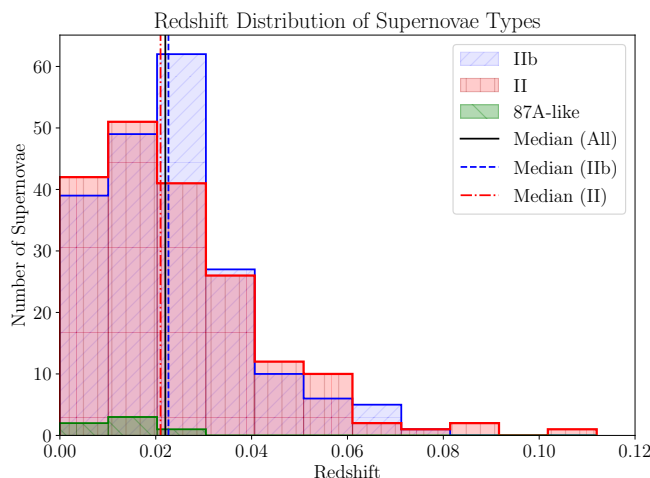


Fig. 2. Redshift distribution for the 393 SNe in our sample. The vertical lines indicated the median of the whole sample (solid black line) at 0.022, SNe II (dashed-dotted red line) at 0.021 and IIb (dashed blue line) at 0.023.

the number of spectra by SN type. Table B.5 presents the whole dataset (Appendix B).

The redshift distribution of our sample is shown in Figure 2. The Figure shows that most of the sample has a redshift below 0.06. The median of the redshift distribution is 0.021 and 0.023 for SNe II and IIb, respectively. These median values indicate that the central tendency of both distributions is very similar, suggesting that our sample is well-balanced in terms of redshift. This makes it suitable for the analysis.

2.2. Explosion date

We compute the explosion epoch for each SN in our sample following the methodology outlined in Gutiérrez et al. (2017). This approach uses the last non-detection³ and the first detection for each object, estimating the explosion date as the middle point between these two epochs. The detection limits were determined using publicly available photometry from the Asteroid Terrestrial-impact Last Alert System (ATLAS; Tonry et al. 2018c; Smith et al. 2020b) forced photometry server (Shingles et al. 2021) and the Zwicky Transient Facility (ZTF; Bellm et al. 2019; Graham et al. 2019) public stream through the Lasair⁴ broker (Smith et al. 2019). The average uncertainty in the estimated explosion dates is ~ 2.5 days. When this method was not applicable either due to the absence of deep non-detections or the lack of any non-detections, we estimated the explosion epoch using spectral matching, as described in Gutiérrez et al. (2017). Thus, we compared our SN spectrum with templates of other SNe with well-established explosion dates. For this, we employed the Supernova Identification⁵ (SNID; Blondin & Tonry 2007) and the NGSF⁶ (Next Generation SuperFit; Goldwasser et al. 2022;

³ Non-detections correspond to fluxes below the detection threshold. In these cases, ATLAS and ZTF report upper-limit magnitudes based on the image depth, typically 3σ for forced photometry in ATLAS, and 5σ in ZTF.

⁴ <https://lasair.roe.ac.uk/>

⁵ Following Blondin & Tonry (2007), we only considered matches with $r_{\text{lap}} \geq 5$ and $\text{lap} \geq 0.4$.

⁶ The best-fitting SN template is identified via a χ^2 minimisation procedure.

Howell et al. 2005), a Python-based implementation of the SUPERFIT template-matching classification tool. Finally, for the sample of SNe II analysed in Gutiérrez et al. (2017), we adopted their explosion dates.

2.3. Measurements

We analyse the spectra of our SNe by characterising the strength/intensity of the absorption component of specific spectral lines. To achieve this, we compute the pseudo-Equivalent Width (pEW) and Full Width at Half Maximum (FWHM). Our methodology follows similar approaches presented in the literature, including works by Liu et al. (2016); Gutiérrez et al. (2017); Holmbo et al. (2023).

The pEW is defined as:

$$\text{pEW} = \sum_{i=1}^N \left(1 - \frac{f(\lambda_i)}{f_0(\lambda_i)}\right) \Delta\lambda_i , \quad (1)$$

where λ_1 and λ_N are the wavelength boundaries of the spectral line to be measured, and $\Delta\lambda$ is the difference between two consecutive points, $f(\lambda_i)$ corresponds to the flux observed at λ_i and $f_0(\lambda_i)$ the continuum flux. The pEW quantifies the overall strength of a spectral line relative to the pseudo-continuum, with higher pEW values indicating a stronger contribution of that feature in the SN spectrum. Variations in pEW can signal changes in the physical conditions of the ejecta, such as temperature, density, or ionisation state of the emitting or absorbing material. Therefore, its analysis provides valuable insights into the composition of the SN ejecta.

To define this continuum, we developed an interactive PYTHON code, based on FRT_CONTINUUM⁷. We modified it so that it allows the user to select a specific feature by choosing two regions around it: a lower and an upper wavelength limit. Within those regions, the wavelength boundaries of the line (λ_1 and λ_N) are determined by identifying the points with the maximum slope change on each side. Using these boundary points, a pseudo-continuum is established, and the spectrum is normalised relative to it. Next, the difference between the normalised flux and the continuum is integrated across the absorption region by iterating over the range between λ_1 and λ_N , accumulating the pEW values using the previously defined formula (see Figure 3).

The FWHM is determined by fitting a Gaussian function to the spectral feature. The Gaussian model is widely used in spectral analysis because it can accurately represent symmetric, bell-shaped profiles. The relationship between the FWHM and the parameters of the fitted Gaussian function is given by:

$$\text{FWHM} = 2\sqrt{2 \ln 2} \sigma . \quad (2)$$

Here, σ is the standard deviation of the fitted Gaussian function, which defines the width of the Gaussian curve. To calculate the FWHM, we use the function `SPECUTILS.GAUSSIAN_FWHM`, which derives the FWHM directly from σ based on the Gaussian profile. This value represents the width of the spectral feature at half of its maximum depth. The FWHM represents the velocity dispersion of the material in the line-forming region, directly reflecting how fast the ejecta is expanding along the line of sight. This velocity dispersion is related to the explosion energy of

⁷ https://github.com/tdejaeger/Astronomy/blob/master/Codes/fit_continuum.py

the SN, as more energetic explosions produce higher velocity spreads, resulting in broader spectral features.

The errors associated with the FWHM and pEW measurements were estimated by systematically varying the boundaries of the selected wavelength region and performing the measurements three times. The region boundaries were adjusted for each predefined shift, the continuum measured, and the FWHM and pEW recalculated, generating a set of shifted measurements. These measurements quantify the sensitivity of the FWHM and pEW to variations in the selection of the wavelength region. The deviations between the shifted and original measurements (obtained from the unshifted region) were analysed statistically. To calculate the errors, statistical metrics such as the standard deviation or root mean square error (RMSE) were used to characterise the spread of the shifted measurements. These values provide a robust estimate of uncertainties in the FWHM and pEW measurements.

To address noisy spectra, we incorporated a smoothing option into the code. This allows users to apply a smoothing degree before selecting the regions, ensuring accurate spectral line identification and measurements, without significantly affecting the pEW or FWHM values. After smoothing, the modified spectrum overlaps the original data. An example of how our interactive code works is shown in Figure 3. The top panel shows the two regions selected on each side of a specific line. The smoothed spectrum is shown in cyan. The bottom panel of Figure 3 displays the final measured line after processing.

To validate the accuracy of our developed semi-interactive code, we compared its derived measurements with those obtained using manually IRAF (Tody 1986, 1993). For this comparison, we selected a subsample of spectra and manually measured the pEW and FWHM for the same spectral lines with IRAF. The results of this comparison, presented in the Appendix A (Figure A.1), demonstrate the consistency between the two methods.

Following the explained methodology and using our code, we estimated the pEW and FWHM for the spectral lines across all 866 spectra in our sample. Since the two SN types analysed in this work typically exhibit a blue featureless continuum at very early phases, with spectral features gradually emerging over time, we adopted the methodology of Gutiérrez et al. (2017) by assigning a value of zero to a line measurement when the line is absent. Accordingly, a value of $pEW = 0$ indicates that a specific line is not visible at that phase.

3. Analysis

3.1. Re-classification

Before starting our analysis, we inspected all SN spectra in our sample to verify the accuracy of the assigned classifications. We visually checked the main features in the spectra and the LC morphology. For objects with multiple spectroscopic follow-up observations, the appearance of some spectral lines allows us to easily identify possible misclassifications. Through this inspection, we found 16 misclassified SNe. Table 1 summarises these objects and their re-classifications. As seen, 14 objects were initially classified as SNe II, and we re-classified them as SNe IIb. SN 2015Y was classified as a SN Ib; however, its earliest spectra show signatures of hydrogen features, leading to its re-classification as IIb (Childress et al. 2016). Additionally, SN 2020abah was reclassified from SN II to SN 87A-like.

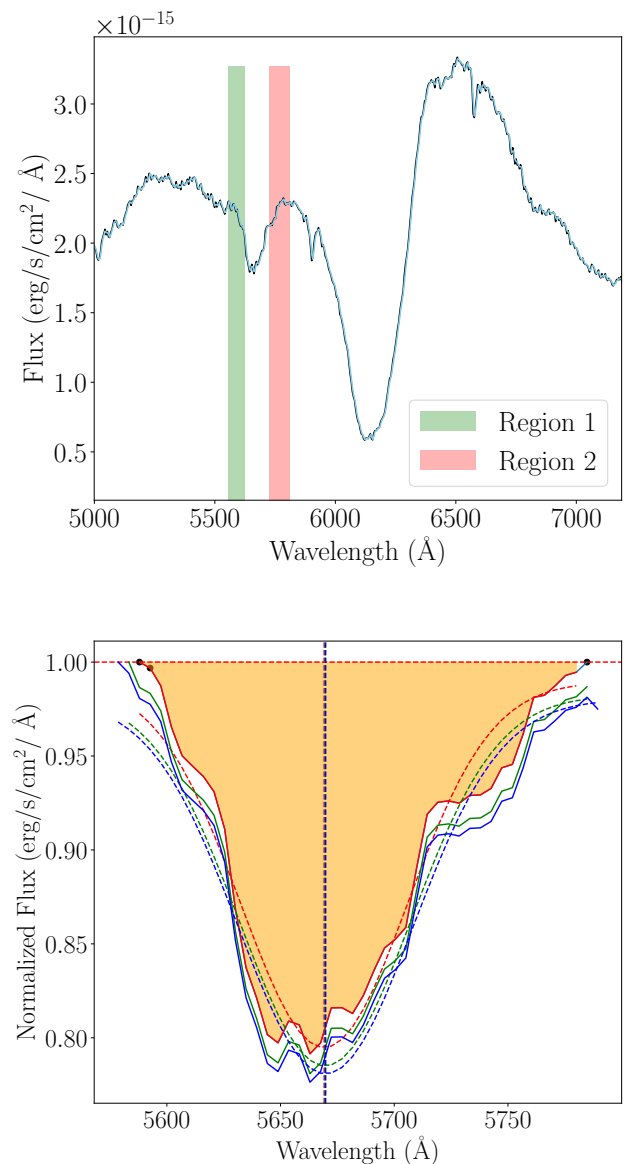


Fig. 3. An example of the pEW and FWHM measurement for the He I line. On the top panel, we show the selection of the two regions to define the line to be measured. The defined line and the Gaussian fitting for the pEW and FWHM computation are shown in the bottom panel. The different line colours represent the shifted measurements used to estimate the uncertainties.

3.2. Spectral line identification

Given that the spectra of SNe II and IIb appear similar at early phases due to the presence of H and He I $\lambda 5876$, we investigate whether they exhibit distinguishable properties. To do so, we examine how prototypical objects of each SN type evolve over time. Figure 4 shows the spectral evolution from the explosion to 30 days post-explosion for the type II SNe 1999em and 2013ej and the type IIb SNe 1993J and 2011dh.

By examining the spectral evolution in each SN, we identified specific features that exhibit distinct tendencies based on their classification. In the first days after the explosion, both SNe II and IIb often display a featureless blue continuum (Matheson et al. 2000a; Arcavi 2017; Hillier & Dessart 2019), which is the result of the high temperatures of the ejected material during that phase. As the ejecta cools down, broader lines, such as the

Table 1. Reclassified SNe based on their spectral evolution and/or photometry properties.

SN name	Classification	Reference	Re-classification
SN 2015Y	Ib	[1]	IIb
SN 2016bam	II	[2]	IIb
SN 2018bti	II	[3]	IIb
SN 2020adnx	II	[4]	IIb
SN 2019aax	II	[5]	IIb
SN 2019abu	II	[6]	IIb
SN 2019lqo	II	[7]	IIb
SN 2019lsk	II	[8]	IIb
SN 2019luz	II	[8]	IIb
SN 2019mrz	II	[9]	IIb
SN 2019rwd	II	[10]	IIb
SN 2019sox	II	[11]	IIb
SN 2019tua	II	[12]	IIb
SN 2020abah	II	[13]	87A-like
SN 2020aqe	II	[14]	IIb
SN 2021afdx	II	[15]	IIb

Reclassifications done before performing the analysis. Objects considered in our sample with the new classification.

References. [1] Zheng & Filippenko (2015), [2] Hosseinzadeh et al. (2016a), [3] Hiramatsu et al. (2018), [4] Srivastav et al. (2021), [5] Piranomonte et al. (2019b), [6] Piranomonte et al. (2019a), [7] Bose et al. (2019), [8] Angus et al. (2019), [9] Wiseman et al. (2019), [10] Arcavi et al. (2019), [11] Cartier & Ugarte (2019), [12] Burke et al. (2019), [13] Sit (2022), [14] Burke et al. (2020), [15] Ragosta et al. (2021).

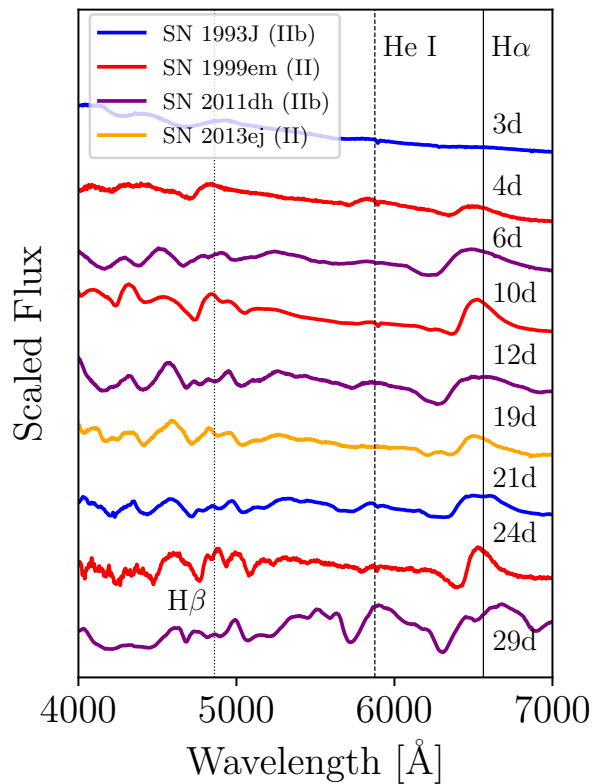


Fig. 4. Evolution of type II SNe 1999em (Leonard et al. 2001) (red) and 2013ej (Valenti et al. 2013) (orange) and type IIb SNe 1993J (Barbon et al. 1995) (blue) and 2011dh (Valenti et al. 2013; Ergon et al. 2014) (purple). The epoch of each of the spectra is computed from the explosion date. The dotted vertical line marks the rest-wavelength corresponding to $H\beta$; the dashed line is the $\text{He I } \lambda 5876$ feature, and the continued line is $H\alpha$.

3.3. Median spectra

To visualise the main spectroscopic differences between SNe II, IIb and 87A-like, we compute the median spectrum of each type by including all the spectra in our final sample, following a similar procedure as Liu et al. (2016). This includes 188 SNe II, 199 SNe IIb and 6 SNe 87A-like between 0–40 days after explosion. Due to the limited number of SN 87A-like objects, the median spectrum for this group may not fully represent its characteristics. Nevertheless, we decided to include it because some SNe 87A-like are often misclassified (see Section 4.1). The resulting median spectra for the three SN types are plotted in Figure A.2. The spectra were normalised by scaling them to the median value of a common reference wavelength range, ensuring their fluxes match at a specific wavelength. This process allows a direct comparison of spectral features across different objects while preserving their relative shapes. The resolution of the available data constrains the quality of the median spectra. While spectra with very poor resolution were excluded from our sample, some noisy spectra worsened the quality of the median spectrum, which is evident in Figure A.2.

A comparison between the three median spectra reveals common features with notable differences in the strength and width of the line depending on their type. In SNe IIb, both $H\alpha$ and $\text{He I } \lambda 5876$ are broader than in SNe II and 87A-like. In contrast, the spectrum of SNe II appears to be still dominated by the continuum, with $H\alpha$ and $\text{He I } \lambda 5876$ barely seen. For SNe 87A-like, spectral differences are also observed, although they are classified

hydrogen Balmer series and $\text{He I } \lambda 5876$, emerge. Given that the H and He I lines are present in both SN types, we considered them as primary indicators. However, despite being shared in these two classes, notable differences in the evolution and shape of $H\alpha$ and $\text{He I } \lambda 5876$ are apparent (Figure 4). In the first one to two weeks, both types exhibit strong H lines, but their evolutionary patterns begin to diverge. For instance, for SNe II, $H\alpha$ develops a well-defined P-Cygni profile. In contrast, in SNe IIb, $H\alpha$ transitions towards a flat-topped profile, which eventually begins to split into two components due to the emergence of $\text{He I } \lambda 6678$ (Holmbo et al. 2023). The presence and strength of this He I line can vary significantly between individual SNe, which can complicate the analysis of the $H\alpha$ emission profile.

Subtle differences in the spectra of SNe II and IIb are also visible in the $H\alpha$ absorption and He I line $\lambda 5876$. The $H\alpha$ absorption profile is typically much broader throughout the evolution of SNe IIb compared to SNe II. Additionally, the He I line $\lambda 5876$ emerges earlier and is generally stronger in SNe IIb. This behaviour is likely a result of the partial stripping of the H envelope in SNe IIb.

We also examined the $H\beta$ ($\lambda 4861$) line, which, like $H\alpha$, shows differences between SNe II and IIb. However, given that $H\beta$ is affected by the Iron lines around it, we excluded it from our analysis due to the complexities in its characterisation. The feature is marked with a dotted vertical line in Figure 4. In consequence, our analysis is focused only on the $H\alpha$ absorption feature and the $\text{He I } \lambda 5876$ line.

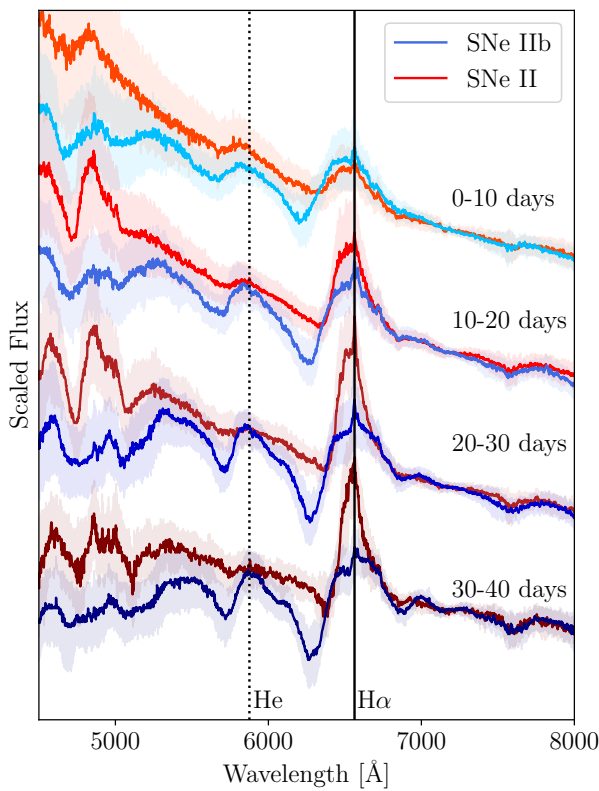


Fig. 5. Comparison between the median spectra of SNe II and IIb in different time ranges: 0 – 10 days post-explosion, 10 – 20 days, 20 – 30 days and 30 – 40 days. Blue spectra correspond to SNe IIb, and red spectra to SNe II. The dashed vertical line marks the rest wavelength of He I ($\lambda 5876$), while the continuous line marks the rest wavelength of $H\alpha$. The shaded regions represent the Median Absolute Deviation (MAD), which represents dispersion around the median.

based on their photometry. The SN 87A-like median spectrum displays a well-defined $H\alpha$ P-Cygni profile with a broad emission line. The He I $\lambda 5876$ is also prominent. These findings align with our visual inspection.

Given that the spectral features change based on the SN phase, we perform a more detailed analysis of the median spectra over time. We computed it for SNe II and IIb within the four-time intervals: 0 – 10 days post-explosion, 10 – 20 days, 20 – 30 days and 30 – 40 days. The resulting median spectra are presented in Figure 5, where SNe IIb are represented in blue and SNe II in red. Due to the limited data for SNe 87A-like, we could not compute their median spectra for specific time intervals.

The median spectra constructed within time intervals show more explicit evolutionary tendencies for each SN type. Notably, the $H\alpha$ line dominates the spectrum of both classes. In the early phases, the absorption of the H lines ($H\alpha$ and $H\beta$) is stronger in SNe IIb and remains so throughout their evolution up to 40 days. Furthermore, the He I line emerges within the first 10 days in SNe IIb, whereas in SNe II, it appears at ~ 10 days post-explosion. In SNe II, both $H\alpha$ and He I also increase their strength over time, which can complicate classification depending on the specific characteristics of each SN. However, a key distinction lies in the shape of the lines, particularly $H\alpha$. In SNe II, the emission component remains strong at all phases, and the P-Cygni profile is well-defined.

Furthermore, a comparison between the median spectra of our SNe IIb sample and those presented by Liu et al. (2016) reveals strong similarities. In both cases, the $H\alpha$ line shows broad

absorption with a flattened-topped emission component, accompanied by a strengthening He I line that becomes more prominent as the SN evolves. Although Liu et al. (2016) sample does not cover phases as early as those analysed in this work, the median spectra between 10 and 40 days post-explosion are consistent across both works.

Examining the early spectra of SNe II, IIb, and 87A-like reveals significant observational differences in the strength and shape of the H and He lines among the different classes. These subtle differences enable early characterisation and more reliable classifications. Therefore, the following analysis is focused on the $H\alpha$ absorption feature and the He I $\lambda 5876$ lines.

4. Results

4.1. Spectral measurements

In this section, we present the results of our measurements. The values for the pEW and FWHM covering the first 40 days after the explosion are presented in Figure 6. The colour bars on the right side indicate the SN phase. The analysis across the full-time interval (0 – 40 days) does not reveal a distinct separation into two clusters; instead, it shows a continuum where SNe IIb tend to dominate at higher values.

We examined the spectral features across smaller time intervals to investigate whether the observed continuum is intrinsic or a consequence of the broad time range considered (0 – 40 days). The results for the earliest two intervals (0 – 10 and 10 – 20 days) are presented in Figure 7. Within these intervals, the pEW and FWHM parameters reveal clear trends: SNe IIb consistently exhibit stronger $H\alpha$ and He I features throughout the entire early time range. Notably, an intermediate region is observed around 25 Å in the pEW of both $H\alpha$ and He I, as well as around 125 Å for $H\alpha$ and 200 Å for He I in the FWHM. This overlap between the two populations further supports the continuum observed in the full-time interval (0 – 40 days). However, we note that the overlap between the groups becomes more significant as time passes. Specifically, the later the analysed time range, the greater the overlap, as the SNe II values grow stronger as time passes (see Figures A.3 and A.4 in the Appendix A). This highlights the important role that the epoch of the SN will have in our analysis and the development of our method. A summary of the pEW and FWHM values for each SN type at each time interval is presented in Appendix B (see Table B.4).

We also find that, although SNe 87A-like are spectroscopically similar at all phases to SNe II, they exhibit notably higher values, especially in the $H\alpha$ absorption feature (Figures 6 and 7). Despite this, we excluded them from further analyses due to their low numbers.

To evaluate the statistical significance of our results, we applied the Kolmogorov-Smirnov test (KS test). This non-parametric method computes the maximum difference between the Cumulative Distribution Function (CDF) of two data sets under the null hypothesis that both groups are drawn from populations with identical distributions. The KS test results for the comparison of the pEW and FWHM of $H\alpha$ and He I between SNe II and IIb are summarised in Table 2. The Table includes the KS statistic (greatest difference between the two CDFs) and the corresponding p-value (significance of the difference obtained) for each time interval. A p-value < 0.05 indicates the rejection of the null hypothesis, suggesting a statistically significant difference between the two groups.

From Table 2, we observe that most distributions have p-values significantly below the 0.05 threshold, indicating a mean-

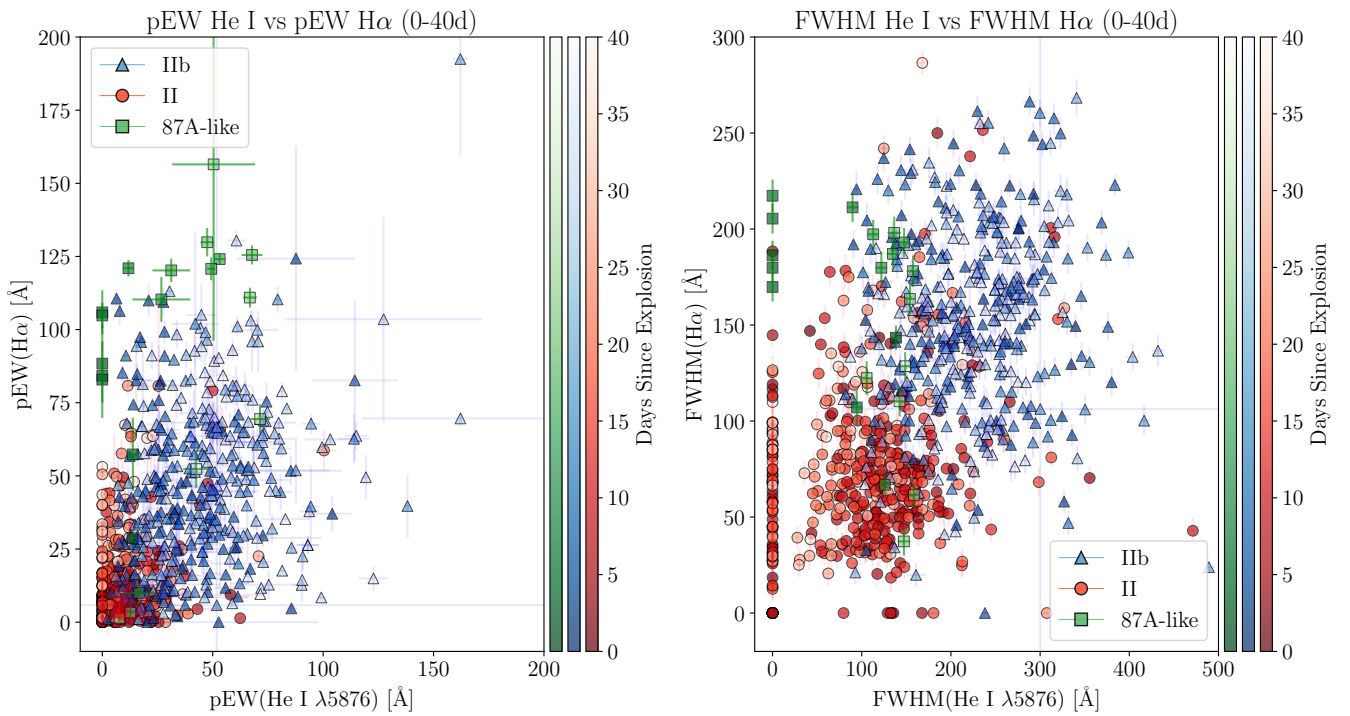


Fig. 6. *Left panel:* pEW of the H α absorption profile versus the pEW of the He I $\lambda 5876$ line measured across the full-time interval (0 – 40 days). The markers are established by SN type: SNe IIb are shown as blue triangles, SNe II as red circles, and SNe 87A-like as green squares. The colour bars on the right side indicate the SN phase. *Right panel:* Same as the left panel, but for the FWHM measurements.

Table 2. The KS-statistic run for our measurements. Separately for the pEW and FWHM results for the lines of H α and He I.

Time range	# Sp.	pEW				FWHM			
		He I		H α		He I		H α	
		KS-statistic	p-value	KS-statistic	p-value	KS-statistic	p-value	KS-statistic	p-value
0-10d	220	0.349	0.0002	0.281	0.005	0.303	0.002	0.205	0.085
10-20d	278	0.482	2.012e-08	0.439	5.374e-07	0.386	1.609e-05	0.445	3.048e-07
20-30d	233	0.348	1.494e-04	0.264	8.490e-03	0.340	2.366e-04	0.275	5.434e-03
30-40d	135	0.205	0.227	0.141	0.667	0.195	0.273	0.259	0.063
0-40d	866	0.732	7.914e-51	0.675	1.530e-42	0.635	3.131e-37	0.624	7.170e-36

The table shows the two values returned by the KS-test: the KS-statistic and the p-value. Values that are not statistically significant are shown in italics.

ingful separation between the SN II and IIb. The two samples exhibit statistically significant differences in the earliest 30 days post-explosion, with the most clear separation occurring within a 10 to 20-day interval. These findings support our hypothesis that SNe II and IIb display differences in their early spectral evolution, reinforcing the possibility of identifying them based on pEW and FWHM values.

The obtained KS test values suggest that while early-time observations can effectively differentiate between the two types based on pEW values, this distinction becomes less clear as SNe evolve. Interestingly, the greatest difference between SN II and IIb is observed during the 10 – 20-day interval rather than the earlier range (0 – 10 days). This is likely because both types are characterised by a blue featureless spectrum without prominent features soon after the explosion. Even as H lines emerge, they may still be weak, lacking sufficient signatures to differentiate between SNe II and IIb. Consistent with this, we find no significant difference in the H α FWHM distribution during the first 10 days post-explosion.

From 30 days post-explosion, classifying SNe II and IIb based on the analysed spectral features becomes increasingly challenging due to the significant overlap between the two populations. For the 30 – 40-day interval, the p-values exceed the significance threshold across all analysed distributions, indicating that the differences between the pEW and FWHM of the two SN types decrease as their spectra evolve. Although the reduced number of spectra may influence the results, the physical convergence of spectral features also contributes. Around 30 days after explosion, the H α line in SNe II typically strengthens, reaching intensities comparable to those observed in SNe IIb. At the same time, the He I line is often blended with the emerging Na I feature, particularly for SNe II (Gutiérrez et al. 2017). Nevertheless, the distinction between the two types remains clear at this stage when considering additional spectral features beyond H α and He I. Indeed, by ~ 30 days post-explosion, the H α P-Cygni profile in SNe IIb begins to exhibit distinct characteristics of this subtype. Notably, the He I $\lambda 6678$ feature, located near the peak of H α becomes more prominent, indicating an interference in the emission of the H feature. Additionally, He I lines emerge at

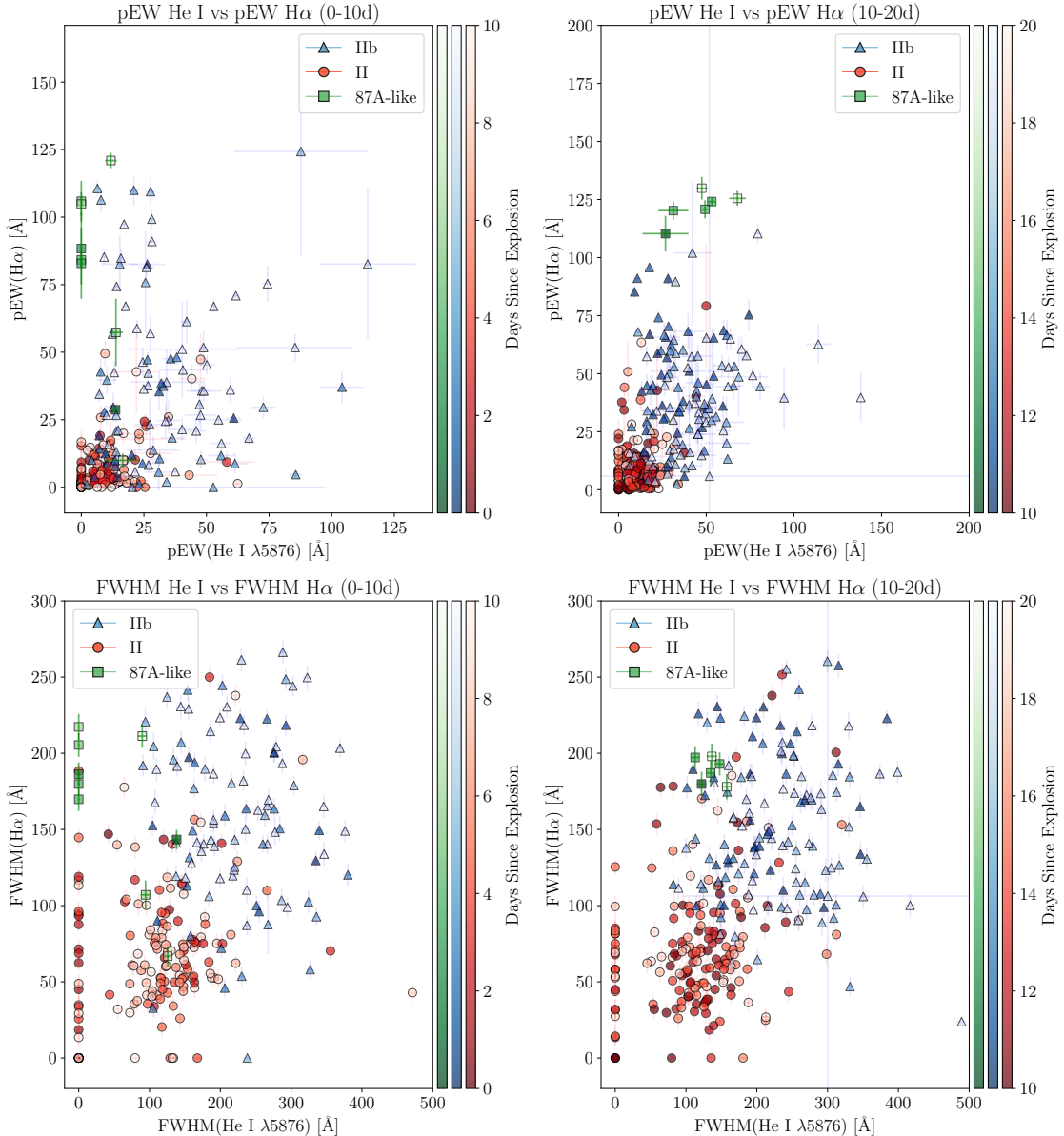


Fig. 7. pEW and FWHM values of H α line and He I λ 5876 for 0 – 10 days and 10 – 20 days. The markers are established by SN type: SNe IIb are shown as blue triangles, SNe II as red circles, and SNe 87A-like as green squares. The colour bars on the right side indicate the SN phase. The pEW measurements are in the top panels, and the FWHM measurements are in the bottom panels. In the left panels, we show the measurements within 0 – 10 days and in the right panels, between 10 – 20 days.

this phase, providing robust criteria for distinguishing between SNe II and IIb.

4.2. Machine learning methods

Machine learning methods offer powerful tools for identifying and analysing differences between the studied classes. These techniques are particularly useful for uncovering patterns and relationships that may remain hidden by traditional approaches. By handling complex, non-linear patterns, machine learning methods can effectively identify the features that distinguish the classes. This subsection explores our previous results by employing various machine-learning techniques. These include density contours, Quadratic Discriminant Analysis (QDA), t-SNE (T-distributed Stochastic Neighbour Embedding), Linear Discriminant Analysis (LDA), and Random Forest Classifier (RFC).

4.2.1. Density Contours

To further investigate the effect of overlapping values and the potential separation between the two SN types, we analysed their density evolution using a kernel density estimate (KDE). This method, which applies a Gaussian kernel with bandwidth= 1.0 by default, smooths the observations and produces a continuous estimate of the bivariate probability density. As a result, KDE offers a clearer representation of the data through continuous probability density curves.

Figure 8 illustrates the density contours of the pEW measurements. The comparison between the pEW of the H α and He I demonstrates that SN II measurements are intensely concentrated within a narrow region below (20, 20) Å throughout the 0 – 40-day period. However, a noticeable increase in the density contours for SNe II appears after approximately 20 days, with the contours continuing to expand over time. Along the y-axis, a

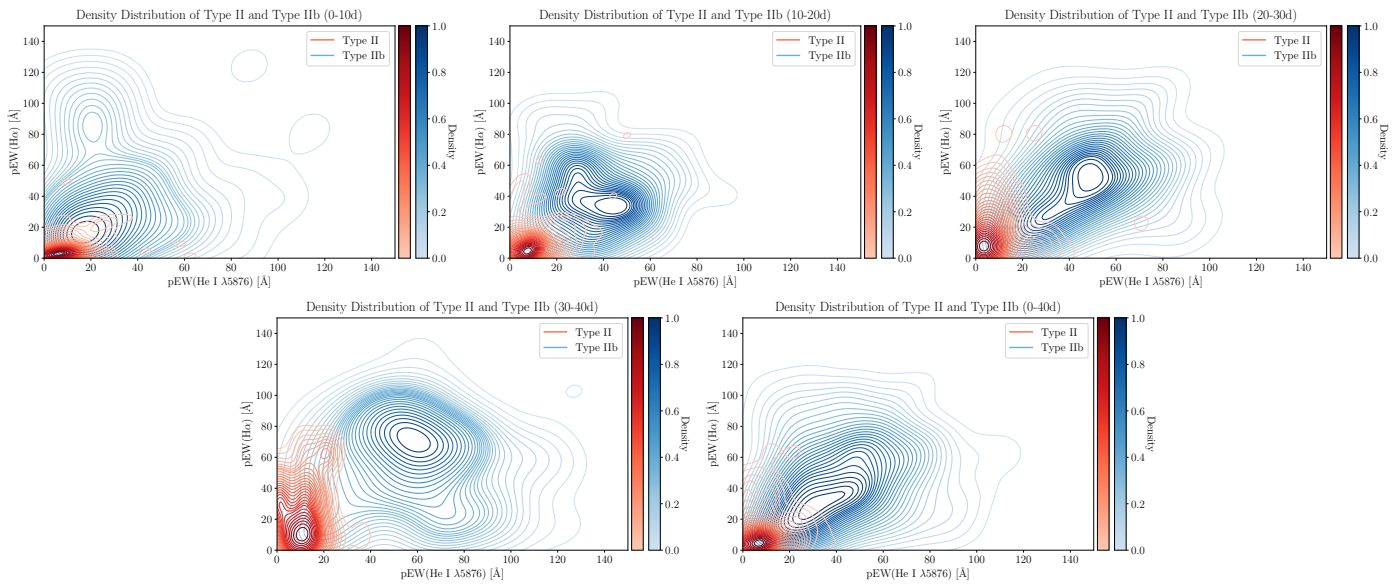


Fig. 8. Density contours of SNe II (in red) and IIb (in blue) based on the pEW measurements. The colour bars on the right side indicate the normalised density values, with darker colours representing higher densities. Each plot represents the density contours at different time intervals, as indicated at the top of the figure.

significant strengthening of the H α absorption is observed, reaching values of approximately 80 Å by 20 days post-explosion. In contrast, the He I feature gradually increases, extending its outer density contours to around 40 Å.

In comparison, the SN IIb population exhibit a broader range of values and less concentration compared to SNe II. Although some overlap exists between SNe IIb and II, their density contours separate with distinct central values. For SNe IIb, the central values shift over time, increasing from approximately (30, 30) Å in the early phases to around (70, 70) Å at later epochs. Notably, during the later epochs, the values for SNe IIb start to disperse, mimicking the behaviour observed in SNe II. This dispersion is particularly evident in the 30 – 40-day interval, where a secondary high-density contour emerges closer to the SN II contour centre, resulting in a broader overlap between the two populations. The increasing pEW values for both SN types contribute to this overlap, as highlighted in the comparison plots presented in the previous section.

A similar density contour analysis was also performed for the FWHM measurements (Figure A.5 in Appendix A). The results also indicate a separation between the two SN populations. However, the overlap between the datasets is significantly more pronounced, and the concentration of points within specific regions for each population is less distinct.

4.2.2. Quadratic Discriminant Analysis

Considering the significance of the separation between the two SN types confirmed by the KS test for both pEW and FWHM across time intervals, we define the separation boundaries using a machine-learning approach. Specifically, we apply the Quadratic Discriminant Analysis (QDA) to establish the optimal decision boundary for classifying our data points. QDA uses quadratic decision surfaces to discriminate between the measurements of the two samples. It can be considered a generalisation of the Linear Discriminant Analysis (LDA), as it is not limited to dividing the data by a straight line.

Defining these regions not only demonstrates that the two populations are separable but also visually captures the distinct evolution of the pEW and FWHM. In Figure 9, we present the separation defined by the QDA classifier for our sample, using the pEW measurements of He I λ 5876 and H α . The decision boundaries are shown for the full dataset over the first 40 days post-explosion and for the 0 – 10 and 10 – 20-day intervals. Notably, the overlap between the two SN types is significantly reduced in the earliest intervals compared to the full 40-day range, as the 90% probability region is more compact. A similar analysis was performed for other time intervals and for the FWHM measurements (details in Appendix A, Figures A.8 and A.10). However, as demonstrated by the density contours and the KS test results (Table 2), the separation based on FWHM values is less distinct than that based on the pEWs.

4.2.3. tSNE + LDA:

As an alternative method to demonstrate and visualise the behaviour of the two SN populations, we applied the t-SNE (t-distributed Stochastic Neighbour Embedding; Van der Maaten & Hinton 2008). This statistical technique is designed for visualising high-dimensional data by reducing it to lower-dimensional spaces, offering intuitive insights into how data is structured in higher dimensions. Unlike linear methods, t-SNE can separate data that cannot be divided by a straight line, overcoming the limitations posed by the shape of our measurements. This approach is particularly useful for uncovering underlying patterns and relationships within the data.

We use t-SNE to visualise our data, incorporating all the measured values for each SNe. This process reduced our 5D dataset—including the pEW and FWHM of H α and He I, along with the SNe epoch—into a 2D representation. The two resulting t-SNE components represent the reduced dimensions, capturing the spatial arrangement of the data points while preserving the relationships from the high-dimensional space. Additionally, to further analyse the 2D t-SNE distribution, we classified the data using LDA.

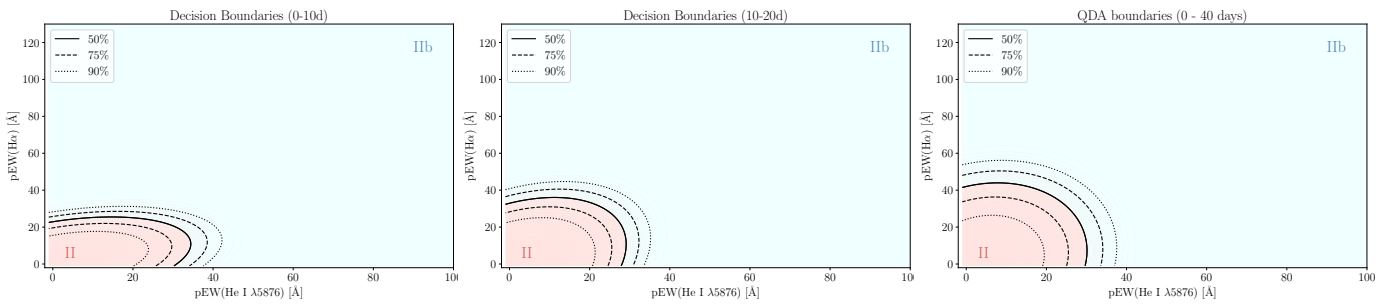


Fig. 9. Decision boundaries defined by the QDA classifier based on the pEW measurements for SN II and IIb pEW are shown across three time intervals: 0 – 10 days (left), 10 – 20 days (middle) and 0 – 40 days after the explosion (right). The red region corresponds to predictions for SNe II, while the blue region represents SNe IIb. The decision regions with a filled contour indicate where the model assigns a given SN type. Black contour lines represent classification probability thresholds, with a solid line marking a 50% probability, dashed lines for 75%, and a dotted line for 90% of belonging to a specific class.

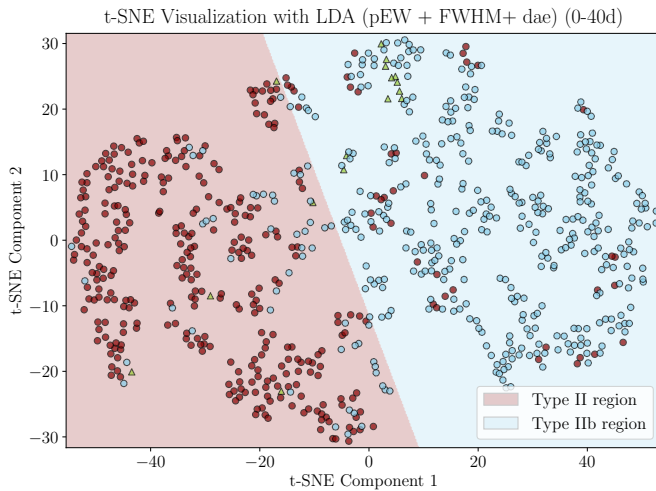


Fig. 10. Resulting t-SNE 2D reduced plot, using a perplexity value of 20. The red and blue dots represent SNe II and IIb, respectively, while green triangles indicate 87A-like events. The figure is separated into two regions defined by the LDA, with the solid line representing the decision boundary found for the t-SNE projection.

The resulting 2D distribution for the 0 – 40-day interval is presented in Figure 10. The plot reveals a separation between SNe II and IIb, with each type exhibiting a higher distribution in distinct regions of the plot. This finding supports the hypothesis that the two SN types can be distinguished based on the observed features (pEW, FWHM, and epoch). However, a complete separation is not evident. This continuity aligns with the trends observed in the individual pEW and FWHM comparisons of H α and He I. Visualising the data with the t-SNE method, as opposed to the QDA analysis, highlights a noticeable density decrease between the two populations, delineating two primary clusters, even though a mixed region remains visible. This 2D visualisation highlights, as discussed in Section 4, the behaviour of the 87A-like SNe, which appear in the region predominantly occupied by SNe IIb. This may be a consequence of the strong H α line exhibited by the 87A-like events (see Figure 6). Results for the 2D distributions in other time intervals are shown in Appendix A (Figure A.12).

4.2.4. Random Forest Classifier

Finally, we employed a Random Forest Classifier (RFC) to analyse the differences in the behaviour of the two SN types. This machine learning approach utilises multiple decision trees to

	RFC (averaged)	RFC (random)	t-SNE+LDA	QDA
Precision	II	0.813	0.848	pEW FWHM
	IIb	0.950	0.907	0.837 0.871
Recall	II	0.938	0.890	0.909 0.879
	IIb	0.844	0.871	0.925 0.890

Table 3. Comparison of precision and recall scores for the different classification methods.

classify SNe based on their specific characteristics. To prepare the data for the RFC, we constructed a feature matrix combining the spectral parameters (FWHM and pEW for both H α and He I) with the SN phase. The dataset was split into training and testing sets using a 60/40 ratio, ensuring a robust training sample while maintaining a significant portion for testing predictive accuracy. The classifier was trained on the training sample and evaluated on the test sample, predicting the SN types based on the input parameters. Importantly, we introduced only one value per parameter for each SN to ensure accurate outputs.

To evaluate the RFC's effectiveness in distinguishing between the two SN types, we applied two different sampling strategies. In the first approach, for SNe with multiple spectra, we randomly selected a single spectrum per object for inclusion in the analysis. In the second approach, we computed the average of all available spectra for each SN, including the phase, and used these averaged measurements as input to the RFC. Figure 11 presents the predicted probabilities for test sample SNe classified as Type II under both strategies. As shown in Table 3, the classifier performed slightly better with the random selection method.

Based on the RFC probabilities, SNe classified as Type II (in red) consistently received a high probability of obtaining the same classification by the RFC. Conversely, SNe IIb (in blue) were assigned a low probability of being classified as Type II. These results confirm that the measured features used in our analysis effectively distinguish the two SN types. We also tested alternative data combinations introduced in the RFC, which resulted in less effective classifications; For comparison, these results are presented in Appendix A (see Figures A.13 and A.14).

The RFC provides a statistical method for identifying differences between these two SN types and is a practical tool for classifying or reclassifying new SNe. By adjusting the training sample percentage from 60% to the entire dataset and using the values of interest for a specific SN as the test sample, it is possible to estimate the likelihood of that SN belonging to each type. For this purpose, and given the demonstrated utility of the method, we selected the RFC model based on averaged spectral values as

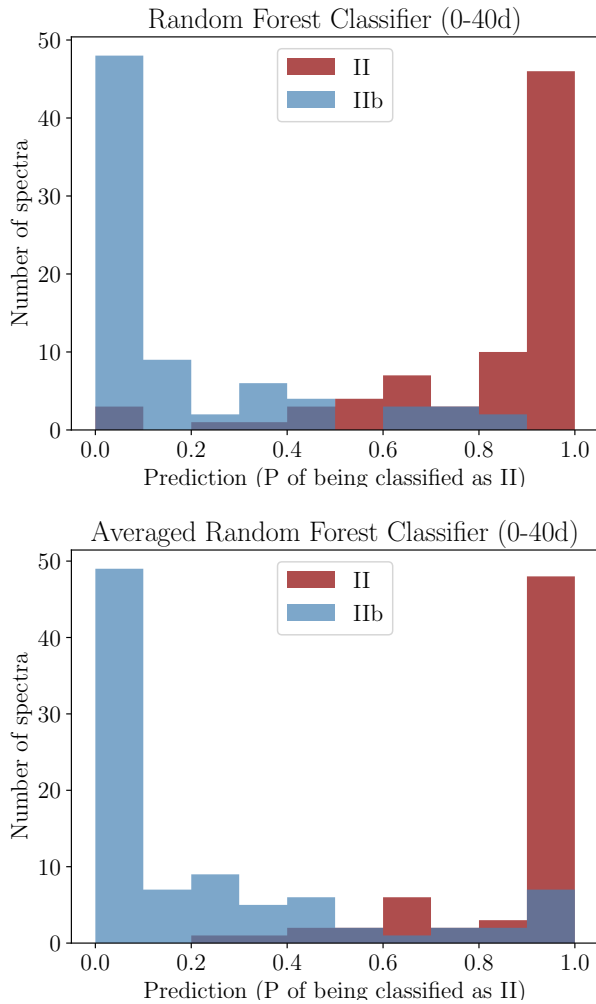


Fig. 11. Probabilities assigned by the RFC based on five parameters (pEW and FWHM of H α and He I, along with the epoch) within the first 40 days post-explosion. **Top panel:** Top panel: Classification probabilities obtained by randomly selecting one spectrum per SN from those with multiple observations. **Bottom panel:** Probabilities computed using the average spectrum for each SN, combining all available spectra.

our preferred classification tool. This approach ensures consistent, non-variable input for each SN by integrating all available spectral data from the main sample.

5. Discussion

5.1. A continuum in the H α pEW and FWHM?

The diversity observed in CCSNe arises from the varying amounts of outermost layers retained by their progenitor stars before the explosion. SNe IIb exhibit a transitional behaviour, evolving from hydrogen-dominated to helium-dominated spectra, suggesting that their progenitors retained less hydrogen before explosion than those of SNe II.

Our results show a complex picture: **(i)** while the pEW and FWHM of H α and He I are generally higher in SNe IIb than in SNe II, **(ii)** no definite separation exists between these parameters, indicating a continuum. The first finding is somewhat counterintuitive, as one might expect SNe II, which retain a more significant amount of H, to exhibit stronger spectral features. However, this can be explained by the differences in progenitor structure. In progenitor stars with a substantial hydrogen envelope, a greater

fraction of the shock-deposited energy is radiated away, leading to lower kinetic energy per unit mass (E_{kin}/M_{ej}) and, consequently, slower expansion velocities and narrower spectral lines. In contrast, SNe IIb, with their low-mass hydrogen envelopes, experience faster ejecta expansion, resulting in broader spectral lines (Dessart et al. 2024).

As for the second finding, theoretical models with varying orbital separations predict a continuum of light-curve morphologies for Type Ib, IIb, and II SNe, reflecting a range of H-rich envelope masses (Dessart et al. 2024). However, the distinct differences in the LCs of SNe II and IIb suggest their progenitors have different properties (e.g. Arcavi et al. 2012; Pessi et al. 2019), challenging the idea of a continuous distribution in spectral parameters. Our results indicate that, while hydrogen retention plays a key role in shaping the observed properties of SNe II and IIb, other factors likely contribute to their observed diversity. Even if hydrogen retention follows a continuum, this does not necessarily imply that their progenitors belong to a single, continuous evolutionary sequence. Instead, they likely represent distinct endpoints influenced by multiple parameters.

5.2. Effectiveness of our method

After applying several statistical techniques to quantitatively analyse the behaviour and differences between H α and He I in SNe II and IIb, we evaluated the potential utility and reliability of these findings as a foundation for a novel classification method.

Having already included all available higher-resolution spectra in our primary sample, we tested our results using SNe with lower-resolution spectra. To this end, we gathered all available SEDM spectra for SNe II and IIb from the Transient Name Server (TNS⁸), comprising 609 SNe II and 25 SNe IIb. Objects without accompanying light curve information were excluded, as the explosion date was necessary to constrain the SN phase. Thus, the final sample consisted of 106 SNe, as detailed in Table B.1 (Appendix B). We note the significant disparity in the number of SEDM spectra classified as SNe II versus SNe IIb: among the 106 SNe, 92 were classified as SNe II and 14 as SNe IIb. Additionally, we incorporated newly classified SNe that were released after compiling our main sample. This includes 36 newly classified objects (28 SNe II and 8 SNe IIb) along with two SNe (SN 2013gg and SN 2015dj) that were classified as SNe II on TNS but as SNe IIb on WISEREP and SN 2019oxi, which is a type II but was showing broad features. As a result, the comparison sample comprised 123 SNe II and 22 SNe IIb.

Following the same procedure as before, we measured the pEW and FWHM of H α and He I $\lambda 5876$ for the newly collected spectra. The results were then plotted within the density contours (Figure 12) and the QDA decision regions (Figure A.9, in Appendix A). Each SN was represented according to its official classification type as recorded in TNS. This approach enabled us to validate our method by re-evaluating the classification of spectra that exhibited potential signs of misclassification.

As shown in Figure 12, most of the objects from the comparison sample were correctly classified; however, a few SNe exhibit spectroscopic properties that more closely align with the opposite class. For instance, some SNe initially classified as Type II display characteristics of SNe IIb (i.e. higher pEW values), and vice versa. In these cases, we cross-verified the classification by examining their LC shapes and rise times. Specifically, this decision is based on the observation that SNe II typically have shorter rise times than SNe IIb (Pessi et al. 2019) and that most of

⁸ <https://www.wis-tns.org/>

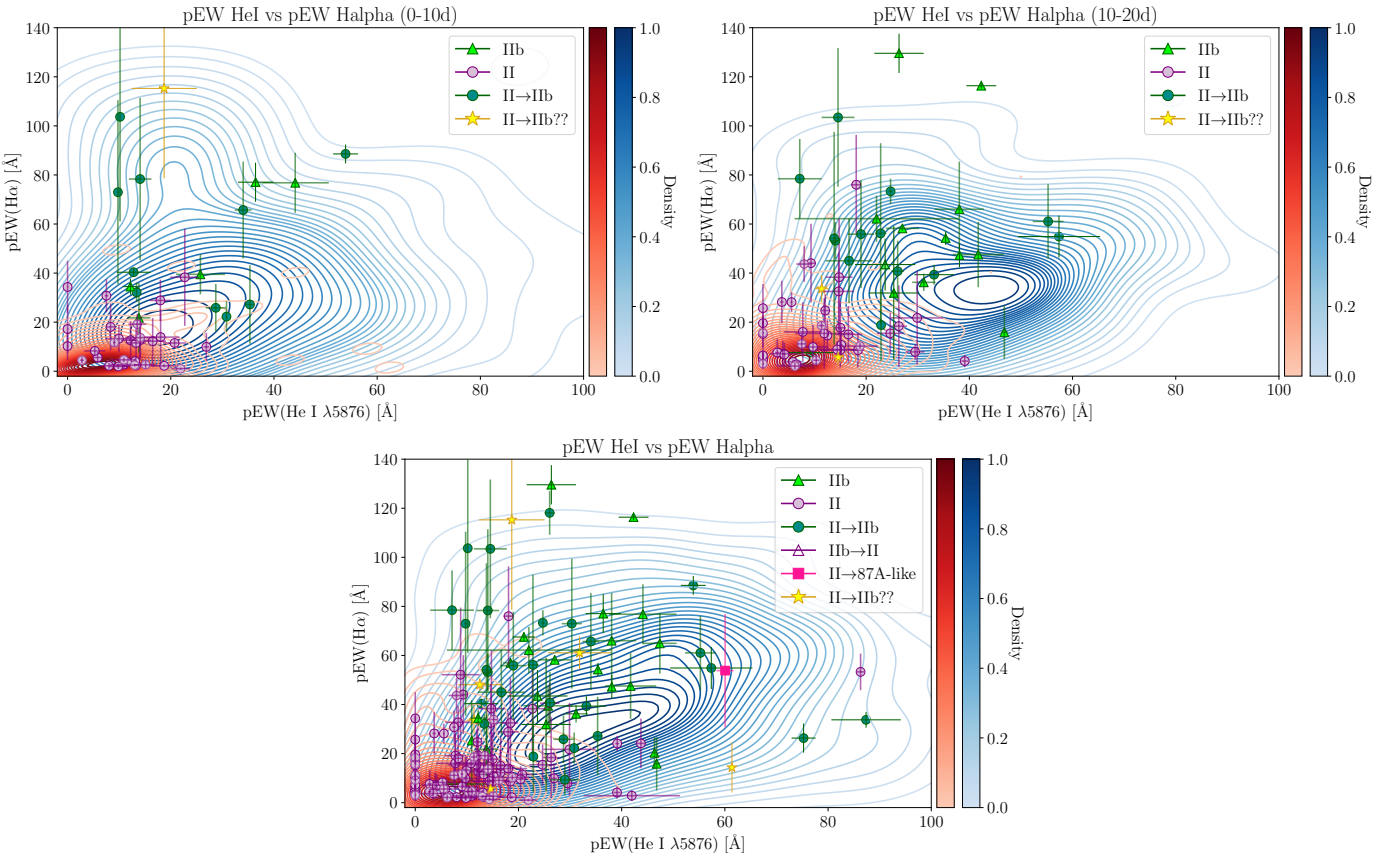


Fig. 12. pEW measurements of H α and He I for the comparison sample (SEDM plus newly classified SNe) overlaid on the density contours of SNe II (red) and IIb (blue) obtained in Section 4.2.1 (same as Figure 9), for three time intervals: 0 – 10 days (left), 10 – 20 days (middle) and 0 – 40 days (right). The comparison sample is represented by SNe II as filled purple dots and SNe IIb as filled green triangles. Dark green circles correspond to SNe initially classified as Type II but exhibiting SNe IIb-like properties. Open purple triangles represent SNe, which were initially classified as Type IIb but spectroscopically belong to the SN II class. Pink squares denote SNe II showing 87A-like characteristics. Yellow stars highlight SNe II that appear to exhibit SNe IIb characteristics but lack sufficient data to confirm this classification.

the SNe II exhibit a quasi-constant luminosity (a plateau) lasting several months. However, when the LC did not provide definitive confirmation, we conducted a more detailed spectral matching to refine the classification.

Through this re-evaluation process, we proved a potential misclassification of 34 SNe. Among these, 26 objects initially classified as Type II were found to align more closely with the properties of SNe IIb, while one SN, originally classified as SNe IIb, was determined to be better matched with SNe II. Notably, six SNe with insufficient photometric data (SN 2013gg, SNe 2018hqt, 2019noj, 2019oxi, 2024cgi and 2024lsl) show characteristics of both classes, providing inconclusive classifications. Lastly, SN 2020rmk was reclassified as a 87A-like event based on its spectral properties and exceptionally long-rise time (> 50 days). The re-classified objects are shown in Figure 12 and summarised in Tables B.2 and B.3 in the Appendix B.

To achieve a more accurate classification for those objects without a conclusive designation, we developed a Monte Carlo simulation with 500 iterations to compute their uncertainty. In each iteration, we resampled the base training set using bootstrapping, where some objects may be repeated and others omitted, and retrained the RFC model. This process yielded a distribution of classification probabilities for each object, enabling a more informed assessment of SN type in cases where photometric classification is not feasible. As a result, we classified SNe 2024lsl and 2018hqt as Type II and SNe 2024cgi and 2019noj as Type

IIb. For the SN 2019oxi and SN 2013gg, the RFC assigned 83% probability of being a SN II and 17% of being a SN IIb, and 55.6% and 44.4%, respectively, for the latter.

To evaluate how well each model balances the trade-off between identifying SNe of each type, we computed the precision and recall scores for each classification method. These metrics provide an overview of each method's ability to classify the sample accurately. The precision measures the classifier's ability to identify positive samples while minimising false positives correctly. This measures the proportion of correctly classified SNe among all predicted SNe, ensuring reliability. The recall reflects the classifier's ability to identify all actual positive samples, minimising false negatives. It quantifies the proportion of actual SNe that were correctly identified by the model, ensuring completeness. Then, a high precision score indicates fewer false positives, while a high recall score means fewer wrong classifications. The equations for each of these metrics are as follows:

$$\text{Precision: } \frac{TP}{TP + FP}, \quad (3)$$

$$\text{Recall: } \frac{TP}{TP + FN}, \quad (4)$$

where TP are the true positives, cases where the model correctly classifies a SN, FP are false positives, where the given classification is incorrect, and FN are false negatives, cases where

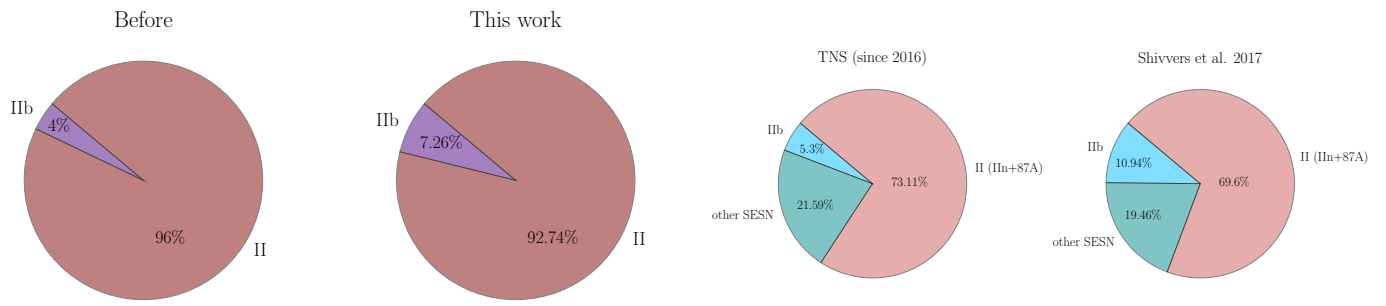


Fig. 13. Comparison of the fraction of SEDM spectra of each SN type before and after the performance of our re-classifications.

the model fails to identify the SN type. The metric scores for the methods are presented in Table 3. They all have similar precision and recall scores above 0.8 for both types.

5.3. Relative SN fractions

Once all SNe in our test sample were assigned a SN type following the methodology previously described, we compared these results with their initial classifications. We specifically analysed the impact of re-examined SEDM spectra on the original SN-type fractions. This comparison, presented in Figure 13, reveals a noticeable increase in the fraction of SNe IIb, with a $3.26\% \pm 0.13\%$ rise (almost twice the initial fraction) in SEDM spectra classified as SNe IIb.

The rates of CCSNe using the Lick Observatory Supernova Search volume-limited sample have been estimated in several works (e.g. Leaman et al. 2011; Li et al. 2011b,a; Maoz et al. 2011) and recently revised by Shivvers et al. (2017). They found that SNe II constitute approximately 70% of all CCSNe, while SESNe account for about 30%. Within SESNe, there are SNe Ib, Ic, and IIb. Based on known classifications and reclassifications, they estimated the true CCSNe fractions to be 69.6% for SNe II, 10.94% for SNe IIb, and 19.46% for other SESNe. More recently, Perley et al. (2020), using the ZTF Bright Transient Survey (BTS) magnitude-limited sample, found that hydrogen-rich SNe (SNe II, IIb, IIIn, and superluminous SNe II) constitute 72.2% of all CCSNe. Within the hydrogen-rich SN class, SNe II are 69.05% of all the CCSNe, while the fraction corresponding to IIb is 5.10%. The remaining 25.85% is formed by SNe Ib, Ic, Ic-BL and Ibn SESNe. These percentages correspond to the fractions excluding the SLSNe that were included in the analysis of (Perley et al. 2020).

Based on the subtype ratio presented in Shivvers et al. (2017), we performed a similar analysis, including the same SN types, using publicly available TNS data collected from 2016 to 2024. Our results, presented in Figure 14, reveal discrepancies compared to Shivvers et al. (2017). The fraction of SNe II differs by 3.5%, while the SNe IIb fraction shows a disagreement of 5.6%. Compared to Perley et al. (2020), the SNe IIb fraction is almost the same, but their SNe II fraction is 4% smaller (this percentage is added to the SESN). While we recognise that this comparison is neither direct nor entirely equitable, since different selection effects than ours influence the referenced samples, we include it to provide a general perspective on how the relative fractions of SNe II and IIb vary when comparing our results with those of other studies.

Considering our findings, even just the reanalysis of SEDM spectra resulted in a measurable shift in the SNe IIb fraction.

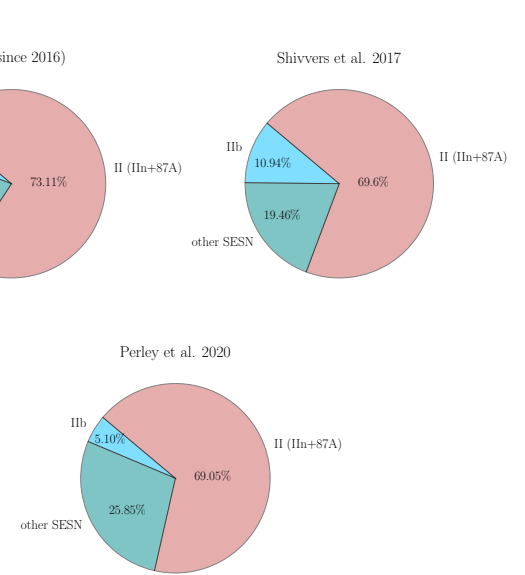


Fig. 14. CC-SNe fractions computed by Shivvers et al. (2017) (right-top), Perley et al. (2020) (bottom) and the fractions computed in this work by using the available data on TNS since 2016 (left-top).

This suggests that classification uncertainties, especially in distinguishing SNe II and IIb at early times, could significantly impact the CCSNe fraction estimates. If SNe IIb are not followed long enough, they may be misclassified as SNe II. This effect could partly explain the observed difference in the SN IIb fractions between our TNS analysis and previous works.

5.4. Transitional events

During our analysis, we identified several peculiar objects, which are discussed in this section. SNe showing ambiguous behaviour in their spectra or LCs are considered "transitional objects". These cases present conflicting classification indicators, as their photometry and spectroscopic characteristics suggest different SN types. The type II SNe 2019nyn, 2019uqp, 2019yyf, 2021agle, 2023rhj and 2024dgy were included in this discussion after their luminosity decay over 30 days post-peak was measured, revealing a magnitude difference comparable to that of the SNe IIb. Similarly, SN 2018arx (classified as a SN IIb) exhibited a LC shape similar to that of SNe II. For each transitional event, we also computed the RFC probability of belonging to each classification category (II/IIb/87A-like).

5.4.1. SNe II with Type IIb-like luminosity declines

The SNe presented in Table 4 were classified as Type II based on their spectral features; however, their luminosity decline within 30 days after peak is more consistent with SNe IIb. This discrepancy raises questions about their classification, suggesting possible transitional properties between the two types.

The similar post-peak decline rates observed could be indicative of fast-declining SNe II (SNe IIL) or SNe IIb, both of which exhibit comparable light-curve behaviour during this phase. However, their early-time evolution diverges, with SNe IIb typically showing a slower rise to maximum light (Pessi et al. 2019). Some studies have suggested a degree of overlap between SNe IIL and IIb (e.g., Faran et al. 2014; Reguitti et al. 2024), which can complicate photometric classification. Nevertheless,

Table 4. RFC probabilities for the 'transitional objects' identified through luminosity decline measurements.

SN	Probabilities		
	II	IIb	87A-like
2019yn	1.0	0.0	0.0
2019uqp	0.76	0.21	0.03
2019yyf	0.99	0.01	0.0
2021agle	0.74	0.25	0.01
2023rhj	1.0	0.0	0.0
2024dgy (10d)	1.0	0.0	0.0
2024dgy (17d)	0.99	0.01	0.0

the spectroscopic features in our data strongly support a Type II classification, making a IIb interpretation unlikely. Indeed, the probabilities assigned by the RFC strongly support their official classification as SNe II.

5.4.2. SNe II with mixed spectral and photometric properties

Some SNe display a combination of spectral and photometric characteristics that place them in the overlapping region between SNe II and IIb.

- **SN 2019oxi:** Officially classified as a SN II, this object present notable deviations from the typical properties of SNe II. Its spectral features closely resemble those of SNe IIb, suggesting a possible reclassification. Although its photometric data benefits from a well-coverage follow-up, it does not provide a clear type identification, as it shows a slow rise over ~ 40 days followed by a slow decline. By applying the RFC classification method combined with a Monte Carlo approach, we found that both techniques favour a Type IIb classification. RFC probabilities: II: 0.60; IIb: 0.40; 87-like: 0.0.
- **SN 2018hoa:** Officially classified as SNe II. The spectral line measurements are consistent with this classification, showing small values typical for SNe II. However, the LC exhibits a clear double peak morphology, a feature more commonly associated with SNe IIb. RFC probabilities: II: 0.50; IIb: 0.49; 87-like: 0.0.
- **SN 2024ehs:** Officially classified as a SN II, it shows a bell-like shape LC, with a rising time of about 20 days and a rapid decline after the peak. The spectral measurements of H and He lines are not conclusive either, as they fall into the overlapping region. RFC probabilities at 2 days post-explosion: II: 0.32; IIb: 0.67; 87A-like: 0.01; RFC probabilities at 16 days post-explosion: II: 0.60; IIb: 0.39; 87A-like: 0.01.

5.4.3. SNe IIb showing Type II-like photometric evolution

These SNe were classified as Type IIb based on spectral features, yet their photometric behaviour resembles SNe II.

- **SN 2018arx:** Although classified as a SN IIb and exhibiting a broad, flat-topped $H\alpha$, the He I line is very weak, causing it to fall into the overlapping region between the two populations. Regarding the photometry, it shows a peculiar, relatively constant luminosity that resembles a plateau. The RFC probabilities for this SN are: II: 0.36; IIb: 0.64; 87A-like: 0.00.
- **SN 2022emz:** Spectroscopically, it exhibits the characteristics of a slowly evolving SN IIb, with a broad and deep He I line and a flat top $H\alpha$. However, upon analysing its LC, a constant luminosity is observed for nearly 100 days after

the peak. This behaviour is usual of slow-declining SNe II (SNe IIP). On the other hand, the rise to the peak aligns with the average time exhibited by SNe IIb (Pessi et al. 2019). The RFC probabilities for this object are as follows: II:0.0; IIb:1.00; 87A-like:0.00.

5.5. A new tool to classify SNe II and IIb based on early spectra

We also defined two alternative classification methods that could indeed be used to complement the density contours and QDA regions. First, we performed again a RFC (see section 4.2.4), taking this time our entire sample as a training sample and a newly measured SN as a test sample. This way, we achieve the probabilities for that SN to belong to each type. The probabilities for the SEDM spectra and new classifications are presented in Table B.3 and B.2. Second, we developed the possibility of plotting the newly measured SNe on our t-SNE plots. So far, we can see if it falls in the cluster formed by a majority of type II or IIb SNe. This would allow us to have different perspectives on interpreting the values obtained for the new SN.

6. Conclusions

In this paper, we presented a detailed analysis of the early spectra of SNe II and IIb to uncover their diversity. The 866 spectra of 393 SNe, composing our main sample, were analysed using the pEW and FWHM of the $H\alpha$ and He I $\lambda 5876$ features. Statistical methods and machine-learning techniques were applied to identify differences between SNe II and IIb. Our main results are:

- We find that pEW and FWHM of $H\alpha$ and He I $\lambda 5876$ in SNe IIb display larger values than those of SNe II during the entire evolution, with most significant differences occurring in early phases, particularly in the 10 – 20-day interval.
- Population density evolution reveals a clear separation in the pEW of SNe II and IIb. SNe II consistently exhibit high-density concentrations around 20 Å, while SNe IIb reach 60–80 Å values. Despite this distinction, the two populations seem to form a continuum in spectral properties.
- The QDA analysis shows that SNe II and IIb exhibit distinct pEW evolution patterns, with the greatest separation occurring within the first 10 days. In contrast, differences based on FWHM measurements are less pronounced.
- t-SNE+LDA effectively separated the two types, supporting their distinction based on observed features. However, continuity between the two clusters persists, suggesting a gradual transition rather than a strict boundary between the populations.
- The RFC confirms the distinct characteristics of the two groups and demonstrates the effectiveness of these parameters (pEW and FWHM of $H\alpha$ and He I) as classification criteria. Additionally, it enables the classification of newly observed SNe.
- We demonstrate the method validation using low-resolution SEDM spectra and newly classified SNe. We identify 34 possible misclassified SNe within the re-analysed sample. Based on these revised classifications, we recalculated the SEDM fraction for each SNe type, leading to a notable increase in the percentage of SNe IIb reported in WISERep from 4.0% to 7.26% (see Figure 13), nearly doubling its original value.

We have developed a new classification method for early SNe II and IIb based on quantified differences in spectral features during their early evolution. Using the obtained results,

we computed classification probabilities with the RF classifier and plotted the measurements within defined regions, enabling a clear classification assessment. This approach not only improves our understanding of the early phases of SN evolution but also serves as a valuable tool for enhancing classification accuracy in future observations. Our findings indicate that misclassification significantly impacts the actual CCSNe rate. The reclassification of SEDM spectra has improved the accuracy of previously available classification data, highlighting the robustness of our method.

All classification tools developed in this study, along with the computed median spectra for each time interval, are publicly available at <https://doi.org/10.5281/zenodo.15756198> (<https://zenodo.org/communities/sndata/>) to facilitate broader use.

Acknowledgements. We thank the anonymous referee for the comments and suggestions that have helped us to improve the paper. We thank the anonymous referee for the comments and We thank Maria Kopsacheili, Koraljka Muzic, Joseph Anderson, Luc Dessart and Bastián Ayala for valuable discussions. M.G.B.’s work has been carried out within the framework of the doctoral program in Physics of the Universitat Autònoma de Barcelona. The M.G.B., C.P.G., L.G. research group acknowledges financial support from the Spanish Ministerio de Ciencia e Innovación (MCIN) and the Agencia Estatal de Investigación (AEI) 10.13039/501100011033 under the PID2020-115253GA-I00 HOSTFLOWS and PID2023-151307NB-I00 SNNEXT project, from Centro Superior de Investigaciones Científicas (CSIC) under the projects PIE 20215AT016, ILINK23001, COOPB2304, and the program Unidad de Excelencia María de Maeztu CEX2020-001058-M, and from the Departament de Recerca i Universitats de la Generalitat de Catalunya through the 2021-SGR-01270 grant. C.P.G. acknowledges financial support from the Secretary of Universities and Research (Government of Catalonia) and by the Horizon 2020 Research and Innovation Programme of the European Union under the Marie Skłodowska-Curie and the Beatriu de Pinós 2021 BP 00168 programme.

References

- Al, M. S. E. 2019, Transient Name Server Discovery Report, 2019-1509, 1
 Anderson, J. P., Dessart, L., Gutiérrez, C. P., et al. 2018, Nature Astronomy, 2, 574
 Anderson, J. P., González-Gaitán, S., Hamuy, M., et al. 2014, The Astrophysical Journal, 786, 67
 Angel, C. J., Perez-Fournon, I., Poidevin, F., et al. 2020, Transient Name Server Discovery Report, 2020-2821, 1
 Angus, C. 2020a, Transient Name Server Classification Report, 2020-1392, 1
 Angus, C. 2020b, Transient Name Server Classification Report, 2020-3109, 1
 Angus, C. 2021, Transient Name Server Classification Report, 2021-1049, 1
 Angus, C. 2022, Transient Name Server Classification Report, 2022-3613, 1
 Angus, C. 2023, Transient Name Server Classification Report, 2023-1681, 1
 Angus, C. 2024, Transient Name Server Classification Report, 2024-434, 1
 Angus, C. & Izzo, L. 2021, Transient Name Server Classification Report, 2021-831, 1
 Angus, C., Wiseman, P., Swann, E., Frohmaier, C., & Irani, I. 2019, Transient Name Server Classification Report, 2019-1371, 1
 Angus, C., Wiseman, P., Swann, E., et al. 2019, Transient Name Server Classification Report, 2019, 1
 Angus, C., Wiseman, P., Swann, E., et al. 2019, Transient Name Server Classification Report, 2019-1379, 1
 Angus, C., Jones, S., Yaron, O., & Knezevic, N. 2017, Transient Name Server Classification Report, 2017-1477, 1
 Arbour, R., Armstrong, M., Boles, T., et al. 2004, IAU Circular, 8406
 Arcavi, I. 2017, arXiv preprint arXiv:1710.03759
 Arcavi, I., Burke, J., Hiramatsu, D., et al. 2019, Transient Name Server Classification Report, no abstract available
 Arcavi, I., Burke, J., Hiramatsu, D., et al. 2019, Transient Name Server Classification Report, 2019-2059, 1
 Arcavi, I., Gal-Yam, A., Cenko, S. B., et al. 2012, The Astrophysical Journal Letters, 756, L30
 Arcavi, I., Gal-Yam, A., Kasliwal, M. M., et al. 2010, ApJ, 721, 777
 Arcavi, I., Gal-Yam, A., Yaron, O., et al. 2011, ApJ, 742, L18
 Armstrong, M., Hamuy, M., Morrell, N., Arias, J., & Barba, R. 2003, IAU Circular, 8173
 Atapin, K., Dodin, A., Tatarnikov, A., et al. 2020, Transient Name Server Classification Report, 2020-3698, 1
 Ayala, B., Ramirez, M., Dastidar, R., et al. 2023, Transient Name Server Classification Report, 2023-2482, 1
 Baek, M. & Li, W. 2005, IAU Circular, 8641
 Balakina, E. A., Pruzhinskaya, M. V., Moskvitin, A. S., & Blinnikov, S. I. 2019, in The multi-messenger astronomy: gamma-ray bursts, search for electromagnetic counterparts to neutrino events and gravitational waves, 32–36
 Balam, D. 2018, Transient Name Server Classification Report, 2018-788, 1
 Balon, C. 2023, Transient Name Server Classification Report, 2023-3314, 1
 Barbarino, C., Carracedo, A. S., Tartaglia, L., & Yaron, O. 2019, Transient Name Server Classification Report, 2019-287, 1
 Barbon, R., Benetti, S., Cappellaro, E., et al. 1995, Astronomy and Astrophysics Supplement, v. 110, p. 513, 110, 513
 Barbon, R., Ciatti, F., & Rosino, L. 1979, Astronomy and Astrophysics, vol. 72, no. 3, Feb. 1979, p. 287-292. Research supported by the Consiglio Nazionale delle Ricerche., 72, 287
 Bauer, F. E., Forster, F., Pignata, G., et al. 2019, Transient Name Server Discovery Report, 2019-2342, 1
 Bellm, E. C., Kulkarni, S. R., Graham, M. J., et al. 2019, PASP, 131, 018002
 Benetti, S. 2017, Transient Name Server Classification Report, 2017-258, 1
 Benetti, S., Pastorello, A., Elias-Rosa, N., et al. 2014, The Astronomer’s Telegram, 6185, 1
 Bersten, M. C., Benvenuto, O. G., Nomoto, K., et al. 2012, The Astrophysical Journal, 757, 31
 Blagorodnova, N., Neill, J. D., Walters, R., et al. 2018, PASP, 130, 035003
 Blanchard, P., Zheng, W., Cenko, S., et al. 2013, Central Bureau Electronic Telegrams, 3422, 1
 Blondin, S., Modjaz, M., Kirshner, R., et al. 2006, Central Bureau Electronic Telegrams, 455, 1
 Blondin, S. & Tonry, J. L. 2007, The Astrophysical Journal, 666, 1024
 Bock, G., Milisavljevic, D., Parrent, J., et al. 2012, Central Bureau Electronic Telegrams, 3197, 1
 Bock, G. & Stanek, K. Z. 2019, Transient Name Server Discovery Report, 2019-1601, 1
 Bock, G., Stanek, K. Z., & Kochanek, C. S. 2019, Transient Name Server Discovery Report, 2019-1548, 1
 Boles, T. 2009, Central Bureau Electronic Telegrams, 1985
 Boles, T., Khandrika, H., Madison, D. R., et al. 2005, IAU Circular, 8604
 Borsato, L., Nascimbeni, V., Benetti, S., et al. 2012, Central Bureau Electronic Telegrams, 2993
 Bose, S., Holmbo, S., Mattila, S., et al. 2019, Transient Name Server Classification Report, no abstract available
 Bose, S., Holmbo, S., Mattila, S., et al. 2019, Transient Name Server Classification Report, 2019-1332, 1
 Bose, S., Holoién, T., Prieto, J. L., et al. 2018, Transient Name Server Classification Report, 2018-640, 1
 Bose, S., Kumar, K., Sutaria, F., et al. 2013, in Astronomical Society of India Conference Series, Vol. 9, 134
 Bostroem, K. A., Valenti, S., Horesh, A., et al. 2019, MNRAS, 485, 5120
 Bredall, J., Do, A., Payne, A., et al. 2019a, Transient Name Server Classification Report, 2019-980, 1
 Bredall, J., Payne, A., Do, A., et al. 2019b, Transient Name Server Classification Report, 2019-981, 1
 Brennan, S., Callis, E., Ihaneč, N., Gromadzki, M., & Irani, I. 2019a, Transient Name Server Classification Report, 2019-1773, 1
 Brennan, S., Fraser, M., Ihaneč, N., Gromadzki, M., & Yaron, O. 2019b, Transient Name Server Classification Report, 2019-1595, 1
 Brimacombe, J., Bersier, D., & Stanek, K. Z. 2019, Transient Name Server Discovery Report, 2019-314, 1
 Brimacombe, J., Brown, J. S., Stanek, K. Z., et al. 2015, The Astronomer’s Telegram, 8153, 1
 Brimacombe, J. & Valley, P. 2019, Transient Name Server Discovery Report, 2019-723, 1
 Brinnel, V., Carracedo, A. S., Barbarino, C., Tartaglia, L., & Yaron, O. 2019, Transient Name Server Classification Report, 2019-417, 1
 Brivio, R., Ferro, M., Benetti, S., Reguitti, A., & Yaron, O. 2024, Transient Name Server Classification Report, 2024-303, 1
 Brown, J. 2016, Transient Name Server Discovery Report, 2016, 1
 Brown, J. S., Stanek, K. Z., Holoién, T. W. S., et al. 2015, The Astronomer’s Telegram, 7989, 1
 Bruch, R., Anderson, J., Gutierrez, C., & Irani, I. 2021a, Transient Name Server Classification Report, 2021-3405, 1
 Bruch, R. J., Gal-Yam, A., Schulze, S., et al. 2021b, ApJ, 912, 46
 Bufano, F., Pignata, G., Bersten, M., et al. 2014, MNRAS, 439, 1807
 Burke, J., Arcavi, I., Hiramatsu, D., et al. 2019a, Transient Name Server Classification Report, 2019-1039, 1
 Burke, J., Arcavi, I., Hiramatsu, D., et al. 2019b, Transient Name Server Classification Report, 2019-2020, 1
 Burke, J., Hiramatsu, D., Howell, D. A., McCully, C., & Pellegrino, C. 2019c, Transient Name Server Classification Report, 2019-1748, 1

- Burke, J., Hiramatsu, D., Howell, D. A., McCully, C., & Pellegrino, C. 2019, Transient Name Server Classification Report, no abstract available
- Burke, J., Hiramatsu, D., Howell, D. A., McCully, C., & Pellegrino, C. 2020, Transient Name Server Classification Report, no abstract available
- Burke, J., Hiramatsu, D., Howell, D. A., McCully, C., & Pellegrino, C. 2020, Transient Name Server Classification Report, 2020-304, 1
- Burke, J., Howell, D. A., Hiramatsu, D., et al. 2021, Transient Name Server Classification Report, 2021-1132, 1
- Burke, J., Howell, D. A., Hiramatsu, D., McCully, C., & Pellegrino, C. 2019a, Transient Name Server Classification Report, 2019-2406, 1
- Burke, J., Itagaki, K., Hiramatsu, D., et al. 2019b, Transient Name Server Classification Report, 2019-2517, 1
- Burket, J., Li, W., Blondin, S., Prieto, J. L., & the ESSENCE Project. 2005, IAU Circular, 8464
- Byrne, R., Fitzpatrick, B., Fraser, M., & Yaron, O. 2023, Transient Name Server Classification Report, 2023-2299, 1
- Caimmi, M. 2017, Transient Name Server Discovery Report, 2017-973, 1
- Callis, E., Brennan, S., Ihane, N., Gromadzki, M., & Yaron, O. 2019, Transient Name Server Classification Report, 2019-1662, 1
- Campbell, H., Blagorodnova, N., Fraser, M., et al. 2014, The Astronomer's Telegram, 5937, 1
- Carini, R., Palazzi, E., Cappellaro, E., Fiore, A., & Yaron, O. 2019, Transient Name Server Classification Report, 2019-228, 1
- Carini, R., Ragosta, F., Benetti, S., Tartaglia, L., & Strotjohann, N. L. 2021a, Transient Name Server Classification Report, 2021-3762, 1
- Carini, R., Ragosta, F., Benetti, S., Tartaglia, L., & Strotjohann, N. L. 2021b, Transient Name Server Classification Report, 2021-3787, 1
- Carracedo, A. S., Barbarino, C., Brinnel, V., Tartaglia, L., & Yaron, O. 2019, Transient Name Server Classification Report, 2019-355, 1
- Carrasco, F., Hamuy, M., Antezana, R., et al. 2013, Central Bureau Electronic Telegrams, 3437, 1
- Cartier, R., Briceno, C., Gomez, D., Espinoza, J., & Estay, O. 2019a, Transient Name Server Classification Report, 2019-824, 1
- Cartier, R., Contreras, C., Pasten, A., & Fuentes, C. 2020, Transient Name Server Classification Report, 2020-3731, 1
- Cartier, R., Olivares, F., Pineda, J., et al. 2019b, Transient Name Server Classification Report, 2019-817, 1
- Cartier, R. & Ugarte, P. 2019, Transient Name Server Classification Report, 2019, 1
- Challis, P., Kirshner, R., Mandel, K., et al. 2016, The Astronomer's Telegram, 9505, 1
- Chambers, K., Huber, M., Flewelling, H., et al. 2016a, Transient Name Server Discovery Report, 2016, 1
- Chambers, K., Huber, M., Flewelling, H., et al. 2016b, Transient Name Server Discovery Report, 2016, 1
- Chambers, K., Huber, M., Flewelling, H., et al. 2017a, Transient Name Server Discovery Report, 2017, 1
- Chambers, K., Huber, M., Flewelling, H., et al. 2017b, Transient Name Server Discovery Report, 2017, 1
- Chambers, K. C., Boer, T. D., Bulger, J., et al. 2023, Transient Name Server Discovery Report, 2023-567, 1
- Chambers, K. C., Boer, T. D., Bulger, J., et al. 2021a, Transient Name Server Discovery Report, 2021-777, 1
- Chambers, K. C., Boer, T. D., Bulger, J., et al. 2021b, Transient Name Server Discovery Report, 2021-1947, 1
- Chambers, K. C., Boer, T. D., Bulger, J., et al. 2021c, Transient Name Server Discovery Report, 2021-2706, 1
- Chambers, K. C., Boer, T. D., Bulger, J., et al. 2021d, Transient Name Server Discovery Report, 2021-2936, 1
- Chambers, K. C., Boer, T. D., Bulger, J., et al. 2021e, Transient Name Server Discovery Report, 2021-2949, 1
- Chambers, K. C., Boer, T. D., Bulger, J., et al. 2021f, Transient Name Server Discovery Report, 2021-3040, 1
- Chambers, K. C., Boer, T. D., Bulger, J., et al. 2021g, Transient Name Server Discovery Report, 2021-3307, 1
- Chambers, K. C., Boer, T. D., Bulger, J., et al. 2022a, Transient Name Server Discovery Report, 2022-863, 1
- Chambers, K. C., Boer, T. D., Bulger, J., et al. 2022b, Transient Name Server Discovery Report, 2022-207, 1
- Chambers, K. C., Boer, T. D., Bulger, J., et al. 2019a, Transient Name Server Discovery Report, 2019-1605, 1
- Chambers, K. C., Boer, T. D., Bulger, J., et al. 2019b, Transient Name Server Discovery Report, 2019-1939, 1
- Chambers, K. C., Boer, T. D., Bulger, J., et al. 2019c, Transient Name Server Discovery Report, 2019-2363, 1
- Chambers, K. C., Boer, T. D., Bulger, J., et al. 2019d, Transient Name Server Discovery Report, 2019-2722, 1
- Chambers, K. C., Huber, M. E., Flewelling, H., et al. 2016c, Transient Name Server Discovery Report, 2016-765, no abstract available
- Chambers, K. C., Huber, M. E., Flewelling, H., et al. 2018, Transient Name Server Discovery Report, 2018-153, 1
- Chambers, K. C., Huber, M. E., Flewelling, H., et al. 2019e, Transient Name Server Discovery Report, 2019-223, 1
- Chambers, K. C., Huber, M. E., Flewelling, H., et al. 2019f, Transient Name Server Discovery Report, 2019-665, 1
- Childress, M. J., Tucker, B. E., Yuan, F., et al. 2016, Publications of the Astronomical Society of Australia, 33, e055
- Chornock, R., Filippenko, A. V., Li, W., et al. 2011, ApJ, 739, 41
- Chu, J., Li, W., & Filippenko, A. V. 2008, Central Bureau Electronic Telegrams, 1271
- Chu, M., Dahiwale, A., & Fremling, C. 2021a, Transient Name Server Classification Report, 2021-2534, 1
- Chu, M., Dahiwale, A., & Fremling, C. 2021b, Transient Name Server Classification Report, 2021-2683, 1
- Chu, M., Dahiwale, A., & Fremling, C. 2021c, Transient Name Server Classification Report, 2021-3202, 1
- Chu, M., Dahiwale, A., & Fremling, C. 2021d, Transient Name Server Classification Report, 2021-3339, 1
- Chu, M., Dahiwale, A., & Fremling, C. 2021e, Transient Name Server Classification Report, 2021-4130, 1
- Ciabattari, F., Mazzoni, E., Donati, S., et al. 2013a, Central Bureau Electronic Telegrams, 3557, 1
- Ciabattari, F., Mazzoni, E., & Petroni, G. 2017, Transient Name Server Discovery Report, 2017, 1
- Ciabattari, F., Tomasella, L., Benetti, S., et al. 2013b, Central Bureau Electronic Telegrams, 3615, 1
- Cifuentes, M., Pignata, G., Apostolovski, Y., et al. 2012, Central Bureau Electronic Telegrams, 3347, 1
- Clark, P., Smartt, S., Yaron, O., & Knezevic, N. 2018, Transient Name Server Classification Report, 2018-678, 1
- Clocchiatti, A. 2002, International Astronomical Union Circular, 7793, 2
- Consel, E., Dong, S., Brown, J. S., et al. 2016, Transient Name Server Discovery Report, 2016-1, no abstract available
- Csoernyei, G., Taubenberger, S., Vogl, C., Blondin, S., & Zimmerman, E. A. 2024a, Transient Name Server Classification Report, 2024-615, 1
- Csoernyei, G., Taubenberger, S., Vogl, C., Blondin, S., & Zimmerman, E. A. 2024b, Transient Name Server Classification Report, 2024-624, 1
- Csoernyei, G., Taubenberger, S., Vogl, C., Blondin, S., & Zimmerman, E. A. 2024c, Transient Name Server Classification Report, 2024-672, 1
- Csoernyei, G., Taubenberger, S., Vogl, C., et al. 2021, Transient Name Server Classification Report, 2021-2990, 1
- Csoernyei, G., Taubenberger, S., Vogl, C., et al. 2023, Transient Name Server Classification Report, 2023-3231, 1
- Dahiwale, A., Dugas, A., & Fremling, C. 2019a, Transient Name Server Classification Report, 2019-1854, 1
- Dahiwale, A. & Fremling, C. 2019a, Transient Name Server Classification Report, 2019-2184, 1
- Dahiwale, A. & Fremling, C. 2019b, Transient Name Server Classification Report, 2019-2894, 1
- Dahiwale, A. & Fremling, C. 2019c, Transient Name Server Classification Report, 2019-2468, 1
- Dahiwale, A. & Fremling, C. 2020a, Transient Name Server Classification Report, 2020-25, 1
- Dahiwale, A. & Fremling, C. 2020b, Transient Name Server Classification Report, 2020-1410, 1
- Dahiwale, A. & Fremling, C. 2020c, Transient Name Server Classification Report, 2020-3837, 1
- Dahiwale, A. & Fremling, C. 2021a, Transient Name Server Classification Report, 2021-193, 1
- Dahiwale, A. & Fremling, C. 2021b, Transient Name Server Classification Report, 2021-206, 1
- Dahiwale, A. & Fremling, C. 2021c, Transient Name Server Classification Report, 2021-479, 1
- Dahiwale, A. & Fremling, C. 2021d, Transient Name Server Classification Report, 2021-502, 1
- Dahiwale, A. & Fremling, C. 2021e, Transient Name Server Classification Report, 2021-1234, 1
- Dahiwale, A., Fremling, C., & Dugas, A. 2019b, Transient Name Server Classification Report, 2019-1952, 1
- Dahiwale, A., Fremling, C., & Dugas, A. 2019c, Transient Name Server Classification Report, 2019-1961, 1
- Dahiwale, A., Fremling, C., & Dugas, A. 2019d, Transient Name Server Classification Report, 2019-1985, 1
- Dahiwale, A., Fremling, C., & Dugas, A. 2019e, Transient Name Server Classification Report, 2019-2050, 1
- Dall'Ora, M., Botticella, M. T., Pumo, M. L., et al. 2014, ApJ, 787, 139
- Das, K., Meynardie, W., Chu, M., & Fremling, C. 2023, Transient Name Server Classification Report, 2023-855, 1

- Davis, A. B., Shappee, B. J., Stanek, K. Z., et al. 2014, The Astronomer's Telegram, 6151, 1
- Davis, K. W., Siebert, M. R., Rojas-Bravo, C., et al. 2021, Transient Name Server Classification Report, 2021-3046, 1
- De, K. 2019, Transient Name Server Discovery Report, 2019-2609, 1
- De, K. 2021a, Transient Name Server Discovery Report, 2021-74, 1
- De, K. 2021b, Transient Name Server Discovery Report, 2021-85, 1
- De, K. 2021c, Transient Name Server Discovery Report, 2021-2740, 1
- De, K. 2021d, Transient Name Server Discovery Report, 2021-3802, 1
- De Cia, A., Yaron, O., Vreeswijk, P., et al. 2013, The Astronomer's Telegram, 5249, 1
- de Jaeger, T., Zheng, W., Stahl, B. E., et al. 2019, MNRAS, 490, 2799
- Deckers, M., Dimitriadis, G., Harvey, L., Terwel, J., & Yaron, O. 2021, Transient Name Server Classification Report, 2021-3198, 1
- Delgado, A., Harrison, D., Hodgkin, S., et al. 2017a, Transient Name Server Discovery Report, 2017, 1
- Delgado, A., Harrison, D., Hodgkin, S., et al. 2017b, Transient Name Server Discovery Report, 2017, 1
- Delgado, A., Harrison, D., Hodgkin, S., et al. 2017c, Transient Name Server Discovery Report, 2017, 1
- Delgado, A., Harrison, D., Hodgkin, S., et al. 2019a, Transient Name Server Discovery Report, 2019-613, 1
- Delgado, A., Harrison, D., Hodgkin, S., et al. 2019b, Transient Name Server Discovery Report, 2019-776, 1
- Delgado, A., Harrison, D., Hodgkin, S., et al. 2019c, Transient Name Server Discovery Report, 2019-896, 1
- della Valle, M. & Bianchini, A. 1992, International Astronomical Union Circular, 5558, 3
- Dennefeld, M., Murieta, A. S. D., Magee, M., & Yaron, O. 2023, Transient Name Server Classification Report, 2023-3160, 1
- Desai, D. 2022, Transient Name Server Classification Report, 2022-2064, 1
- Desai, D. D., Ashall, C., Shappee, B. J., et al. 2023, MNRAS, 524, 767
- Dessart, L., Gutiérrez, C. P., Ercolino, A., Jin, H., & Langer, N. 2024, Astronomy & Astrophysics, 685, A169
- Dimai, A., Koff, R. A., Tomasella, L., et al. 2011, Central Bureau Electronic Telegrams, 2887, 2
- Dimitriadis, G. 2019, Transient Name Server Classification Report, 2019-1707, 1
- Dimitriadis, G. & Foley, R. J. 2019, Transient Name Server Classification Report, 2019-389, 1
- Dimitriadis, G., Pan, Y. C., Rojas-bravo, C., & Foley, R. J. 2018, Transient Name Server Classification Report, 2018-196, 1
- Dimitriadis, G., Pursiainen, M., Smith, M., et al. 2016, The Astronomer's Telegram, 9660, 1
- Dimitriadis, G., Siebert, M. R., Taggart, K., Tinyanont, S., & Foley, R. J. 2020, Transient Name Server Classification Report, 2020-2840, 1
- Do, A. 2021, Transient Name Server Classification Report
- Do, A. 2022, Transient Name Server Classification Report, 2022-2394, 1
- Duev, D. 2020a, Transient Name Server Discovery Report, 2020-3660, 1
- Duev, D. 2020b, Transient Name Server Discovery Report, 2020-3685, 1
- Dyer, M. J., Koivisto, N., Davies, B., et al. 2024, Transient Name Server Classification Report, 2024-371, 1
- Ergon, M., Sollerman, J., Fraser, M., et al. 2014, Astronomy Astrophysics, 562, A17
- Evans, R., White, B., & Bembrick, C. 2001, International Astronomical Union Circular, 7772, 1
- Farah, J. R., Howell, D. A., Terreran, G., et al. 2025, ApJ, 984, 60
- Faran, T., Poznanski, D., Filippenko, A. V., et al. 2014, Monthly Notices of the Royal Astronomical Society, 442, 844
- Faran, T., Poznanski, D., Filippenko, A. V., et al. 2014, MNRAS, 445, 554
- Figuero, S., McKinnon, K., Nunez, R., et al. 2022, Transient Name Server Classification Report, 2022-488, 1
- Filippenko, A., Desroches, L., Ganeshalingam, M., Chornock, R., & Serduke, F. 2004, International Astronomical Union Circular, 8331, 2
- Filippenko, A. V. 1988, Astronomical Journal (ISSN 0004-6256), vol. 96, Dec. 1988, p. 1941-1948. Research supported by the University of California., 96, 1941
- Filippenko, A. V., Matheson, T., & Ho, L. C. 1993, ApJ, 415, L103
- Folatelli, G., Bersten, M. C., Benvenuto, O. G., et al. 2014a, The Astrophysical Journal Letters, 793, L22
- Folatelli, G., Bersten, M. C., Kuncarayakti, H., et al. 2014b, The Astrophysical Journal, 792, 7
- Forster, F. 2019a, Transient Name Server Discovery Report, 2019-1575, 1
- Forster, F. 2019b, Transient Name Server Discovery Report, 2019-1609, 1
- Forster, F. 2019c, Transient Name Server Discovery Report, 2019-1647, 1
- Forster, F. 2019d, Transient Name Server Discovery Report, 2019-1653, 1
- Forster, F. 2019e, Transient Name Server Discovery Report, 2019-1758, 1
- Forster, F. 2019f, Transient Name Server Discovery Report, 2019-1962, 1
- Forster, F. 2019g, Transient Name Server Discovery Report, 2019-2073, 1
- Forster, F., Bauer, F. E., Galbany, L., et al. 2020a, Transient Name Server Discovery Report, 2020-1187, 1
- Forster, F., Bauer, F. E., Galbany, L., et al. 2020b, Transient Name Server Discovery Report, 2020-1791, 1
- Forster, F., Bauer, F. E., Munoz-Arcibia, A., et al. 2020c, Transient Name Server Discovery Report, 2020-3526, 1
- Forster, F., Bauer, F. E., Munoz-Arcibia, A., et al. 2020d, Transient Name Server Discovery Report, 2020-3595, 1
- Forster, F., Bauer, F. E., Munoz-Arcibia, A., et al. 2021a, Transient Name Server Discovery Report, 2021-1, 1
- Forster, F., Bauer, F. E., Munoz-Arcibia, A., et al. 2021b, Transient Name Server Discovery Report, 2021-2956, 1
- Forster, F., Bauer, F. E., Pignata, G., et al. 2019a, Transient Name Server Discovery Report, 2019-2392, 1
- Forster, F., Bauer, F. E., Pignata, G., et al. 2019b, Transient Name Server Discovery Report, 2019-2613, 1
- Forster, F., Bauer, F. E., Pignata, G., et al. 2019c, Transient Name Server Discovery Report, 2019-2631, 1
- Forster, F., Bauer, F. E., Pignata, G., et al. 2020e, Transient Name Server Discovery Report, 2020-914, 1
- Forster, F., Bauer, F. E., Pignata, G., et al. 2022, Transient Name Server Discovery Report, 2022-3658, 1
- Forster, F., Munoz-Arcibia, A., Bauer, F. E., et al. 2021c, Transient Name Server Discovery Report, 2021-2396, 1
- Forster, F., Pignata, G., Bauer, F. E., et al. 2023, Transient Name Server Discovery Report, 2023-2574, 1
- Fraser, M., Brennan, S., Gromadzki, M., Ihane, N., & Irani, I. 2019a, Transient Name Server Classification Report, 2019-1571, 1
- Fraser, M., Brennan, S., Gromadzki, M., Ihane, N., & Irani, I. 2019b, Transient Name Server Classification Report, 2019-1587, 1
- Fraser, M., Eappachen, D., Maguire, K., & Jonker, P. 2019c, Transient Name Server Classification Report, 2019-1061, 1
- Fraser, M., Reynolds, T., Inserra, C., & Yaron, O. 2016, Transient Name Server Classification Report, 2016-490, 1
- Fremling, C. 2018a, Transient Name Server Discovery Report, 2018-943, 1
- Fremling, C. 2018b, Transient Name Server Discovery Report, 2018-1048, 1
- Fremling, C. 2019a, Transient Name Server Discovery Report, 2019-586, 1
- Fremling, C. 2019b, Transient Name Server Discovery Report, 2019-778, 1
- Fremling, C. 2019c, Transient Name Server Discovery Report, 2019-1973, 1
- Fremling, C. 2020, Transient Name Server Discovery Report, 2020-3684, 1
- Fremling, C. 2021a, Transient Name Server Discovery Report, 2021-713, 1
- Fremling, C. 2021b, Transient Name Server Discovery Report, 2021-947, 1
- Fremling, C. 2021c, Transient Name Server Discovery Report, 2021-2352, 1
- Fremling, C. 2021d, Transient Name Server Discovery Report, 2021-3248, 1
- Fremling, C. 2021e, Transient Name Server Discovery Report, 2021-3280, 1
- Fremling, C. 2021f, Transient Name Server Discovery Report, 2021-3710, 1
- Fremling, C. 2021g, Transient Name Server Discovery Report, 2021-3950, 1
- Fremling, C. 2022, Transient Name Server Discovery Report, 2022-978, 1
- Fremling, C. 2023a, Transient Name Server Discovery Report, 2023-801, 1
- Fremling, C. 2023b, Transient Name Server Discovery Report, 2023-2133, 1
- Fremling, C. 2023c, Transient Name Server Discovery Report, 2023-2966, 1
- Fremling, C. 2024, Transient Name Server Discovery Report, 2024-12, 1
- Fremling, C. & Dahiwale, A. 2019a, Transient Name Server Classification Report, 2019-1774, 1
- Fremling, C. & Dahiwale, A. 2019b, Transient Name Server Classification Report, 2019-2854, 1
- Fremling, C., Dahiwale, A., & Dugas, A. 2019a, Transient Name Server Classification Report, 2019-1923, 1
- Fremling, C., Dugas, A., & Sharma, Y. 2019b, Transient Name Server Classification Report, 2019-329, 1
- Fremling, C., Dugas, A., & Sharma, Y. 2019c, Transient Name Server Classification Report, 2019-685, 1
- Fremling, C., Dugas, A., & Sharma, Y. 2019d, Transient Name Server Classification Report, 2019-747, 1
- Fremling, C., Dugas, A., & Sharma, Y. 2019e, Transient Name Server Classification Report, 2019-799, 1
- Fremling, C., Dugas, A., & Sharma, Y. 2019f, Transient Name Server Classification Report, 2019-875, 1
- Fremling, C., Dugas, A., & Sharma, Y. 2019g, Transient Name Server Classification Report, 2019-940, 1
- Fremling, C., Dugas, A., & Sharma, Y. 2019h, Transient Name Server Classification Report, 2019-1273, 1
- Fremling, C., Dugas, A., & Sharma, Y. 2019i, Transient Name Server Classification Report, 2019-2831, 1
- Fremling, C., Dugas, A., & Sharma, Y. 2019j, Transient Name Server Classification Report, 2019-1277, 1
- Fremling, C., Sollerman, J., Taddia, F., et al. 2016, A&A, 593, A68
- Fremling, U., Chu, M., Dahiwale, A., & Fremling, C. 2022, Transient Name Server Classification Report, 2022-1684, 1
- Frohmaier, C. 2019, Transient Name Server Classification Report, 2019-397, 1

- Frohmaier, C., Swann, E., Short, P., Nicholl, M., & Yaron, O. 2019, Transient Name Server Classification Report, 2019-990, 1
- Fulton, M., Srivastav, S., Smith, K. W., et al. 2022, Transient Name Server Classification Report, 2022-3299, 1
- Gagliano, R., Post, R., Weinberg, E., Newton, J., & Puckett, T. 2017, Transient Name Server Discovery Report, 2017, 1
- Gal-Yam, A. 2016, arXiv preprint arXiv:1611.09353
- Gal-Yam, A., Bufano, F., Barlow, T., et al. 2008, *The Astrophysical Journal*, 685, L117
- Gal-Yam, A., Nugent, P., Quimby, R., et al. 2011, *The Astronomer's Telegram*, 3403, 1
- Galbany, L., Gutiérrez, C. P., Piscarreta, L., et al. 2025, arXiv preprint arXiv:2501.19108
- Galbany, L., Hamuy, M., Phillips, M. M., et al. 2016, *The Astronomical Journal*, 151, 33
- Galbany, L., Lavers, A. L. C., Stritzinger, M., et al. 2020, Transient Name Server Classification Report, 2020-1269, 1
- Gillanders, J., Srivastav, S., Fulton, M., Shingles, L. J., & Zimmerman, E. 2021, Transient Name Server Classification Report, 2021-49, 1
- Gkini, A., Pessi, P., Brennan, S., et al. 2022a, Transient Name Server Classification Report, 2022-3654, 1
- Gkini, A., Pessi, P., Brennan, S., et al. 2022b, Transient Name Server Classification Report, 2022-3690, 1
- Goldwasser, S., Yaron, O., Sass, A., et al. 2022, Transient Name Server AstroNote, 191, 1
- Gonzalez-Banuelos, M., Kopsacheili, M., Gutierrez, C., & Yaron, O. 2023, Transient Name Server Classification Report, 2023-3017, 1
- González-Gaitán, S., Tominaga, N., Molina, J., et al. 2015, *MNRAS*, 451, 2212
- Graham, M. J., Kulkarni, S. R., Bellm, E. C., et al. 2019, *PASP*, 131, 078001
- Graham, M. L., Dahiwale, A., & Fremling, C. 2020a, Transient Name Server Classification Report, 2020-27, 1
- Graham, M. L., Dahiwale, A., & Fremling, C. 2020b, Transient Name Server Classification Report, 2020-205, 1
- Graham, M. L., Dahiwale, A., & Fremling, C. 2021, Transient Name Server Classification Report, 2021-1157, 1
- Green, D. W. E. 2005a, IAU Circular, 8473
- Green, D. W. E. 2005b, IAU Circular, 8476
- Green, D. W. E. 2006a, Supernova 2006ba in NGC 2980, Electronic Telegram No. 443
- Green, D. W. E. 2006b, Supernova 2006iv in UGC 6774, Electronic Telegram No. 662
- Green, D. W. E. 2006c, Supernova 2006T in NGC 3054, Electronic Telegram No. 385
- Green, D. W. E. 2006d, Supernovae 2006ba, 2006bb, 2006bc, 2006bd, 2006be, 2006bf, Circular No. 8693
- Green, D. W. E. 2006e, Supernovae 2006ek, 2006el, 2006em, Electronic Telegram No. 605
- Green, D. W. E. 2010, Central Bureau Electronic Telegrams
- Green, D. W. E. 2015, Electronic Telegram No. 4198
- Griffith, C., Cenko, S. B., Li, W., & Filippenko, A. V. 2009, Central Bureau Electronic Telegrams, 1685
- Gromadzki, M. & Wyrzykowski, L. 2019, Transient Name Server Discovery Report, 2019-1679, 1
- Groot, P. & Tranin, H. 2024, Transient Name Server Discovery Report, 2024-63, 1
- Gutiérrez, C. P., Anderson, J. P., Hamuy, M., et al. 2017, *The Astrophysical Journal*, 850, 89
- Hamuy, M., Deng, J., Mazzali, P. A., et al. 2009, *The Astrophysical Journal*, 703, 1612
- Hamuy, M., Pinto, P. A., Maza, J., et al. 2001, *The Astrophysical Journal*, 558, 615
- Harmanen, J. 2018, Transient Name Server Classification Report, 2018-231, 1
- Hillier, D. J. & Dessart, L. 2019, *Astronomy & Astrophysics*, 631, A8
- Hinds, K. & Perley, D. 2022, Transient Name Server Classification Report, 2022-1037, 1
- Hinkle, J. 2022, Transient Name Server Classification Report, 2022-2170, 1
- Hinkle, J. 2023, Transient Name Server Classification Report, 2023-1521, 1
- Hiramatsu, D., Arcavi, I., Burke, J., et al. 2018, Transient Name Server Classification Report, 2018, 1
- Hiramatsu, D., Arcavi, I., Burke, J., et al. 2019a, Transient Name Server Classification Report, 2019-1118, 1
- Hiramatsu, D., Arcavi, I., Burke, J., et al. 2019b, Transient Name Server Classification Report, 2019-1572, 1
- Hiramatsu, D., Arcavi, I., Burke, J., et al. 2019c, Transient Name Server Classification Report, 2019-1644, 1
- Hiramatsu, D., Arcavi, I., Howell, D. A., et al. 2019d, Transient Name Server Classification Report, 2019-1522, 1
- Hiramatsu, D., Burke, J., Arcavi, I., et al. 2019e, Transient Name Server Classification Report, 2019-659, 1
- Hiramatsu, D., Howell, D. A., Moriya, T. J., et al. 2021a, *ApJ*, 913, 55
- Hiramatsu, D., Howell, D. A., Moriya, T. J., et al. 2021b, *ApJ*, 913, 55
- Hodgkin, S. T., Breedt, E., Delgado, A., et al. 2023, Transient Name Server Discovery Report, 2023-3152, 1
- Holmbo, S., Stritzinger, M., Karamehmetoglu, E., et al. 2023, *Astronomy & Astrophysics*, 675, A83
- Hoogendam, W. 2023, Transient Name Server Classification Report, 2023-3008, 1
- Hosseinzadeh, G., Arcavi, I., Howell, D. A., McCully, C., & Valenti, S. 2016, Transient Name Server Classification Report, 2016-219, 1
- Hosseinzadeh, G., Arcavi, I., Valenti, S., Howell, D. A., & McCully, C. 2016a, TNS Classification Report, 2016TNSCR.213....1H
- Hosseinzadeh, G., Arcavi, I., Valenti, S., et al. 2016b, Transient Name Server Classification Report, 2016-263, 1
- Hosseinzadeh, G., Valenti, S., Arcavi, I., McCully, C., & Howell, D. A. 2015, *The Astronomer's Telegram*, 7997, 1
- Hosseinzadeh, G., Yang, Y., McCully, C., et al. 2016c, Transient Name Server Classification Report, 2016-162, 1
- Howell, D. A., Sullivan, M., Perrett, K., et al. 2005, *The Astrophysical Journal*, 634, 1190
- Howerton, S., Drake, A., Djorgovski, S., et al. 2013, *Central Bureau Electronic Telegrams*, 3466, 1
- Hu, D., Zhao, Z., Li, Y., et al. 2024, Transient Name Server Discovery Report, 2024-360, 1
- Huang, X.-B., Wang, X.-G., Li, L., et al. 2024, *ApJ*, 970, 103
- Huber, M., Chambers, K. C., Flewelling, H., et al. 2015, *The Astronomer's Telegram*, 7153, 1
- Huber, M. E. 2020, Transient Name Server Classification Report, 2020-3719, 1
- Huber, M. E. 2021a, Transient Name Server Classification Report, 2021-2168, 1
- Huber, M. E. 2021b, Transient Name Server Classification Report, 2021-3294, 1
- Huber, M. E. 2021c, Transient Name Server Classification Report, 2021-3408, 1
- Huber, M. E. 2022a, Transient Name Server Classification Report, 2022-296, 1
- Huber, M. E. 2022b, Transient Name Server Classification Report, 2022-3052, 1
- Hung, T. 2019, Transient Name Server Classification Report, 2019-2038, 1
- Ihanec, N., Wevers, T., Callis, E., Gromadzki, M., & Irani, I. 2019, Transient Name Server Classification Report, 2019-2552, 1
- Inserra, C., Müller-Bravo, T., Gromadzki, M., et al. 2023, ePESSTO+, the advanced Public ESO Spectroscopic Survey of Transient Objects, eSO program IDs 1103.D-0328 and 106.216C; dataset accessed via <https://archive.eso.org/doidownload/script/ePESSTOplus>
- Itagaki, K. 2016, Transient Name Server Discovery Report, 2016, 1
- Itagaki, K. 2017, Transient Name Server Discovery Report, 2017, 1
- Itagaki, K. 2018, Transient Name Server Discovery Report, 2018-1614, 1
- Itagaki, K. 2019, Transient Name Server Discovery Report, 2019-2480, 1
- Itagaki, K. 2020, Transient Name Server Discovery Report, 2020-310, 1
- Itagaki, K., Nakano, S., Matheson, T., et al. 2003, IAU Circular, 8129
- Izzo, L., Malesani, D. B., Kilpatrick, C. D., et al. 2022, Transient Name Server AstroNote, 132, 1
- Jacques, C., Pimentel, E., Monard, L. A. G., et al. 2004, IAU Circular, 8418
- Janka, H.-T., Langanke, K., Marek, A., Martínez-Pinedo, G., & Müller, B. 2007, *Physics Reports*, 442, 38
- Jha, S. 2016, Transient Name Server Classification Report, 2016-699, 1
- Jha, S. W., Jones, D., & Do, A. 2020, Transient Name Server Classification Report, 2020-2050, 1
- Jones, D. O., Dimitriadis, G., Pan, Y. C., & Foley, R. J. 2017, Transient Name Server Classification Report, 2017-1464, 1
- Jones, D. O., French, K. D., Agnello, A., et al. 2022, Transient Name Server Discovery Report, 2022-3453, 1
- Jones, D. O., French, K. D., Agnello, A., et al. 2023, Transient Name Server Discovery Report, 2023-1569, 1
- Kand rashoff, M., Cenko, S., Li, W., & Filippenko, A. 2010, Central Bureau Electronic Telegrams, 2329, 1
- Karambelkar, V., Meynardie, W., Chu, M., & Fremling, C. 2023, Transient Name Server Classification Report, 2023-254, 1
- Kawabata, M. 2018, Transient Name Server Classification Report, 2018-2159, 1
- Khlat, L., Prieto, J. L., & Dong, S. 2018, Transient Name Server Classification Report, 2018-988, 1
- Kilpatrick, C. D., Foley, R. J., Abramson, L. E., et al. 2017, *MNRAS*, 465, 4650
- Kim, M., Zheng, W., Li, W., et al. 2013, *Central Bureau Electronic Telegrams*, 3606, 1
- Kiyota, S., Holoi en, T. W. S., Stanek, K. Z., et al. 2015, *The Astronomer's Telegram*, 6945, 1
- Kopsacheili, M., Gonzalez-Banuelos, M., Gutierrez, C., et al. 2023a, Transient Name Server Classification Report, 2023-3082, 1
- Kopsacheili, M., Gonzalez-Banuelos, M., Gutierrez, C., & Yaron, O. 2023b, Transient Name Server Classification Report, 2023-3005, 1
- Kostrzewska-rutkowska, Z., Callis, E., Fraser, M., & Yaron, O. 2018, Transient Name Server Classification Report, 2018-1212, 1
- Kumar, B., Pandey, S., Sahu, D., et al. 2013, *Monthly Notices of the Royal Astronomical Society*, 431, 308

- Kunkel, W., Madore, B., & Shelton, I. 1987, 4316
- Leadbeater, R. 2018, Transient Name Server Classification Report, 2018-1638, 1
- Leadbeater, R. 2024a, Transient Name Server Classification Report, 2024-811, 1
- Leadbeater, R. 2024b, Transient Name Server Classification Report, 2024-872, 1
- Leaman, J., Li, W., Chornock, R., & Filippenko, A. V. 2011, Monthly Notices of the Royal Astronomical Society, 412, 1419
- Leibundgut, B., Spyromilio, J., Vogl, C., et al. 2019, Transient Name Server Classification Report, 2019-2149, 1
- Leloudas, G., Charalampopoulos, P., Malesani, D., et al. 2019a, Transient Name Server Classification Report, 2019-2141, 1
- Leloudas, G., Charalampopoulos, P., Malesani, D. B., et al. 2019b, Transient Name Server AstroNote
- Leonard, D. & Cenko, S. 2005, The Astronomer's Telegram, 431, 1
- Leonard, D. C., Filippenko, A. V., Gates, E. L., et al. 2001, Publications of the Astronomical Society of the Pacific, 114, 35
- Li, L., Cai, Y., Zhai, Q., et al. 2024, Transient Name Server Classification Report, 2024-724, 1
- Li, L., Zhai, Q., Zhang, J., & Wang, X. 2022, Transient Name Server Classification Report, 2022-25, 1
- Li, L., Zhai, Q., Zhang, J., & Wang, X. 2023, Transient Name Server Classification Report, 2023-2827, 1
- Li, W., Armstrong, M., Boles, T., et al. 2003, IAU Circular, 8245
- Li, W., Cenko, S. B., Filippenko, A. V., & Challis, P. 2009, Central Bureau Electronic Telegrams, 1647
- Li, W., Chornock, R., Leaman, J., et al. 2011a, Monthly Notices of the Royal Astronomical Society, 412, 1473
- Li, W., Leaman, J., Chornock, R., et al. 2011b, Monthly Notices of the Royal Astronomical Society, 412, 1441
- Lin, H., Xiang, D., Rui, L., et al. 2017, Transient Name Server Classification Report, 2017-1488, 1
- Lipunov, V., Shurpakov, S., Denisenko, D., et al. 2014, Central Bureau Electronic Telegrams, 3962, 1
- Liu, Y.-Q., Modjaz, M., Bianco, F. B., & Graur, O. 2016, The Astrophysical Journal, 827, 90
- Lyman, J., Homan, D., Leloudas, G., & Yaron, O. 2017a, Transient Name Server Classification Report, 2017-907, 1
- Lyman, J., Homan, D., Maguire, K., & Yaron, O. 2017b, Transient Name Server Classification Report, 2017-894, 1
- Ma, E., Zheng, W., & Filippenko, A. V. 2019, Transient Name Server Discovery Report, 2019-1728, 1
- Malesani, D. B., Charalampopoulos, P., Angus, C., Izzo, L., & Yaron, O. 2019, Transient Name Server Classification Report, 2019-2284, 1
- Maoz, D., Mannucci, F., Li, W., et al. 2011, Monthly Notices of the Royal Astronomical Society, 412, 1508
- Marion, G. & Berlind, P. 2011, Central Bureau Electronic Telegrams, 2894, 1
- Matheson, T., Challis, P., Kirshner, R., et al. 2003, Supernovae 2003ke, 2003kg, 2003kh, 2003ih, 2003ki, IAU Circular No. 8246, central Bureau for Astronomical Telegrams
- Matheson, T., Filippenko, A. V., Barth, A. J., et al. 2000a, The Astronomical Journal, 120, 1487
- Matheson, T., Filippenko, A. V., Ho, L. C., Barth, A. J., & Leonard, D. C. 2000b, The Astronomical Journal, 120, 1499
- Matheson, T., Filippenko, A. V., Li, W., Leonard, D. C., & Shields, J. C. 2001, The Astronomical Journal, 121, 1648
- Maund, J. R. 2019, The Astrophysical Journal, 883, 86
- Maund, J. R., Fraser, M., Smartt, S. J., et al. 2013, MNRAS, 431, L102
- Maund, J. R., Smartt, S. J., Kudritzki, R. P., Podsiadlowski, P., & Gilmore, G. F. 2004, Nature, 427, 129
- Maza, J., Hamuy, M., Antezana, R., et al. 2010, Central Bureau Electronic Telegrams, 2215
- Medler, K., Mazzali, P. A., Teffs, J., et al. 2022, MNRAS, 513, 5540
- Meza, N., Gromadzki, M., & Yaron, O. 2021, Transient Name Server Classification Report, 2021-3312, 1
- Milisavljevic, D., Fesen, R., Soderberg, A., Pickering, T., & Kotze, P. 2011, Central Bureau Electronic Telegrams, 2902
- Milisavljevic, D., Margutti, R., Soderberg, A. M., et al. 2013a, The Astrophysical Journal, 767, 71
- Milisavljevic, D., Marion, G., Hsiao, E., et al. 2013b, The Astronomer's Telegram, 4943, 1
- Minkowski, R. 1979, in A Source Book in Astronomy and Astrophysics, 1900–1975 (Harvard University Press), 478–480
- Modjaz, M., Blondin, S., Kirshner, R. P., et al. 2014, The Astronomical Journal, 147, 99
- Moller, A., Tucker, B., Zhang, B., et al. 2017, Transient Name Server Discovery Report, 2017, 1
- Monard, L., Childress, M., Scalzo, R., Yuan, F., & Schmidt, B. 2012, Central Bureau Electronic Telegrams, 3201, 1
- Monard, L. A. G. 2009, Central Bureau Electronic Telegrams, 2071
- Monard, L. A. G., Boles, T., Puckett, T., et al. 2004, IAU Circular, 8405
- Moore, T., Ramsden, P., Aamer, A., et al. 2023, Transient Name Server Classification Report, 2023-2869, 1
- Morales-Garoffolo, A., Elias-Rosa, N., Bersten, M., et al. 2015, Monthly Notices of the Royal Astronomical Society, 454, 95
- Morrell, N., Phillips, M., & Folatelli, G. 2007, Central Bureau Electronic Telegrams, 946, 1
- Mostardi, R. & Li, W. 2007, Central Bureau Electronic Telegrams, 905
- Mostardi, R., Li, W., & Filippenko, A. V. 2008, Central Bureau Electronic Telegrams, 1280
- Muller, T., Antilen, J., Wiseman, P., & Yaron, O. 2019, Transient Name Server Classification Report, 2019-2732, 1
- Munoz-Arcancibia, A., Bauer, F. E., Forster, F., et al. 2023a, Transient Name Server Discovery Report, 2023-3204, 1
- Munoz-Arcancibia, A., Bauer, F. E., Forster, F., et al. 2022a, Transient Name Server Discovery Report, 2022-1221, 1
- Munoz-Arcancibia, A., Bauer, F. E., Forster, F., et al. 2024a, Transient Name Server Discovery Report, 2024-599, 1
- Munoz-Arcancibia, A., Bauer, F. E., Forster, F., et al. 2023b, Transient Name Server Discovery Report, 2023-2181, 1
- Munoz-Arcancibia, A., Bauer, F. E., Pignata, G., et al. 2023c, Transient Name Server Discovery Report, 2023-639, 1
- Munoz-Arcancibia, A., Forster, F., Bauer, F. E., et al. 2020a, Transient Name Server Discovery Report, 2020-3652, 1
- Munoz-Arcancibia, A., Forster, F., Bauer, F. E., et al. 2020b, Transient Name Server Discovery Report, 2020-3732, 1
- Munoz-Arcancibia, A., Forster, F., Bauer, F. E., et al. 2020c, Transient Name Server Discovery Report, 2020-3535, 1
- Munoz-Arcancibia, A., Forster, F., Bauer, F. E., et al. 2020d, Transient Name Server Discovery Report, 2020-3558, 1
- Munoz-Arcancibia, A., Forster, F., Bauer, F. E., et al. 2021a, Transient Name Server Discovery Report, 2021-966, 1
- Munoz-Arcancibia, A., Forster, F., Bauer, F. E., et al. 2021b, Transient Name Server Discovery Report, 2021-1986, 1
- Munoz-Arcancibia, A., Forster, F., Bauer, F. E., et al. 2021c, Transient Name Server Discovery Report, 2021-2009, 1
- Munoz-Arcancibia, A., Forster, F., Bauer, F. E., et al. 2021d, Transient Name Server Discovery Report, 2021-2663, 1
- Munoz-Arcancibia, A., Forster, F., Bauer, F. E., et al. 2021e, Transient Name Server Discovery Report, 2021-2944, 1
- Munoz-Arcancibia, A., Forster, F., Bauer, F. E., et al. 2021f, Transient Name Server Discovery Report, 2021-3056, 1
- Munoz-Arcancibia, A., Forster, F., Bauer, F. E., et al. 2022b, Transient Name Server Discovery Report, 2022-2109, 1
- Munoz-Arcancibia, A., Mourao, A., Forster, F., et al. 2024b, Transient Name Server Discovery Report, 2024-687, 1
- Munoz-Arcancibia, A., Pignata, G., Bauer, F. E., et al. 2022c, Transient Name Server Discovery Report, 2022-3638, 1
- Munoz-Arcancibia, A., Pignata, G., Forster, F., et al. 2023d, Transient Name Server Discovery Report, 2023-2154, 1
- Munoz-Arcancibia, A., Pignata, G., Forster, F., et al. 2022d, Transient Name Server Discovery Report, 2022-3637, 1
- Murieta, A. S. D., Dennefeld, M., Magee, M., & Zimmerman, E. A. 2023, Transient Name Server Classification Report, 2023-3190, 1
- Nakano, S. 2014, Central Bureau Electronic Telegrams, 3787, 1
- Nakano, S., Aoki, M., Garnavich, P., Kirshner, R., & Berlind, P. 1996, International Astronomical Union Circular, 6524, 1
- Nakano, S., Aoki, M., Garnavich, P., Kirshner, R., & Stanek, K. 1997, International Astronomical Union Circular, 6724, 1
- Nakano, S., Itagaki, K., Yusa, T., et al. 2014, Central Bureau Electronic Telegrams, 3963, 1
- Nakaoka, T., Kawabata, K. S., Yamanaka, M., Takaki, K., & Kawabata, M. 2016, Transient Name Server Classification Report, 2016-11, 1
- Nakar, E. & Piro, A. L. 2014, ApJ, 788, 193
- Narla, A., Cenko, S. B., Li, W., & Filippenko, A. V. 2009, Central Bureau Electronic Telegrams, 1859
- Narla, A., Cenko, S. B., Li, W., et al. 2011, Central Bureau Electronic Telegrams, 2627
- Nicholl, M., Cartier, R., Pelisoli, I., et al. 2019a, Transient Name Server Classification Report, 2019-693, 1
- Nicholl, M., Ridley, E., Gompertz, B., Galbany, L., & Strotjohann, N. L. 2021, Transient Name Server Classification Report, 2021-2718, 1
- Nicholl, M., Short, P., Angus, C., Muller, T., & Yaron, O. 2019b, Transient Name Server Classification Report, 2019-782, 1
- Nicholl, M., Short, P., Swann, E., et al. 2019c, Transient Name Server Classification Report, 2019-700, 1
- Nissinen, M., Hentunen, V.-P., & Oksanen, A. 2008, Central Bureau Electronic Telegrams, 1324
- Nordin, J., Brinnel, V., Giomi, M., et al. 2019a, Transient Name Server Discovery Report, 2019-141, 1

- Nordin, J., Brinnel, V., Giomi, M., et al. 2019b, Transient Name Server Discovery Report, 2019-236, 1
- Nordin, J., Brinnel, V., Giomi, M., et al. 2019c, Transient Name Server Discovery Report, 2019-278, 1
- Nordin, J., Brinnel, V., Giomi, M., et al. 2019d, Transient Name Server Discovery Report, 2019-335, 1
- Nordin, J., Brinnel, V., Giomi, M., et al. 2019e, Transient Name Server Discovery Report, 2019-409, 1
- Nordin, J., Brinnel, V., Giomi, M., et al. 2019f, Transient Name Server Discovery Report, 2019-891, 1
- Nordin, J., Brinnel, V., Giomi, M., et al. 2019g, Transient Name Server Discovery Report, 2019-1089, 1
- Nordin, J., Brinnel, V., Giomi, M., et al. 2019h, Transient Name Server Discovery Report, 2019-1095, 1
- Nordin, J., Brinnel, V., Giomi, M., et al. 2019i, Transient Name Server Discovery Report, 2019-1116, 1
- Nordin, J., Brinnel, V., Giomi, M., et al. 2019j, Transient Name Server Discovery Report, 2019-1174, 1
- Nordin, J., Brinnel, V., Giomi, M., et al. 2019k, Transient Name Server Discovery Report, 2019-1287, 1
- Nordin, J., Brinnel, V., Giomi, M., et al. 2019l, Transient Name Server Discovery Report, 2019-1330, 1
- Nordin, J., Brinnel, V., Giomi, M., et al. 2019m, Transient Name Server Discovery Report, 2019-1389, 1
- Nordin, J., Brinnel, V., Giomi, M., et al. 2019n, Transient Name Server Discovery Report, 2019-1567, 1
- Nordin, J., Brinnel, V., Giomi, M., et al. 2019o, Transient Name Server Discovery Report, 2019-1585, 1
- Nordin, J., Brinnel, V., Giomi, M., et al. 2019p, Transient Name Server Discovery Report, 2019-1682, 1
- Nordin, J., Brinnel, V., Giomi, M., et al. 2019q, Transient Name Server Discovery Report, 2019-1732, 1
- Nordin, J., Brinnel, V., Giomi, M., et al. 2019r, Transient Name Server Discovery Report, 2019-1958, 1
- Nordin, J., Brinnel, V., Giomi, M., et al. 2019s, Transient Name Server Discovery Report, 2019-1974, 1
- Nordin, J., Brinnel, V., Giomi, M., et al. 2019t, Transient Name Server Discovery Report, 2019-1984, 1
- Nordin, J., Brinnel, V., Giomi, M., et al. 2019u, Transient Name Server Discovery Report, 2019-2243, 1
- Nordin, J., Brinnel, V., Giomi, M., et al. 2019v, Transient Name Server Discovery Report, 2019-2250, 1
- Nordin, J., Brinnel, V., Giomi, M., et al. 2020, Transient Name Server Discovery Report, 2020-1248, 1
- Oates, S. R., Bayless, A. J., Stritzinger, M. D., et al. 2012, MNRAS, 424, 1297
- Onori, F. 2017, Transient Name Server Classification Report, 2017-964, 1
- Onori, F., Cannizzaro, G., Knezevic, N., & Yaron, O. 2017, Transient Name Server Classification Report, 2017-1258, 1
- Östman, L., Nordin, J., Goobar, A., et al. 2011, A&A, 526, A28
- Otero, S. & Buso, V. 2016, Transient Name Server Discovery Report, 2016, 1
- Parker, S. 2016a, Transient Name Server Discovery Report, 2016, 1
- Parker, S. 2016b, Transient Name Server Discovery Report, 2016, 1
- Parker, S., Brimacombe, J., Childress, M., et al. 2014, Central Bureau Electronic Telegrams, 3955, 1
- Parker, S., Kiyota, S., Brimacombe, J., et al. 2013, Central Bureau Electronic Telegrams, 3665, 1
- Parrag, E., Cosentino, S. P., Inserra, C., et al. 2022, Transient Name Server Classification Report, 2022-1385, 1
- Pastorello, A., Pumo, M., Navasardyan, H., et al. 2012, Astronomy & Astrophysics, 537, A141
- Pastorello, A., Zampieri, L., Turatto, M., et al. 2004, Monthly Notices of the Royal Astronomical Society, 347, 74
- Payne, A. V. 2020, Transient Name Server Classification Report, 2020-3799, 1
- Payne, A. V. 2023, Transient Name Server Classification Report, 2023-1646, 1
- Pellegrino, C., Hiramatsu, D., Arcavi, I., et al. 2023, The Astrophysical Journal, 954, 35
- Perley, D. 2019, Transient Name Server Classification Report, 2019-2724, 1
- Perley, D. 2020a, Transient Name Server Classification Report, 2020-3701, 1
- Perley, D. 2020b, Transient Name Server Classification Report, 2020-3779, 1
- Perley, D. 2020c, Transient Name Server Classification Report, 2020-3838, 1
- Perley, D. & Taggart, K. 2019a, Transient Name Server Classification Report, 2019-2661, 1
- Perley, D. & Taggart, K. 2019b, Transient Name Server Classification Report, 2019-2684, 1
- Perley, D. A., Fremling, C., Sollerman, J., et al. 2020, ApJ, 904, 35
- Pessi, P., Anderson, J. P., Galbany, L., & Irani, I. 2020a, Transient Name Server Classification Report, 2020-3741, 1
- Pessi, P., Gkini, A., Brennan, S., et al. 2022, Transient Name Server Classification Report, 2022-3641, 1
- Pessi, P. & Sollerman, J. 2024, Transient Name Server Classification Report, 2024-780, 1
- Pessi, P. J., Anderson, J., Galbany, L., & Yaron, O. 2020b, Transient Name Server Classification Report, 2020-3712, 1
- Pessi, P. J., Folatelli, G., Anderson, J. P., et al. 2019, Monthly Notices of the Royal Astronomical Society, 488, 4239
- Petrushevska, T., Ihane, N., Gromadzki, M., & Yaron, O. 2024, Transient Name Server Classification Report, 2024-110, 1
- Phan, K., Jiménez-Palau, C., Müller, T., & Yaron, O. 2023, Transient Name Server Classification Report, 2023-321, 1
- Phillips, M., Suntzeff, N., Krisciunas, K., et al. 2001, International Astronomical Union Circular, 7772, 2
- Pignata, G., Maza, J., Hamuy, M., et al. 2008, Central Bureau Electronic Telegrams, 1618
- Pignata, G., Maza, J., Hamuy, M., et al. 2009, Central Bureau Electronic Telegrams, 1781
- Pignata, G., Wang, L., Galbany, L., & Yaron, O. 2017, Transient Name Server Classification Report, 2017-623, 1
- Pineda, J., Bruch, R. J., & Yaron, O. 2021, Transient Name Server Classification Report, 2021-4213, 1
- Piranomonte, S., Carini, R., Benetti, S., & Yaron, O. 2019a, Transient Name Server Classification Report, no abstract available
- Piranomonte, S., Carini, R., Melandri, A., D'avanzo, P., & Yaron, O. 2019b, Transient Name Server Classification Report, 2019, 1
- Pollas, C. & Pennypacker, C. 1987, International Astronomical Union Circular, 4426, 1
- Prentice, S., Maguire, K., Skillen, K., Magee, M., & Clark, P. 2019a, Transient Name Server Classification Report, 2019-2675, 1
- Prentice, S., Maguire, K., Skillen, K., Magee, M., & Clark, P. 2019b, Transient Name Server Classification Report, 2019-2705, 1
- Prentice, S. J., Ashall, C., James, P. A., et al. 2019c, MNRAS, 485, 1559
- Prentice, S. J., Magee, M. R., Skillen, P. C. K., & Maguire, K. 2019d, Transient Name Server Classification Report, 2019-1233, 1
- Prentice, S. J., Maguire, K., Skillen, K., Magee, M. R., & Clark, P. 2019e, Transient Name Server Classification Report, 2019-589, 1
- Prentice, S. J., Maguire, K., Skillen, K., Magee, M. R., & Clark, P. 2019f, Transient Name Server Classification Report, 2019-1276, 1
- Prentice, S. J., Maguire, K., Skillen, K., Magee, M. R., & Clark, P. 2019g, Transient Name Server Classification Report, 2019-1214, 1
- Prentice, S. J., Maguire, K., Skillen, K., Magee, M. R., & Clark, P. 2019h, Transient Name Server Classification Report, 2019-1588, 1
- Prentice, S. J., Maguire, K., Skillen, K., Magee, M. R., & Clark, P. 2019i, Transient Name Server Classification Report, 2019-1598, 1
- Prentice, S. J., Maguire, K., Skillen, K., Magee, M. R., & Clark, P. 2019j, Transient Name Server Classification Report, 2019-1645, 1
- Prentice, S. J., Maguire, K., Skillen, K., Magee, M. R., & Clark, P. 2019k, Transient Name Server Classification Report, 2019-2649, 1
- Pugh, H., Park, S., Li, W., et al. 2004, IAU Circular, 8425
- Pun, C. S., Kirshner, R. P., Sonneborn, G., et al. 1995, Astrophysical Journal Supplement v. 99, p. 223, 99, 223
- Quadri, U., Strabla, L., Girelli, R., et al. 2012, Central Bureau Electronic Telegrams, 3054, 1
- Rabinak, I. & Waxman, E. 2011, ApJ, 728, 63
- Ragosta, F., Carini, R., Tartaglia, L., Benetti, S., & Yaron, O. 2021, Transient Name Server Classification Report
- Ragosta, F., Carini, R., Tartaglia, L., Benetti, S., & Yaron, O. 2021, Transient Name Server Classification Report, 2021-4035, 1
- Reguitti, A., Dastidar, R., Pignata, G., et al. 2024, A&A, 692, A26
- Reynolds, T. M., Fraser, M., Mattila, S., et al. 2020, MNRAS, 493, 1761
- Rich, D., Rosebush, J., Sawyer, C., et al. 2013, Central Bureau Electronic Telegrams, 3484, 1
- Ripero, J., Garcia, F., Rodriguez, D., et al. 1993, International Astronomical Union Circular, 5731, 1
- Rodriguez, O., Pignata, G., Gromadzki, M., & Yaron, O. 2019, Transient Name Server Classification Report, 2019-49, 1
- Rojas-Bravo, C., Taggart, K., & Foley, R. J. 2021, Transient Name Server Classification Report, 2021-2290, 1
- Rui, L., Wang, X., Huang, F., Zhang, T., & Zhai, M. 2016, Transient Name Server Classification Report, 2016-13, 1
- Ruiz-Lapuente, P., Kidger, M., Lopez, R., & Canal, R. 1990, Astronomical Journal (ISSN 0004-6256), vol. 100, Sept. 1990, p. 782-787. Research supported by the Delegacion General de Investigacion Cientifica y Tecnologica., 100, 782
- Russiani, M. 2017, Transient Name Server Discovery Report, 2017, 1
- Rybicki, K., Hodgkin, S. T., Fraser, M., Yaron, O., & Knezevic, N. 2017, Transient Name Server Classification Report, 2017-1053, 1
- Ryder, S. D., Sadler, E., Subrahmanyam, R., et al. 2005, in International Astronomical Union Colloquium, Vol. 192, Cambridge University Press, 123–128
- Ryder, S. D., Van Dyk, S. D., Fox, O. D., et al. 2018, The Astrophysical Journal, 856, 83

- Sanders, E., Li, W., et al. 2002, International Astronomical Union Circular, 7944, 2
- Sanders, N. E., Soderberg, A. M., Gezari, S., et al. 2015, The Astrophysical Journal, 799, 208
- Sapir, N. & Waxman, E. 2017, ApJ, 838, 130
- Schlegel, E. M. 1990, MNRAS, 244, 269
- Schmidt, B. P., Kirshner, R. P., Schild, R., et al. 1993, Astronomical Journal (ISSN 0004-6256), vol. 105, no. 6, p. 2236-2250, 2375., 105, 2236
- Schuldt, S., Vogl, C., Taubenberger, S., et al. 2019, Transient Name Server Classification Report, 2019-317, 1
- Schulze, S., Yaron, O., Sollerman, J., et al. 2021, ApJS, 255, 29
- Schwab, M., Kwok, L., Camacho-Neves, Y., Larison, C., & Jha, S. W. 2023, Transient Name Server Classification Report, 2023-1578, 1
- Sheppard, S. S., Fernandez, Y. R., Jewitt, D., et al. 2004, IAU Circular, 8321
- Shigeyama, T., Suzuki, T., Kumagai, S., et al. 1994, Astrophysical Journal, Part 1 (ISSN 0004-637X), vol. 420, no. 1, p. 341-347, 420, 341
- Shingles, L., Smith, K. W., Young, D. R., et al. 2021, Transient Name Server AstroNote, 7, 1
- Shivvers, I., Filippenko, A. V., Silverman, J. M., et al. 2019, MNRAS, 482, 1545
- Shivvers, I., Filippenko, A. V., Silverman, J. M., et al. 2019, Monthly Notices of the Royal Astronomical Society, 482, 1545
- Shivvers, I., Modjaz, M., Zheng, W., et al. 2017, Publications of the Astronomical Society of the Pacific, 129, 054201
- Short, P., Nicholl, M., Muller, T., Angus, C., & Yaron, O. 2019, Transient Name Server Classification Report, 2019-772, 1
- Siebert, M. R., Davis, K., Tinyanont, S., Foley, R. J., & Strasburger, E. 2021a, Transient Name Server Classification Report, 2021-2383, 1
- Siebert, M. R., Davis, K. W., Taggart, K., Tinyanont, S., & Foley, R. J. 2021b, Transient Name Server Classification Report, 2021-2802, 1
- Silverman, J., Cenko, S., Perley, D., et al. 2010, Central Bureau Electronic Telegrams, 2360, 1
- Silverman, J. M., Cenko, S. B., Filippenko, A. V., et al. 2011, Central Bureau Electronic Telegrams, 2736
- Silverman, J. M., Mazzali, P., Chornock, R., et al. 2009, Publications of the Astronomical Society of the Pacific, 121, 689
- Singer, D., Burkett, J., Li, W., & Armstrong, M. 2004, IAU Circular, 8335
- Singh, A., Sahu, D., Anupama, G., et al. 2019, The Astrophysical Journal Letters, 882, L15
- Sit, T. 2022, Transient Name Server Classification Report, no abstract available
- Sit, T. 2022, Transient Name Server Classification Report, 2022-2319, 1
- Skvarc, J. & Mikuz, H. 2008, Central Bureau Electronic Telegrams, 1493
- Smartt, S., Eldridge, J., Crockett, R., & Maund, J. 2009, Monthly Notices of the Royal Astronomical Society, 395, 1409
- Smartt, S. J., Dobson, M., Vogl, C., et al. 2019, Transient Name Server Classification Report, 2019-2416, 1
- Smartt, S. J., Maund, J. R., Hendry, M. A., et al. 2004, Science, 303, 499
- Smartt, S. J., Valenti, S., Fraser, M., et al. 2015, Astronomy & Astrophysics, 579, A40
- Smith, K., Cikota, A., Magee, M., Inserra, C., & Yaron, O. 2016, Transient Name Server Classification Report, 2016-1065, 1
- Smith, K. W., Williams, R. D., Young, D. R., et al. 2019, Research Notes of the American Astronomical Society, 3, 26
- Smith, M., Fraser, M., Anderson, J., et al. 2015, The Astronomer's Telegram, 7214, 1
- Smith, M., Moller, A., Amenouche, M., Angus, C., & Pursiainen, M. 2020a, Transient Name Server Classification Report, 2020-497, 1
- Smith, K. W. aryd Smartt, S. J., Young, D. R., Tonry, J. L., et al. 2020b, arXiv e-prints, arXiv:2003.09052
- Sollerman, J., Chu, M., Dahiwale, A., & Fremling, C. 2024a, Transient Name Server Classification Report, 2024-734, 1
- Sollerman, J., Covarrubias, S., Meynardie, W., Chu, M., & Fremling, C. 2024b, Transient Name Server Classification Report, 2024-176, 1
- Sollerman, J., Yang, S., Schulze, S., et al. 2021, A&A, 655, A105
- Spiro, S., Pastorello, A., Pumo, M., et al. 2014, Monthly Notices of the Royal Astronomical Society, 439, 2873
- Srivastav, S., Fulton, M., Moore, T., & Yaron, O. 2022, Transient Name Server Classification Report, 2022-667, 1
- Srivastav, S., Moore, T., Smith, K. W., Fulton, M., & Bruch, R. J. 2023, Transient Name Server Classification Report, 2023-83, 1
- Srivastav, S., Smartt, S. J., McBrien, O., Smith, K. W., & Young, D. R. 2020, Transient Name Server Classification Report, 2020-346, 1
- Srivastav, S., Smartt, S. J., McBrien, O., et al. 2021, Transient Name Server Classification Report
- Srivastav, S., Smartt, S. J., McBrien, O., et al. 2021, Transient Name Server Classification Report, 2021-16, 1
- Stanek, K. & Bersier, D. 2016, Transient Name Server Discovery Report, 2016, 1
- Stanek, K., Bock, S., Shappee, B., et al. 2016a, Transient Name Server Discovery Report, 2016, 1
- Stanek, K., Brown, J., Holoién, T., et al. 2016b, Transient Name Server Discovery Report, 2016, 1
- Stanek, K. Z. 2018, Transient Name Server Discovery Report, 2018-136, 1
- Stanek, K. Z. 2018, Transient Name Server Discovery Report, no abstract available
- Stanek, K. Z. 2018, Transient Name Server Discovery Report, 2018-1202, 1
- Stanek, K. Z. 2019a, Transient Name Server Discovery Report, 2019-2, 1
- Stanek, K. Z. 2019b, Transient Name Server Discovery Report, 2019-309, 1
- Stanek, K. Z. 2019c, Transient Name Server Discovery Report, 2019-643, 1
- Stanek, K. Z. 2019d, Transient Name Server Discovery Report, 2019-1053, 1
- Stanek, K. Z., Bersier, D., & Kochanek, C. S. 2019, Transient Name Server Discovery Report, 2019-766, 1
- Stanek, K. Z. & Kochanek, C. S. 2019, Transient Name Server Discovery Report, 2019-686, 1
- Stanek, K. Z. & Valley, P. 2019, Transient Name Server Discovery Report, 2019-954, 1
- Stone, G., Brimacombe, J., & Stanek, K. Z. 2018, Transient Name Server Discovery Report, 2018-645, 1
- Stritzinger, M. & Holmbo, S. 2019, Transient Name Server Classification Report, 2019-574, 1
- Stritzinger, M., Morrell, N., Pignata, G., et al. 2011, Central Bureau Electronic Telegrams, 2777
- Stritzinger, M., Taddia, F., Burns, C., et al. 2018, Astronomy & Astrophysics, 609, A135
- Stritzinger, M. D., Holmbo, S., Morrell, N., et al. 2023, A&A, 675, A82
- Swann, E., Frohmaier, C., Nicholl, M., Short, P., & Yaron, O. 2019a, Transient Name Server Classification Report, 2019-902, 1
- Swann, E., Frohmaier, C., Nicholl, M., Short, P., & Yaron, O. 2019b, Transient Name Server Classification Report, 2019-959, 1
- Swann, E., Frohmaier, C., Nicholl, M., Short, P., & Yaron, O. 2019c, Transient Name Server Classification Report, 2019-963, 1
- Szalai, T., Vinkó, J., Könöves-Tóth, R., et al. 2019, ApJ, 876, 19
- Szalai, T., Vinkó, J., Nagy, A. P., et al. 2016, MNRAS, 460, 1500
- Taddia, F., Barbarino, C., Karamehmetoglu, E., et al. 2017, Transient Name Server Classification Report, 2017-158, 1
- Taddia, F., Johansson, J., Leloudas, G., et al. 2014, The Astronomer's Telegram, 5813, 1
- Taddia, F., Sollerman, J., Fremling, C., et al. 2016, Astronomy & Astrophysics, 588, A5
- Taddia, F., Stritzinger, M. D., Sollerman, J., et al. 2012, A&A, 537, A140
- Taggart, K., Davis, K., & Foley, R. 2023, Transient Name Server Classification Report, 2023-652, 1
- Taguchi, K. & Maeda, K. 2023, Transient Name Server Classification Report, 2023-2163, 1
- Taguchi, K. & Maeda, K. 2024, Transient Name Server Classification Report, 2024-590, 1
- Taubenberger, S., Navasardyan, H., Maurer, J. I., et al. 2011, MNRAS, 413, 2140
- Teja, R. S., Singh, A., Sahu, D. K., et al. 2023, ApJ, 954, 155
- Teja, R. S., Singh, A., Sahu, D. K., et al. 2022, ApJ, 930, 34
- Terreran, G., Howell, D. A., McCully, C., et al. 2023a, Transient Name Server Classification Report, 2023-3376, 1
- Terreran, G., Jerkstrand, A., Benetti, S., et al. 2016, MNRAS, 462, 137
- Terreran, G., Pellegrino, C., Howell, D. A., et al. 2023b, Transient Name Server Classification Report, 2023-2212, 1
- Tinyanont, S., Ridden-Harper, R., Foley, R., et al. 2022, Monthly Notices of the Royal Astronomical Society, 512, 2777
- Tody, D. 1986, in Instrumentation in astronomy VI, Vol. 627, SPIE, 733–748
- Tody, D. 1993, in Astronomical Data Analysis Software and Systems II, Vol. 52, 173
- Tomasella, L. 2017a, Transient Name Server Classification Report, 2017-476, 1
- Tomasella, L. 2017b, Transient Name Server Classification Report, 2017-1459, 1
- Tomasella, L. 2019, Transient Name Server Classification Report, 2019-51, 1
- Tomasella, L., Benetti, S., Cappellaro, E., & Turatto, M. 2019, Transient Name Server Classification Report, 2019-1120, 1
- Tomasella, L., Benetti, S., Pastorello, A., et al. 2013, The Astronomer's Telegram, 4989, 1
- Tomasella, L., Pastorello, A., Valenti, S., & Benetti, S. 2011a, Central Bureau Electronic Telegrams, 2887
- Tomasella, L., Valenti, S., Ochner, P., et al. 2011b, Central Bureau Electronic Telegrams, 2827
- Tonry, J., Denneau, L., Heinze, A., et al. 2019a, Transient Name Server Discovery Report, 2019-21, 1
- Tonry, J., Denneau, L., Heinze, A., et al. 2019b, Transient Name Server Discovery Report, 2019-77, 1
- Tonry, J., Denneau, L., Heinze, A., et al. 2019c, Transient Name Server Discovery Report, 2019-109, 1
- Tonry, J., Denneau, L., Heinze, A., et al. 2019, Transient Name Server Discovery Report, 2019-138, 1

- Tonry, J., Denneau, L., Weiland, H., et al. 2024c, Transient Name Server Discovery Report, 2024-540, 1
- Tonry, J., Denneau, L., Weiland, H., et al. 2024d, Transient Name Server Discovery Report, 2024-585, 1
- Tonry, J., Denneau, L., Weiland, H., et al. 2024e, Transient Name Server Discovery Report, 2024-612, 1
- Tonry, J., Denneau, L., Weiland, H., et al. 2024f, Transient Name Server Discovery Report, 2024-701, 1
- Tonry, J., Stalder, B., Denneau, L., et al. 2017a, Transient Name Server Discovery Report, 2017, 1
- Tonry, J., Stalder, B., Denneau, L., et al. 2017b, Transient Name Server Discovery Report, 2017, 1
- Tonry, J., Stalder, B., Denneau, L., et al. 2017c, Transient Name Server Discovery Report, 2017, 1
- Tonry, J., Stalder, B., Denneau, L., et al. 2018a, Transient Name Server Discovery Report, 2018-662, 1
- Tonry, J., Stalder, B., Denneau, L., et al. 2018b, Transient Name Server Discovery Report, 2018-1195, 1
- Tonry, J. L., Denneau, L., Heinze, A. N., et al. 2018c, Publications of the Astronomical Society of the Pacific, 130, 064505
- Tsuboi, M. 2016, Transient Name Server Discovery Report, 2016-201, 1
- Tucker, M. A. 2021a, Transient Name Server Classification Report, 2021-1718, 1
- Tucker, M. A. 2021b, Transient Name Server Classification Report, 2021-3941, 1
- Tucker, M. A. 2023a, Transient Name Server Classification Report, 2023-7, 1
- Tucker, M. A. 2023b, Transient Name Server Classification Report, 2023-1738, 1
- Tucker, M. A. 2023c, Transient Name Server Classification Report, 2023-1945, 1
- Tucker, M. A. 2023d, Transient Name Server Classification Report, 2023-2787, 1
- Tucker, M. A., Payne, A. V., Do, A., Huber, M. E., & Shappee, B. J. 2019a, Transient Name Server Classification Report, 2019-98, 1
- Tucker, M. A., Payne, A. V., Do, A., Huber, M. E., & Shappee, B. J. 2019b, Transient Name Server Classification Report, 2019-783, 1
- Tucker, M. A., Payne, A. V., Do, A., Huber, M. E., & Shappee, B. J. 2019c, Transient Name Server Classification Report, 2019-1109, 1
- Tucker, M. A. & Shappee, B. J. 2018, Transient Name Server Classification Report, 2018-1209, 1
- Valenti, S., Sand, D., Pastorello, A., et al. 2013, Monthly Notices of the Royal Astronomical Society: Letters, 438, L101
- Valenti, S., Sand, D., Pastorello, A., et al. 2014, MNRAS, 438, L101
- Vallely, P. 2019a, Transient Name Server Discovery Report, 2019-554, 1
- Vallely, P. 2019b, Transient Name Server Discovery Report, 2019-893, 1
- Van der Maaten, L. & Hinton, G. 2008, Journal of machine learning research, 9
- Van Dyk, S. D., Li, W., & Filippenko, A. V. 2003, Publications of the Astronomical Society of the Pacific, 115, 1289
- Van Dyk, S. D., Zheng, W., Fox, O. D., et al. 2014, The Astronomical Journal, 147, 37
- Vincenzi, M., Sullivan, M., Firth, R., et al. 2019, Monthly Notices of the Royal Astronomical Society, 489, 5802
- Wang, Q., Armstrong, P., Zenati, Y., et al. 2023, ApJ, 943, L15
- Weinberg, E., Post, R., & Puchett, T. 2019, Transient Name Server Discovery Report, 2019-1086, 1
- Wiggins, P. 2017, Transient Name Server Discovery Report, 2017, 1
- Wiggins, P. 2018, Transient Name Server Discovery Report, 2018-53, 1
- Williamson, M., Vogl, C., Modjaz, M., et al. 2023, ApJ, 944, L49
- Wise, J., Hinds, K., & Perley, D. 2023, Transient Name Server Classification Report, 2023-832, 1
- Wiseman, P., Angus, C., Frohmaier, C., Swann, E., & Irani, I. 2019, Transient Name Server Classification Report, 2019, 1
- Wood-Vasey, W., Aldering, G., Nügent, P., & Chassagne, R. 2003, IAU Circular, 8082, 1
- Woosley, S., Eastman, R. G., Weaver, T. A., & Pinto, P. A. 1994, The Astrophysical Journal, Part 1 (ISSN 0004-637X), vol. 429, no. 1, p. 300-318, 429, 300
- Wyatt, S., Sand, D., Andrews, J., Daly, P., & Hosseinzadeh, G. 2021, Transient Name Server Classification Report, 2021-3458, 1
- Xu, Z., Xu, J., Tan, H., Sun, G., & Gao, X. 2016, Transient Name Server Discovery Report, 2016, 1
- Xu, Z.-j., Gao, X., Brimacombe, J., Zhang, J.-j., & Wang, X.-f. 2014, Central Bureau Electronic Telegrams, 4010, 1
- Yaron, O. & Gal-Yam, A. 2012, Publications of the Astronomical Society of the Pacific, 124, 668
- Yaron, O., Gal-Yam, A., Schulze, S., & Sollerman, J. 2021, Transient Name Server Classification Report, 2021-2567, 1
- Yuan, F., Quimby, R., Chamarro, D., et al. 2008, Central Bureau Electronic Telegrams, 1395
- Zhai, Q., Zhang, J., Li, W., & Wang, X. 2022, Transient Name Server Classification Report, 2022-3168, 1
- Zhang, J. & Wang, X. 2016, Transient Name Server Classification Report, 2016-27, 1
- Zhang, J., Yin, Y., Wang, X., et al. 2020, Transient Name Server Classification Report, 2020-932, 1
- Zheng, W. & Filippenko, A. V. 2015, The Astronomer's Telegram, 7366, 1
- Zimmerman, E., Adams, W., & Irani, I. 2023, Transient Name Server Discovery Report, 2023-2178, 1
- Zwitter, T., Munari, U., Moretti, S., et al. 2004, IAU Circular, 8413

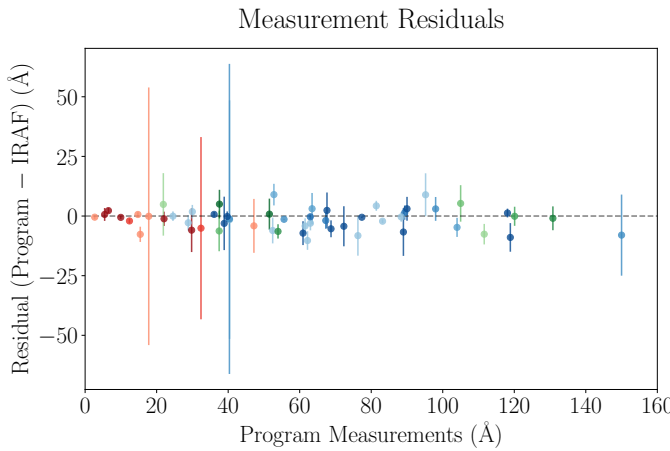


Fig. A.1. Residuals between the pEW and FWHM values measured with our interactive program and those obtained with IRAF are shown as (program – IRAF) plotted against the programme-derived values. Data points are colour-coded by SN type: SNe II are shown in warm colours, while SNe IIb are in cool tones. Different colours represent different SNe.

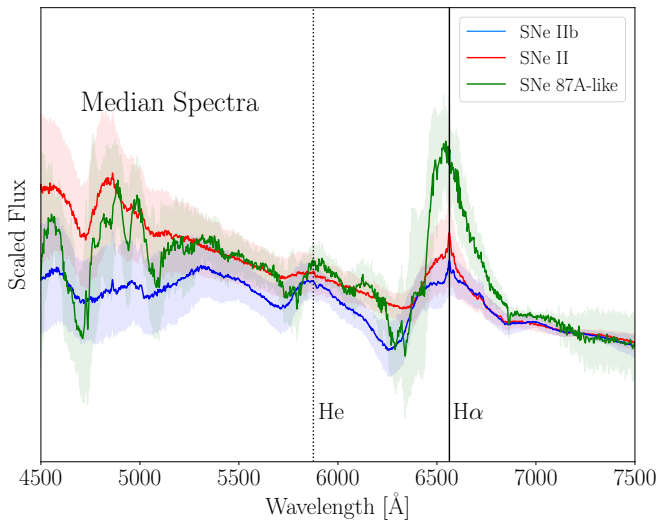


Fig. A.2. Comparison between the median spectrum for SNe II (red), SNe IIb (blue) and SN 87A-like (green) constructed from all spectra in our sample (from explosion to 40 days post-explosion). The shaded regions represent the Median Absolute Deviation (MAD), providing a measure of dispersion around the median.

Appendix A: Figures

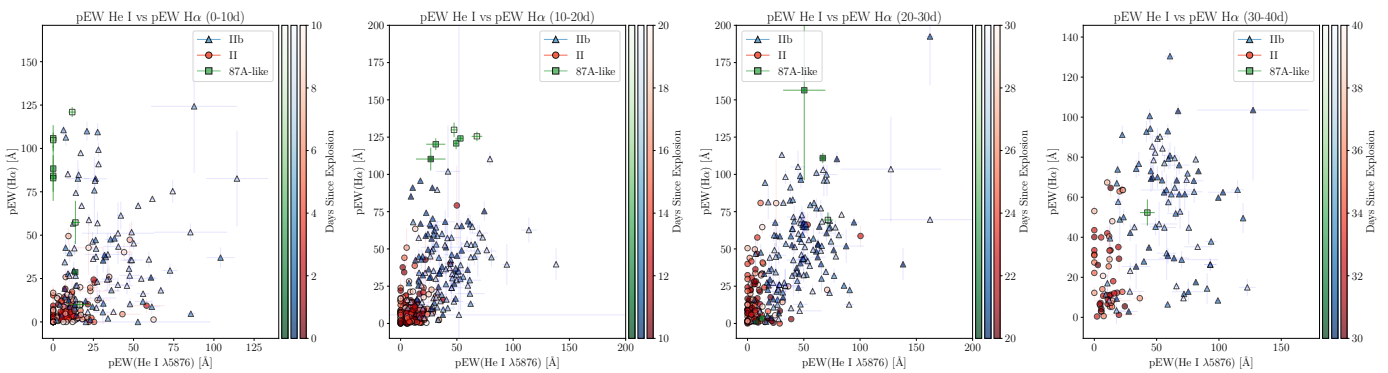


Fig. A.3. pEW values of the H α vs the same measurements for He I λ 5876 for separated time ranges since explosion: 0-10 days, 10-20 days, 20-30 days and 30-40 days. The markers are established by SN type, corresponding to the type SNe IIb, the blue triangles, SNe II, the red circles and SNe 87A-like, the green squares. The colour bars show how the colour intensity changes depending on the number of days since the explosion.

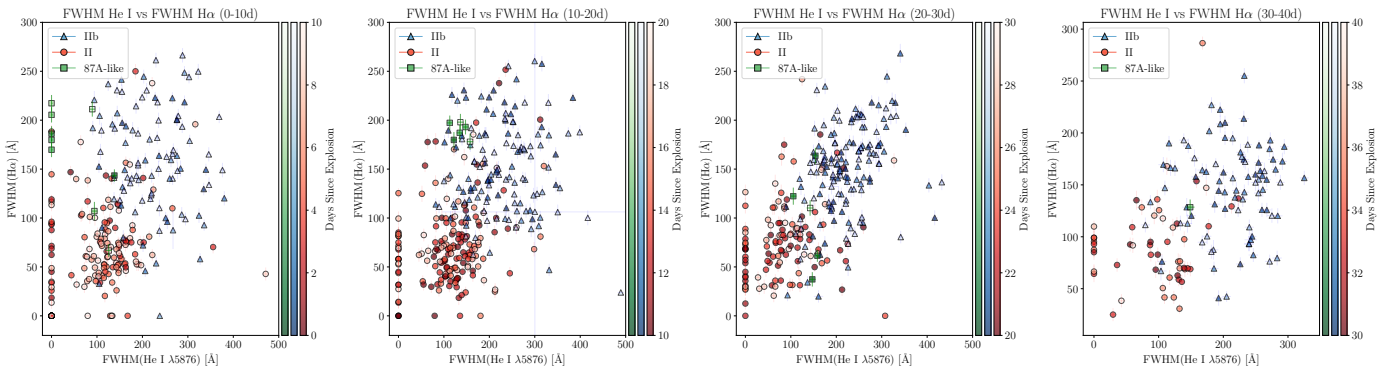


Fig. A.4. FWHM of the H α (λ 6563) line vs the same measurements for the He I (λ 5876) line for separated time ranges since explosion: 0-10 days, 10-20 days, 20-30 days and 30-40 days. The markers are established by SN type, corresponding to the type SNe IIb, the blue triangles, SNe II, the red circles and SNe 87A-like, the green squares. The colour bars show how the colour intensity changes depending on the number of days since the explosion.

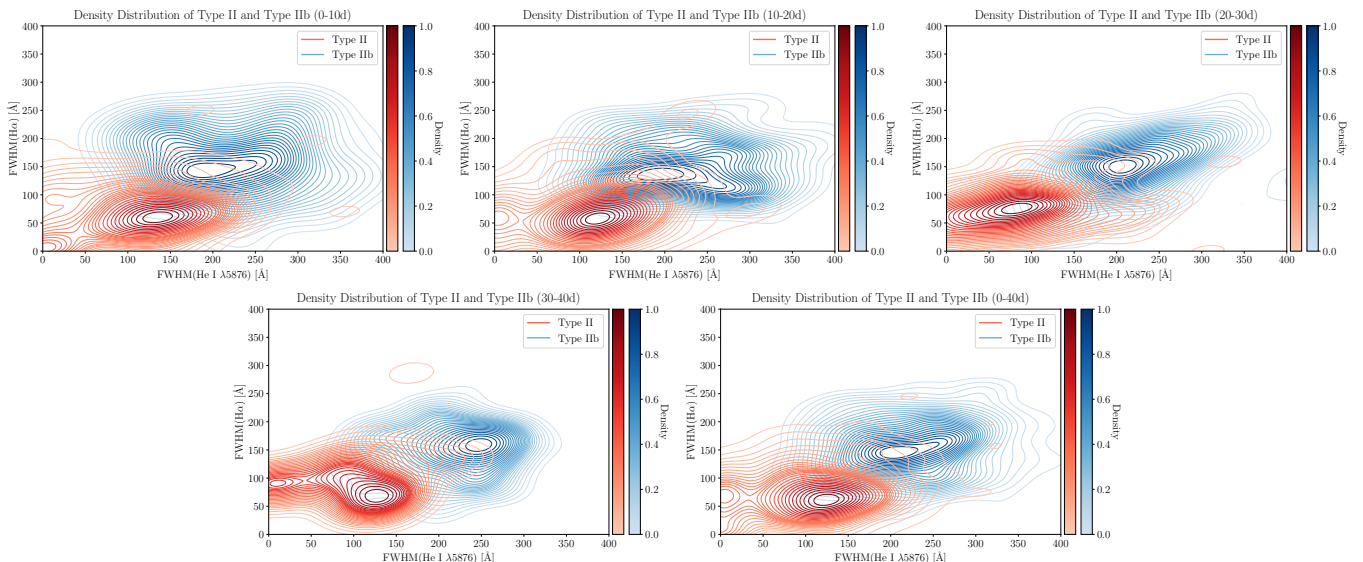


Fig. A.5. The density distribution of type II (in red) and IIb (in blue) population of our sample based on the FWHM measurements. We present the distribution for the different time ranges that we have analysed.

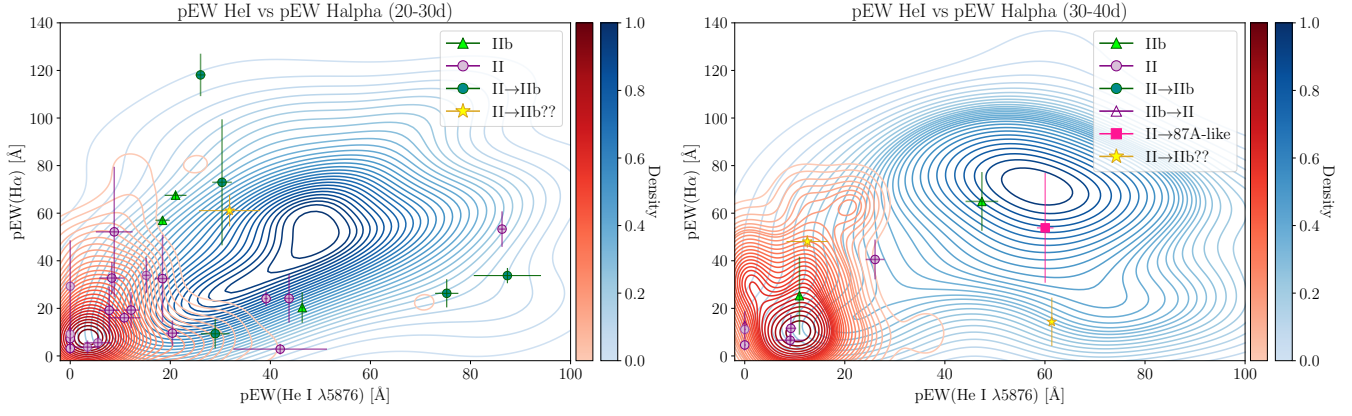


Fig. A.6. The density contours of the pEW along with the SEDM and the new classified SNe used as test sample for 20-30 and 30-40 days after explosion. The comparison sample is represented by SNe II as filled purple dots and SNe IIb as filled green triangles. Dark green circles correspond to SNe initially classified as Type II but exhibiting SNe IIb-like properties. Open purple triangles represent SNe initially classified as Type IIb but spectroscopically belonging to the SN II class. Pink squares denote Type II SNe showing 87A-like characteristics. Yellow stars highlight Type II SNe that appear to exhibit SNe IIb characteristics but lack sufficient data to confirm this classification.

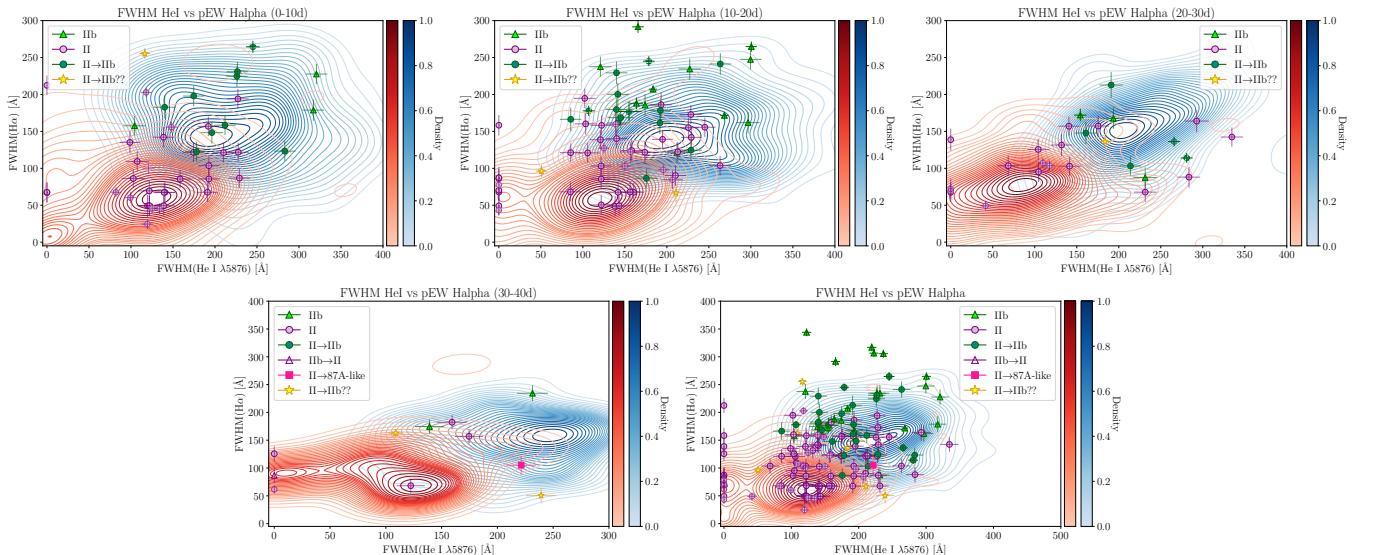


Fig. A.7. The density contours of the FWHM along with the SEDM and the new classified SNe used as test sample, are shown. The comparison sample is represented by SNe II as filled purple dots and SNe IIb as filled green triangles. Dark green circles correspond to SNe initially classified as Type II but exhibiting SNe IIb-like properties. Open purple triangles represent SNe initially classified as Type IIb but spectroscopically belonging to the SN II class. Pink squares denote Type II SNe showing 87A-like characteristics. Yellow stars highlight Type II SNe that appear to exhibit SNe IIb characteristics but lack sufficient data to confirm this classification.

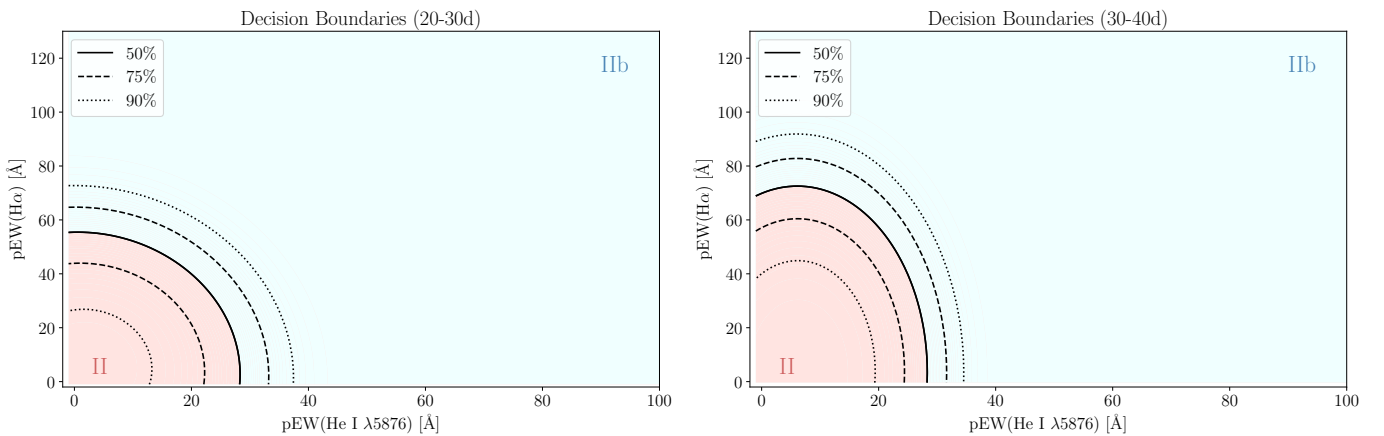


Fig. A.8. The decision boundaries defined by the QDA based on the measures performed for the II and IIb pEW for the following time ranges 20-30 days and 30-40 days after the explosion. The red region corresponds to the type II SNe, and the blue region to the IIb SNe.

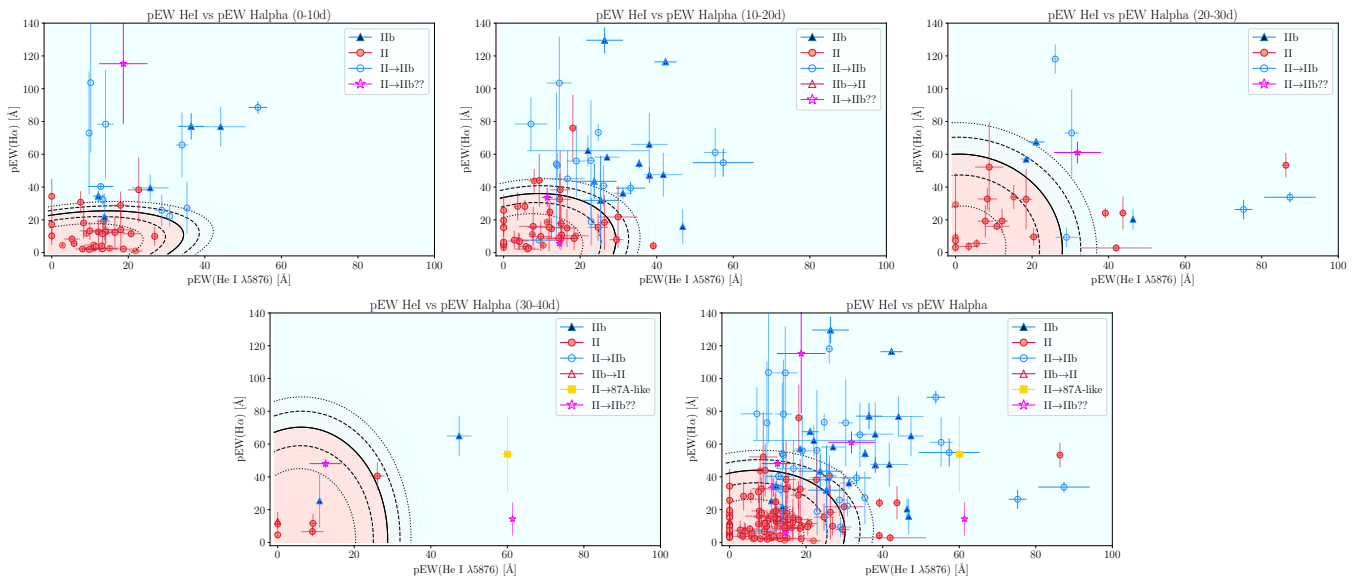


Fig. A.9. The ranges defined by QDA based on the measures performed for the II and IIb pEW along with the SEDM and the new classified SNe. The closed red dots mark the type II data points, the closed blue triangles the type IIb and the yellow square a 87A-like. The open markers are those that have been reclassified based on our method. So the open blue circles belong to the SNe that were first classified as type II and then reclassified as IIb. The open red triangles are those first classified as IIb and then reclassified as II in this work. The purple open stars are SNe classified as II that seem to exhibit characteristics of IIb but could not be confirmed. In Table B.2 are presented plotted spectra with their old and new classifications.

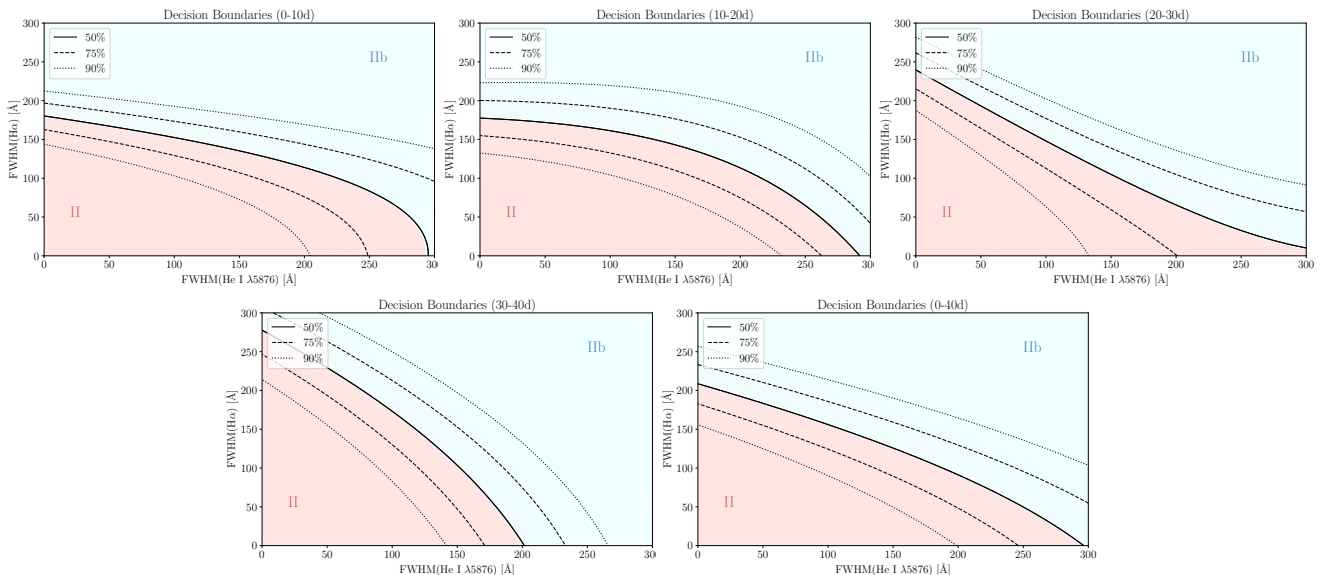


Fig. A.10. Decision boundaries defined by the QDA classifier based on the measures performed for the FWHM of SNe II and IIb at all the analysed time intervals. The red region corresponds to the SNe II, and the blue region to SNe IIb.

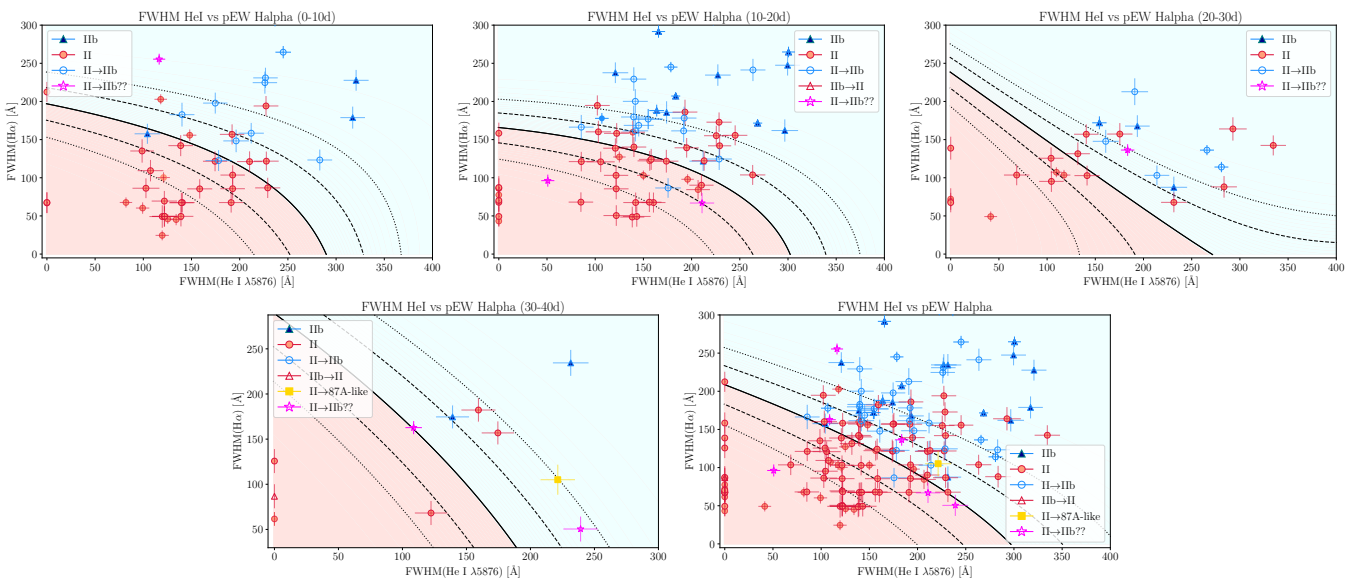


Fig. A.11. The ranges defined by QDA based on the measures performed for the II and IIb FWHM, along with the SEDM and the new classified SNe. The closed red dots mark the type II data points, the closed blue triangles the type IIb and the yellow square a 87A-like. The open markers are those that have been reclassified based on our method. So the open blue circles belong to the SNe that were first classified as type II and then reclassified as IIb. The open red triangles are those first classified as IIb and then reclassified as II in this work. The purple open stars are SNe classified as II that seem to exhibit characteristics of IIb but could not be confirmed. In Table B.2 are presented plotted spectra with their old and new classifications.

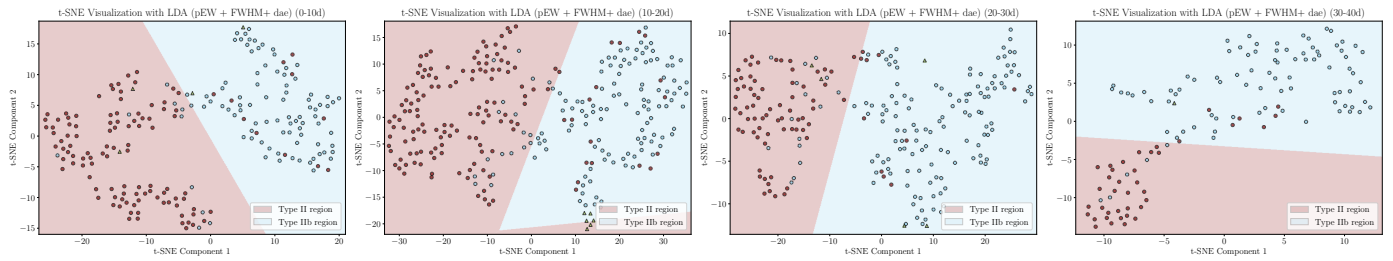


Fig. A.12. The projection of t-SNE with a perplexity value of 20, along with a LDA analysis of the obtained 2D plot for all the analysed time ranges.

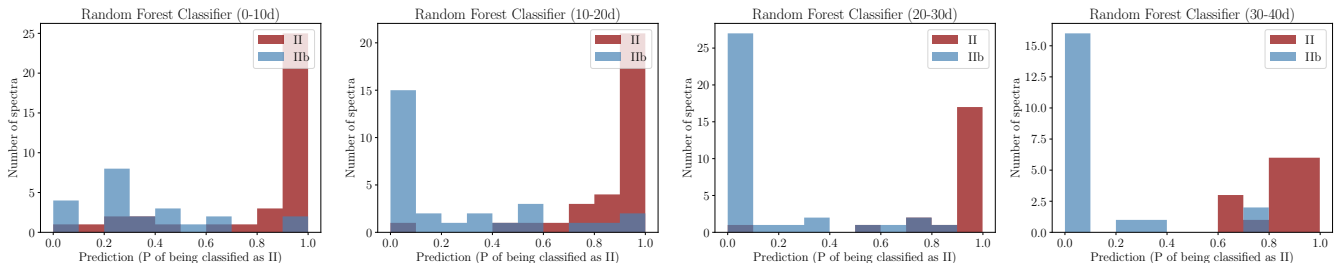


Fig. A.13. Probabilities given by the Random Forest Classifier for supernova spectra, with the data split into four time ranges after the explosion: 0–10 days, 10–20 days, 20–30 days, and 30–40 days. The classifier uses the pEW, FWHM, epoch, and type of each SN spectrum as input parameters, with 60% of the total sample used for training and the remaining 40% for testing. The red and blue bins correspond to SNe II and IIb, respectively.

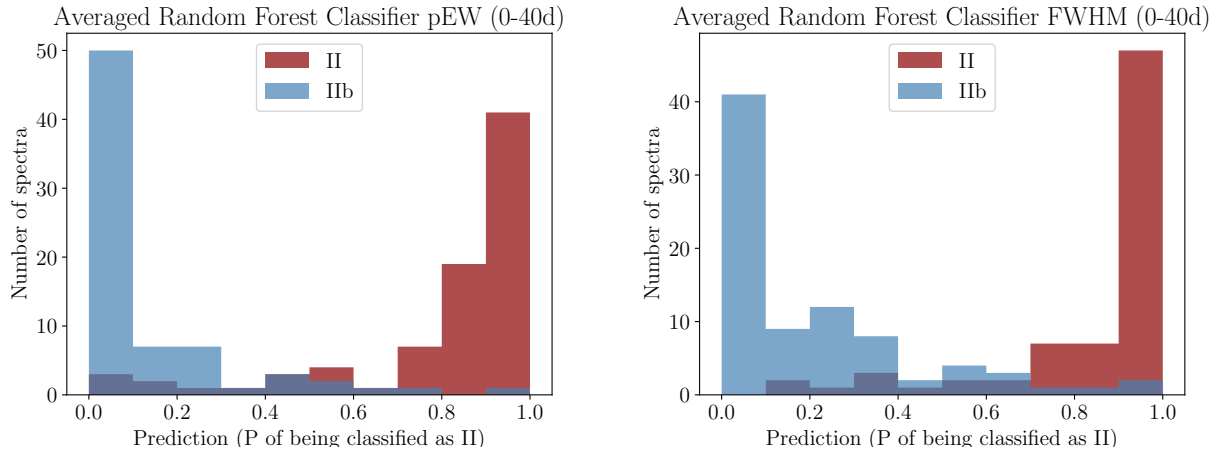


Fig. A.14. **Left panel:** Probabilities given by the Random Forest Classifier for the whole sample, taking into account the pEW measurements for all the spectra within the first 40 days after the explosion the SN, using %60 of the total sample as training sample and the rest as test sample. **Right panel:** Probabilities given by the Random Forest Classifier for the whole sample, taking into account only the FWHM measurements for all the spectra within the first 40 days after the explosion, using %60 of the total sample as training sample and the rest as test sample. The red and blue bins correspond to SNe II and IIb, respectively.

Appendix B: Tables

Table B.1. SNe with lower resolution data

SNe	Classification	SNe	Classification
2016csv	II	2020rmk*	II
2016hgm	II	2020sy	II
2017aub	II	2020tjd*	IIb
2017fys	II	2020uhm	II
2018aex	II	2020urc	IIb
2018amc	II	2020uzx	II
2018dfc	II	2020xcu	II
2018dfi*	II	2020xhs	II
2018fpk	II	2021acma	II
2018ghj	II	2021adlr	II
2018hhs	IIb	2021bkb*	II
2018hmx*	II	2021cah	II
2018hoa	II	2021dru*	II
2018hqt*	II	2021ech	II
2018iby*	II	2021kum	IIb
2018iis	II	2021kww	IIb
2018iwe	II	2021lwd	IIb
2018jbr	II	2021msa*	II
2018kne	II	2021omy*	II
2019bir	II	2021tcv*	II
2019bsq	II	2021uth	IIb
2019cec	II	2021wvz	II
2019cjx*	II	2021xat	II
2019eji	II	2021yke	II
2019ejo	II	2022aasd	II
2019gaf	IIb	2022aber	II
2019hgu	II	2022acri	II
2019hnl	II	2022adtr	IIb
2019hnz	II	2022aek	II
2019hqm	II	2022alw	II
2019hvg*	II	2022ces	II
2019jyw	II	2022hql	II
2019lbi	II	2022irp	II
2019lkx	II	2022lmf	II
2019mfu	II	2022nzs	II
2019noj*	II	2022pxu	II
2019ofk	IIb	2022rgd	II
2019pjs	II	2022sxm	II
2019ply*	II	2022uop*	II
2019rms	II	2022vym	II
2019sgs	II	2022wc*	II
2019sna	IIb	2022ycs*	II
2019szo	II	2022yeg	II
2019wzh	II	2022zjt	II
2019xhb*	II	2022zxt	II
2020aabm	II	2023abdq	II
2020adnx	IIb	2023cf	II
2020boz*	II	2023gwl	IIb
2020cd	II	2023qec	II
2020chy*	II	2023rky*	II
2020cw*	II	2023wf	IIb
2020dyu	II	2023zzk*	II
2020jfo	II	2024frf*	II

The SNe marked with * are those that were reclassified (see Table B.2).

Table B.2. Reclassified SEDM spectra based on the regions we defined.

SNe	Phase (days after explosion)	Initial class.	This work	RF probabilities		
				II	IIb	87A-like
2018dfi	27	II	IIb	0.28	0.72	0.00
2018hmx	5	II	IIb	0.31	0.69	0.00
2018hqt	15	II	II->IIb? (MC: 100.0% II; 0.0% IIb)	0.93	0.05	0.02
2018iby	15	II	IIb	0.22	0.78	0.00
2019cjx	20	II	IIb	0.56	0.40	0.04
2019hvg	5	II	IIb	0.21	0.79	0.00
2019noj	40	II	II->IIb? (MC: 0.0% II; 100.0% IIb)	0.21	0.79	0.00
2019ply	6	II	IIb	0.26	0.71	0.03
2019xhb	17	II	IIb	0.05	0.93	0.02
2020boz	17	II	IIb	0.0	1.0	0.00
2020chy	13	II	IIb	0.07	0.93	0.0
2020cwy	16	II	IIb	0.67	0.33	0.00
2020rmk	35	II	87A-like	0.00	1.00	0.00
2020tjd	34	IIb	II	1.00	0.00	0.00
2021bkb	21	II	IIb	0.00	1.0	0.0
2021dru	14	II	IIb	0.40	0.58	0.02
2021msa	7	II	IIb	0.21	0.79	0.0
2021omy	18	II	IIb	0.01	0.99	0.00
2021tcv	5	II	IIb	0.25	0.75	0.00
2022uop	4	II	IIb	0.25	0.74	0.01
2022wcz	10	II	IIb	0.01	0.99	0.0
2022ycs	12	II	IIb	0.30	0.68	0.02
2023rky	4	II	IIb	0.25	0.75	0.00
2023zzk	21	II	IIb	0.01	0.99	0.00
2024frf	23	II	IIb	0.27	0.70	0.03

For objects denoted as "II->IIb?", the run MC simulation established the classification.

Table B.3. New SN classifications.

SNe	Phase (days after explosion)	Initial class.	This work	RF probabilities		
				II	IIb	87A-like
2013gg	28	II	II->IIb? (MC: 55.6% II; 44.4% IIb)	0.0	1.0	0.00
2015dj	11	II	IIb	0.66	0.34	0.00
	21	II	IIb	0.03	0.97	0.00
	24	II	IIb	0.00	1.00	0.00
2019oxi	32	II	II->IIb? (MC: 83.0% II; 17.0% IIb)	0.60	0.40	0.0
2024jxm	24	II	II			
2024jjd	16	II	II			
2024lor	10	II	II			
2024lls	18	II	II			
2024llc	6	II	II			
2024kqi	22	II	II			
2024kww	15	II	IIb	0.0	1.0	0.0
2024kzf	21	II	II			
2024lby	9	II	II			
2024lgz	32	II	II			
2024lsi	17	II	II->IIb? (MC: 100.0% II; 0.0% IIb)	0.97	0.02	0.01
2024mnp	15	II	II			
2024mxq	16	II	II			
2024neg	2	II	II			
2024nez	2	II	II			
2024opz	7	II	II			
2024oqd	6	II	II			
2024pba	12	II	II			
2024phz	6	II	II			
2024jfg	19	IIb	IIb			
2024ndh	11	IIb	IIb			
2024nak	11	IIb	IIb			
2024fja	16	IIb	IIb			
2024jcf	26	IIb	IIb			
2024iss	13	IIb	IIb			
2024hac	26	II	II			
2024it	9	II	IIb	0.43	0.57	0.0
2024anb	23	II	II			
2024psو	9	II	IIb	0.29	0.71	0.00
2024pom	17	II	II			
2024qiw	16	II	II			
2024rrr	5	IIb	IIb			
2024qrp	14	II	II			
2024sgl	16	II	IIb	0.09	0.91	0.00
2024cgi	10	II	II->IIb? (MC: 0.0% II; 100.0% IIb)	0.23	0.73	0.04
2024uqw	4	IIb	IIb			
	10	IIb	IIb			

For objects denoted as "II->IIb?", the run MC simulation established the classification. For the SN 2015dj, as we have 3 spectra we included the obtained classification probabilities for the three of them.

Table B.4. Evolution of the mean value of pEW and FWHM for each type over the examined time ranges along with their standard deviation.

	FWHM (Å)				pEW (Å)			
	H α		HeI		H α		HeI	
	IIb	II	IIb	II	IIb	II	IIb	II
0-10d	159.68 ± 54.26	68.39 ± 52.08	222.41 ± 71.13	105.63 ± 77.22	39.41 ± 30.51	6.10 ± 7.83	31.83 ± 22.64	9.36 ± 9.93
10-20d	151.51 ± 45.48	74.28 ± 48.54	225.98 ± 72.14	116.24 ± 68.02	40.86 ± 22.61	9.56 ± 11.20	39.27 ± 21.25	9.64 ± 8.44
20-30d	150.26 ± 45.62	77.32 ± 36.51	221.92 ± 62.84	87.42 ± 69.05	50.55 ± 28.91	16.73 ± 16.88	48.13 ± 26.54	8.13 ± 10.02
30-40d	146.03 ± 43.09	95.90 ± 41.46	210.96 ± 54.64	97.34 ± 58.96	53.72 ± 28.74	24.98 ± 19.19	57.77 ± 26.61	10.76 ± 7.95

Table B.5. Full SN sample.

SN	Type	nº Spec	Redshift	Discovery reference	Other references
1986L	II	1	0.00435	Gutiérrez et al. (2017)	Gutiérrez et al. (2017)
1987A	87A-like	10	0.001067	Kunkel et al. (1987)	Pun et al. (1995)
1987K	IIb	4	0.00268	Pollas & Pennypacker (1987)	Filippenko (1988)
1988A	II	2	0.005067	Gutiérrez et al. (2017)	Ruiz-Lapuente et al. (1990)
1990E	II	2	0.00414	Gutiérrez et al. (2017)	Schmidt et al. (1993)
1992af	II	2	0.01847	Gutiérrez et al. (2017)	Gutiérrez et al. (2017); della Valle & Bianchini (1992)
1992ba	II	3	0.00395	Gutiérrez et al. (2017)	Gutiérrez et al. (2017)
1993J	IIb	11	-0.000113	Riperio et al. (1993)	Matheson et al. (2000b,a); Barbon et al. (1995)
1996cb	IIb	3	0.002372	Nakano et al. (1996)	Modjaz et al. (2014)
1997dd	IIb	2	0.01519	Nakano et al. (1997)	Matheson et al. (2001)
1999br	II	4	0.003406	Gutiérrez et al. (2017)	Pastorello et al. (2004)
1999cr	II	1	0.02023	Gutiérrez et al. (2017)	Gutiérrez et al. (2017)
1999em	II	14	0.002392	Gutiérrez et al. (2017)	Gal-Yam et al. (2008); Leonard et al. (2001); Hamuy et al. (2001); Faran et al. (2014)
2001ig	IIb	2	0.003049	Evans et al. (2001)	Silverman et al. (2009); Phillips et al. (2001); Clocchiatti (2002); Ryder et al. (2005)
2002eg	IIb	1	0.026787	Sanders et al. (2002)	Shivvers et al. (2019)
2002gd	II	6	0.00892	Gutiérrez et al. (2017)	Spiro et al. (2014)
2003bg	IIb	7	0.004403	Wood-Vasey et al. (2003)	Hamuy et al. (2009)
2003bn	II	3	0.01276	Gutiérrez et al. (2017)	Gutiérrez et al. (2017)
2003cn	II	2	0.01919	Gutiérrez et al. (2017)	Gutiérrez et al. (2017)
2003E	II	4	0.0148	Gutiérrez et al. (2017)	Gutiérrez et al. (2017)
2003ed	II	1	0.0045	Itagaki et al. (2003)	Shivvers et al. (2017)
2003gu	IIb	2	0.019313	Armstrong et al. (2003)	Shivvers et al. (2019)
2003ib	II	2	0.02402	Gutiérrez et al. (2017)	Gutiérrez et al. (2017)
2003ki	IIb	3	0.025	Li et al. (2003)	Matheson et al. (2003); Shivvers et al. (2019), WISeREP (Yaron & Gal-Yam 2012)
2004bi	IIb	5	0.022	Sheppard et al. (2004)	Filippenko et al. (2004); Shivvers et al. (2019), WISeREP (Yaron & Gal-Yam 2012)
2004bm	IIb	1	0.00419	Singer et al. (2004)	Shivvers et al. (2017)
2004ek	87A-like	2	0.017275	Monard et al. (2004)	Taddia et al. (2016)
2004em	87A-like	1	0.014894	Arbour et al. (2004)	Taddia et al. (2016)
2004et	II	3	0.00016	Zwitter et al. (2004)	Faran et al. (2014)
2004ex	IIb	2	0.017549	Jacques et al. (2004)	Shivvers et al. (2019); Stritzinger et al. (2023)
2004ff	IIb	4	0.022649	Pugh et al. (2004)	Modjaz et al. (2014); Shivvers et al. (2019); Stritzinger et al. (2023); Pessi et al. (2019)
2005an	II	4	0.011014	Gutiérrez et al. (2017)	Shivvers et al. (2017); Gutiérrez et al. (2017)
2005D	IIb	1	0.02837	Burket et al. (2005)	Shivvers et al. (2019)
2005em	IIb	2	0.0253	Boles et al. (2005)	Shivvers et al. (2019); Stritzinger et al. (2023)
2005lr	IIb	2	0.008572	Baek & Li (2005)	Shivvers et al. (2017); Vincenzi et al. (2019)
2005Q	IIb	2	0.0224	Green (2005a)	Stritzinger et al. (2023); Stritzinger et al. (2018)
2005U	IIb	1	0.0103	Green (2005a)	Leonard & Cenko (2005); Modjaz et al. (2014)
2005Z	II	3	0.019233	Green (2005b)	Gutiérrez et al. (2017)
2006ba	IIb	1	0.019	Green (2006a)	Stritzinger et al. (2023)
2006bf	IIb	1	0.024	Green (2006d)	Blondin et al. (2006); Stritzinger et al. (2023)
2006el	IIb	1	0.017	Green (2006e)	Shivvers et al. (2019)
2006it	II	2	0.0155	Gutiérrez et al. (2017)	Gutiérrez et al. (2017)
2006iv	IIb	1	0.0081	Green (2006b)	Shivvers et al. (2019)
2006iw	II	2	0.03073	Gutiérrez et al. (2017)	Gutiérrez et al. (2017)
2006T	IIb	3	0.008091	Green (2006c)	Modjaz et al. (2014); Shivvers et al. (2017)
2007ay	IIb	1	0.01454	Mostardi & Li (2007)	Morrell et al. (2007); Shivvers et al. (2019)

2007bf	II	2	0.0178	Gutiérrez et al. (2017)	Gutiérrez et al. (2017)
2007ld	II	2	0.027	Gutiérrez et al. (2017)	Östman et al. (2011); Gutiérrez et al. (2017)
2007od	II	19	0.00586	Gutiérrez et al. (2017)	Gutiérrez et al. (2017)
2007P	II	3	0.041	Gutiérrez et al. (2017)	Gutiérrez et al. (2017)
2007U	II	5	0.026	Gutiérrez et al. (2017)	Gutiérrez et al. (2017)
2007X	II	5	0.009456666	Gutiérrez et al. (2017)	Gutiérrez et al. (2017)
2008aq	IId	5	0.007972	Chu et al. (2008)	Modjaz et al. (2014)
2008ax	IId	13	0.001931	Mostardi et al. (2008)	Modjaz et al. (2014); Taubenberger et al. (2011); Chornock et al. (2011)
2008bo	IId	5	0.00495	Nissinen et al. (2008)	Modjaz et al. (2014); Shivvers et al. (2019)
2008cw	IId	5	0.0324	Yuan et al. (2008)	Modjaz et al. (2014)
2008fi	IId	2	0.026	Skvarc & Mikuz (2008)	Shivvers et al. (2019)
2008gi	II	3	0.024426	Gutiérrez et al. (2017)	Gutiérrez et al. (2017)
2008hg	II	3	0.018946	Gutiérrez et al. (2017)	Gutiérrez et al. (2017)
2008ho	II	1	0.010273	Gutiérrez et al. (2017)	Gutiérrez et al. (2017)
2008ie	IId	1	0.013673	Pignata et al. (2008)	Shivvers et al. (2019)
2008if	II	4	0.0115	Gutiérrez et al. (2017)	Gutiérrez et al. (2017)
2008in	II	4	0.005224	Gutiérrez et al. (2017)	Gutiérrez et al. (2017)
2008K	II	3	0.026656	Gutiérrez et al. (2017)	Gutiérrez et al. (2017)
2009aj	II	3	0.00961	Gutiérrez et al. (2017)	Gutiérrez et al. (2017)
2009ao	II	1	0.01113	Gutiérrez et al. (2017)	Gutiérrez et al. (2017)
2009au	II	3	0.009396	Gutiérrez et al. (2017)	Gutiérrez et al. (2017)
2009bz	II	3	0.01077	Gutiérrez et al. (2017)	Gutiérrez et al. (2017)
2009C	IId	1	0.023577	Li et al. (2009)	Shivvers et al. (2019)
2009dq	IId	1	0.0047	Pignata et al. (2009)	Stritzinger et al. (2023)
2009gk	IId	2	0.026348	Narla et al. (2009)	Shivvers et al. (2019)
2009ka	IId	1	0.03	Boles (2009)	Shivvers et al. (2019)
2009mg	IId	2	0.0076	Monard (2009)	Oates et al. (2012)
2009Z	IId	4	0.0248	Griffith et al. (2009)	Stritzinger et al. (2023)
2010as	IId	8	0.007315	Maza et al. (2010)	Folatelli et al. (2014b)
2010ei	IId	1	0.01867	Kandashoff et al. (2010)	Green (2010); Shivvers et al. (2019)
2010ej	IId	1	0.05233	Kandashoff et al. (2010)	Silverman et al. (2010); Shivvers et al. (2019)
2010ek	IId	1	0.032046	Kandashoff et al. (2010)	Shivvers et al. (2019)
2011D	IId	1	0.023123	Narla et al. (2011)	Shivvers et al. (2019)
2011dh	IId	10	0.002	Silverman et al. (2011)	Arcavi et al. (2011); Ergon et al. (2014); Shivvers et al. (2019)
2011ei	IId	8	0.009313	Stritzinger et al. (2011)	Milisavljevic et al. (2013a)
2011fu	IId	9	0.018489	Tomasella et al. (2011b)	Kumar et al. (2013); Morales-Garoffolo et al. (2015)
2011hg	IId	1	0.0236	Tomasella et al. (2011a)	Dimai et al. (2011); Marion & Berlind (2011)
2011hs	IId	9	0.0057	Milisavljevic et al. (2011)	Bufano et al. (2014); Smartt et al. (2015)***
2012aw	II	20	0.002595	Quadri et al. (2012)	Dall’Ora et al. (2014)
2012dy	IId	12	0.01	Bock et al. (2012)	Smartt et al. (2015)***
2012ec	II	8	0.0047	Monard et al. (2012)	Maund et al. (2013); Smartt et al. (2015)*; Childress et al. (2016)
2012hs	IId	1	0.006	Cifuentes et al. (2012)	Smartt et al. (2015)*
2012P	IId	5	0.004479	Borsato et al. (2012)	Bose et al. (2013); Fremling et al. (2016)
2013ab	II	4	0.0046	Blanchard et al. (2013)	de Jaeger et al. (2019)
2013ak	IId	4	0.0037	Carrasco et al. (2013)	Milisavljevic et al. (2013b)
2013bb	IId	11	0.019	Howerton et al. (2013)	Smartt et al. (2015)*
2013bl	IId	1	0.0304	Rich et al. (2013)	Tomasella et al. (2013)
2013df	IId	12	0.002395	Ciabattari et al. (2013a)	Van Dyk et al. (2014); Szalai et al. (2016); Childress et al. (2016); Shivvers et al. (2019)
2013ej	II	19	0.002192	Kim et al. (2013)	Valenti et al. (2014); Smartt et al. (2015)*
2013ep	IId	1	0.016888	Ciabattari et al. (2013b)	Balam (2018)
2013fq	IId	2	0.01149	Parker et al. (2013)	Smartt et al. (2015)*; Childress et al. (2016)
2014cq	IId	1	0.011	Parker et al. (2014)	Childress et al. (2016)
2014cw	II	3	0.006	Lipunov et al. (2014)	Smartt et al. (2015)*; Childress et al. (2016)
2014cx	II	9	0.005	Nakano et al. (2014)	Smartt et al. (2015)*; Childress et al. (2016)
2014ds	IId	1	0.01373	Xu et al. (2014)	Smartt et al. (2015)*
2014G	II	5	0.0039	Nakano (2014)	Terreran et al. (2016)

2015au	IIb	1	0.025	Green (2015)	Smartt et al. (2015)*
2015bi	IIb	2	0.016	Conseil et al. (2016)	Rui et al. (2016); Shivvers et al. (2019)
2015bs	II	8	0.027	Chambers et al. (2016c)	Smartt et al. (2015)* ;Anderson et al. (2018)
2015Y	IIb	3	0.008172	Zheng & Filippenko (2015)	Shivvers et al. (2019); Childress et al. (2016)
2016amn	IIb	1	0.0308	Chambers et al. (2016a)	Yaron et al. (2021)
2016aqf	II	9	0.004	Stanek & Bersier (2016)	Hosseinzadeh et al. (2016c)
2016B	II	5	0.004293	Stanek et al. (2016b)	WISeREP (Yaron & Gal-Yam 2012); Smartt et al. (2015)*, Nakaoka et al. (2016) ^a
2016bam	IIb	1	0.014	Tsuboi (2016)	Hosseinzadeh et al. (2016a)
2016bas	IIb	1	0.009	Parker (2016a)	Hosseinzadeh et al. (2016)
2016bhr	IIb	1	0.014	Chambers et al. (2016b)	Hosseinzadeh et al. (2016b)
2016egz	II	8	0.023	Brown (2016)	Fraser et al. (2016); Hiramatsu et al. (2021b)
2016gkg	IIb	12	0.0049	Otero & Buso (2016)	Smartt et al. (2015)*; Jha (2016); Kilpatrick et al. (2017)
2016gsd	II	4	0.06	Itagaki (2016)	Smartt et al. (2015)*; Reynolds et al. (2020)
2016iye	IIb	1	0.03	Parker (2016b)	Smartt et al. (2015)*; Smith et al. (2016)
2016M	IIb	1	0.036	Xu et al. (2016)	Zhang & Wang (2016)
2016X	II	2	0.0044	Stanek et al. (2016a)	de Jaeger et al. (2019)
2017ati	IIb	1	0.016	Delgado et al. (2017b)	Benetti (2017)
2017dgd	IIb	1	0.022	Chambers et al. (2017b)	Tomasella (2017a)
2017eaw	II	12	0.000133	Wiggins (2017)	Szalai et al. (2019)
2017eiy	IIb	1	0.047	Delgado et al. (2017c)	Smartt et al. (2015)*; Pignata et al. (2017)
2017gfh	IIb	1	0.024	Russiani (2017)	Smartt et al. (2015)*; Lyman et al. (2017b)
2017gfz	IIb	1	0.06	Moller et al. (2017)	Smartt et al. (2015)*; Lyman et al. (2017a)
2017gkk	IIb	1	0.004923	Itagaki (2017)	Onori (2017)
2017gpn	IIb	6	0.007388	Caimmi (2017)	Prentice et al. (2019c); Balakina et al. (2019)
2017gth	IIb	1	0.038	Tonry et al. (2017a)	Smartt et al. (2015)*; Rybicki et al. (2017)
2017hyh	IIb	4	0.012	Tonry et al. (2017b)	Smartt et al. (2015)*; Onori et al. (2017); Prentice et al. (2019c)
2017ixz	IIb	2	0.024	Tonry et al. (2017c)	Smartt et al. (2015)*; Jones et al. (2017)
2017iyd	IIb	1	0.0285	Tonry et al. (2017c)	Smartt et al. (2015)*; Angus et al. (2017)
2017jbl	IIb	1	0.015054	Gagliano et al. (2017)	Tomasella (2017b)
2017jdn	IIb	1	0.0317	Ciabattari et al. (2017)	Lin et al. (2017)
2017jo	IIb	1	0.023	Delgado et al. (2017a)	Smartt et al. (2015)*; Taddia et al. (2017)
2017vi	IIb	2	0.04	Chambers et al. (2017a)	Schulze et al. (2021)
2018arx	IIb	1	0.033853	Stanek (2018)	Bose et al. (2018)
2018bsg	IIb	1	0.0217	Stone et al. (2018)	Smartt et al. (2015); Inserra et al. (2023)*; Clark et al. (2018)
2018bti	IIb	1	0.024826	Tonry et al. (2018a)	Hiramatsu et al. (2018)
2018ddr	IIb	1	0.01468	Fremling (2018a)	Khlat et al. (2018)
2018efd	IIb	1	0.03	Fremling (2018b)	Bruch et al. (2021b)
2018fer	IIb	4	0.021	Tonry et al. (2018b)	Smartt et al. (2015); Inserra et al. (2023)*; Tucker & Shappee (2018)
2018fex	IIb	1	0.024	Stanek (2018)	Smartt et al. (2015); Inserra et al. (2023)*; Kostrzewa-rutkowska et al. (2018)
2018gj	II	11	0.004556	Wiggins (2018)	Teja et al. (2023)
2018hna	87A-like	6	0.002408	Itagaki (2018)	Singh et al. (2019); Kawabata (2018) Leadbeater (2018)
2018mc	IIb	1	0.035	Stanek (2018)	Harmanen (2018)
2018ow	IIb	1	0.01	Chambers et al. (2018)	Dimitriadiis et al. (2018)
2019B	II	1	0.021	Stanek (2019a)	Tomasella (2019)
2019aax	IIb	2	0.013	Tonry et al. (2019)	Piranomonte et al. (2019b)
2019abp	IIb	1	0.037628	Nordin et al. (2019a)	Fremling et al. (2019b)
2019abu	IIb	2	0.036379	Tonry et al. (2019)	Piranomonte et al. (2019a)
2019amq	II	1	0.054	Tonry et al. (2019)	Smartt et al. (2015); Inserra et al. (2023)*; Carini et al. (2019)
2019asm	II	1	0.061	Chambers et al. (2019e)	Carini et al. (2019)
2019aur	IIb	1	0.0124	Tonry et al. (2019a)	Fremling et al. (2019d)
2019awk	II	1	0.044	Nordin et al. (2019b)	Fremling et al. (2019d)
2019axz	II	1	0.015	Tonry et al. (2019b)	Smartt et al. (2015); Inserra et al. (2023)*; Barbarino et al. (2019)

2019bao	IIb	3	0.011885	Nordin et al. (2019c)	Smartt et al. (2015); Inserra et al. (2023)*; Schuldt et al. (2019)
2019bju	II	1	0.029	Stanek (2019b)	Smartt et al. (2015); Inserra et al. (2023)*; Carracedo et al. (2019)
2019bkg	II	1	0.037	Brimacombe et al. (2019)	Smartt et al. (2015); Inserra et al. (2023)*; Carracedo et al. (2019)
2019boh	II	1	0.0335	Nordin et al. (2019d)	Fremling et al. (2019c)
2019bph	II	1	0.047	Tonry et al. (2019c)	Frohmaier (2019)
2019btk	II	1	0.074	Tonry et al. (2019d)	Dimitriadis & Foley (2019)
2019bzo	IIb	1	0.065	Nordin et al. (2019e)	Smartt et al. (2015); Inserra et al. (2023)*; Brinnel et al. (2019)
2019ci	II	1	0.04	Tonry et al. (2019a)	Smartt et al. (2015); Inserra et al. (2023)*; Rodriguez et al. (2019)
2019cob	II	1	0.07	Tonry et al. (2019e)	Dahiwale & Fremling (2020b)
2019dke	II	1	0.010637	Vallely (2019a)	Stritzinger & Holmbo (2019)
2019dod	II	1	0.034	Fremling (2019a)	Prentice et al. (2019e)
2019dts	II	1	0.015	Delgado et al. (2019a)	Short et al. (2019)
2019edo	II	1	0.008569	Stanek (2019c)	Hiramatsu et al. (2019e)
2019eff	IIb	1	0.05	Chambers et al. (2019f)	Nicholl et al. (2019a)
2019ejf	II	1	0.025271	Stanek & Kochanek (2019)	Bredall et al. (2019b)
2019ejj	II	1	0.003	Tonry et al. (2019c)	Nicholl et al. (2019c)
2019ekj	II	1	0.04	Tonry et al. (2019d)	Fremling et al. (2019f)
2019etp	II	1	0.015621	Brimacombe & Vallely (2019)	Bredall et al. (2019a)
2019ewu	II	1	0.033	Tonry et al. (2019e)	Williamson et al. (2023)
2019fbv	II	1	0.028	Tonry et al. (2019f)	Tucker et al. (2019b)
2019fcn	II	1	0.003	Stanek et al. (2019)	Nicholl et al. (2019b)
2019fco	IIb	1	0.04058	Tonry et al. (2019g)	Fremling et al. (2019g)
2019ffi	II	1	0.039	Delgado et al. (2019b)	Cartier et al. (2019a)
2019fht	II	1	0.028	Fremling (2019b)	Fremling et al. (2019e)
2019fjp	II	1	0.029	Tonry et al. (2019h)	Cartier et al. (2019a)
2019fks	IIb	1	0.05	Tonry et al. (2019i)	Cartier et al. (2019b)
2019gaf	IIb	1	0.006	Tonry et al. (2019j)	Swann et al. (2019a)
2019ght	II	1	0.047	Nordin et al. (2019f)	Dahiwale et al. (2019a)
2019gql	II	1	0.021	Vallely (2019b)	Swann et al. (2019b)
2019gqm	II	1	0.02	Delgado et al. (2019c)	Swann et al. (2019c)
2019hcn	II	1	0.018	Stanek & Vallely (2019)	Frohmaier et al. (2019)
2019hnl	II	1	0.022869	Tonry et al. (2019f)	Burke et al. (2019a)
2019hyk	II	1	0.014744	Stanek (2019d)	Fraser et al. (2019c)
2019ifm	II	1	0.02308	Weinberg et al. (2019)	Tomasella et al. (2019)
2019igh	IIb	1	0.025	Nordin et al. (2019g)	Fremling & Dahiwale (2019a)
2019ihm	II	1	0.025	Nordin et al. (2019h)	Fremling et al. (2019j)
2019ihw	II	1	0.0325	Nordin et al. (2019h)	Fremling et al. (2019h)
2019ijj	IIb	1	0.02895	Nordin et al. (2019h)	Fremling et al. (2019h)
2019ikb	II	2	0.02	Tonry et al. (2019g)	Tucker et al. (2019c); Fremling et al. (2019i)
2019jyw	II	1	0.01164	Nordin et al. (2019i)	Hiramatsu et al. (2019a)
2019klk	II	1	0.058	Tonry et al. (2019h)	Prentice et al. (2019f)
2019krp	II	1	0.017042	Nordin et al. (2019j)	Prentice et al. (2019f)
2019ktb	II	1	0.112	Tonry et al. (2019i)	Prentice et al. (2019g)
2019lkw	II	2	0.0867	Nordin et al. (2019k)	Hiramatsu et al. (2019b); Fremling & Dahiwale (2019b)
2019lqo	IIb	1	0.0103	Bose et al. (2019)	Bose et al. (2019)
2019lsk	IIb	1	0.019	Angus et al. (2019)	Angus et al. (2019)
2019ltz	II	1	0.0542	Tonry et al. (2019j)	Dahiwale et al. (2019a)
2019lud	II	1	0.04942	Tonry et al. (2019j)	Fremling & Dahiwale (2019a)
2019luo	II	1	0.041	Nordin et al. (2019l)	Angus et al. (2019)
2019luz	IIb	1	0.036	Angus et al. (2019)	Angus et al. (2019)
2019mfu	II	1	0.055	Nordin et al. (2019m)	Wiseman et al. (2019)
2019mrz	IIb	1	0.025	Tonry et al. (2019k)	Wiseman et al. (2019)
2019nqr	II	1	0.084	AI (2019)	Hiramatsu et al. (2019d)
2019yn	II	1	0.024	Bock et al. (2019)	Fraser et al. (2019a)
2019nzy	II	1	0.036	Nordin et al. (2019n)	Prentice et al. (2019i)
2019oba	II	1	0.031462	Tonry et al. (2019l)	Prentice et al. (2019h)
2019obh	IIb	1	0.03555	Nordin et al. (2019n)	Fraser et al. (2019b)
2019odf	II	1	0.029	Nordin et al. (2019o)	Brennan et al. (2019b)
2019oez	II	1	0.039	Forster (2019a)	Brennan et al. (2019b)
2019ofc	II	1	0.021	Tonry et al. (2019m)	Brennan et al. (2019b)
2019ojd	II	1	0.045	Tonry et al. (2019n)	Callis et al. (2019)
2019oje	IIb	1	0.045	Tonry et al. (2019n)	Callis et al. (2019)
2019omb	II	1	0.028	Chambers et al. (2019a)	Prentice et al. (2019j)

2019omo	II	1	0.0335	Bock & Stanek (2019)	Brennan et al. (2019a)
2019oop	II	1	0.05	Forster (2019b)	Callis et al. (2019)
2019osl	II	1	0.010857	Tonry et al. (2019o)	Hiramatsu et al. (2019c)
2019ovq	II	1	0.002	Forster (2019c)	Dahiwale et al. (2019a)
2019oxn	II	1	0.038	Forster (2019d)	Dimitriadis (2019)
2019pad	II	1	0.021	Nordin et al. (2019p)	Dahiwale et al. (2019c)
2019pcr	II	1	0.018883	Gromadzki & Wyrzykowski (2019)	Brennan et al. (2019a)
2019pjs	II	1	0.007415	Ma et al. (2019)	Burke et al. (2019c)
2019pkh	II	1	0.02	Nordin et al. (2019q)	Fremling et al. (2019a)
2019pqa	IIb	1	0.01413	Forster (2019e)	Dahiwale et al. (2019b)
2019rho	II	1	0.01696	Chambers et al. (2019b)	Hung (2019)
2019rn	IIb	1	0.013	Tonry et al. (2019b)	Tucker et al. (2019a)
2019roa	II	1	0.025	Nordin et al. (2019r)	Dahiwale et al. (2019d)
2019rpj	II	1	0.0296	Tonry et al. (2019p)	Burke et al. (2019b)
2019rqe	II	1	0.03	Nordin et al. (2019s)	Hung (2019)
2019rqk	II	1	0.029	Fremling (2019c)	Dahiwale et al. (2019e)
2019rri	II	1	0.0511	Forster (2019f)	Dahiwale & Fremling (2019a)
2019rsw	II	2	0.053	Nordin et al. (2019t)	Leibundgut et al. (2019); Dahiwale & Fremling (2019b)
2019rwd	IIb	1	0.0294	Arcavi et al. (2019)	Arcavi et al. (2019)
2019sna	IIb	1	0.031	Forster (2019g)	Leloudas et al. (2019a,b)
2019sox	IIb	1	0.01	Tonry et al. (2019q)	Cartier & Ugarte (2019)
2019tua	IIb	1	0.010424	Tonry et al. (2019r)	Burke et al. (2019); Huang et al. (2024)
2019tuq	II	1	0.053	Nordin et al. (2019u)	Malesani et al. (2019)
2019tzx	IIb	1	0.0435	Nordin et al. (2019v)	Dahiwale & Fremling (2019c)
2019uhm	II	2	0.010377	Tonry et al. (2019s)	Burke et al. (2019a); Inserra et al. (2023)*
2019uqp	II	1	0.04	Bauer et al. (2019)	Perley & Taggart (2019a)
2019uxh	II	1	0.0326	Chambers et al. (2019c)	Smartt et al. (2019)
2019vb	II	1	0.02	Tonry et al. (2019c)	Prentice et al. (2019d)
2019vdl	II	1	0.025	Forster et al. (2019a)	Prentice et al. (2019k)
2019vrx	II	1	0.037	Tonry et al. (2019t)	Ihanec et al. (2019)
2019vsq	II	1	0.01952	Itagaki (2019)	Burke et al. (2019b)
2019vsr	II	1	0.027	Tonry et al. (2019u)	Perley & Taggart (2019b)
2019vus	II	1	0.025	Tonry et al. (2019)	Prentice et al. (2019a)
2019wqq	IIb	1	0.01123	De (2019)	Graham et al. (2020a)
2019wrx	IIb	1	0.03706	Tonry et al. (2019a)	Dahiwale & Fremling (2020a)
2019wvz	II	1	0.0319	Forster et al. (2019b)	Perley (2019)
2019wzh	II	1	0.0185	Forster et al. (2019c)	Prentice et al. (2019b)
2019yhq	II	1	0.054	Chambers et al. (2019d)	Muller et al. (2019)
2019yjf	II	1	0.043	Tonry et al. (2019b)	Graham et al. (2020b)
2020aapq	II	1	0.03	Tonry et al. (2020c)	Huber (2020)
2020aaasd	II	1	0.025	Forster et al. (2020c)	Perley (2020a)
2020aaun	II	1	0.02815	Munoz-Arcancibia et al. (2020c)	Perley (2020b)
2020aaxf	IIb	1	0.031	Munoz-Arcancibia et al. (2020d)	Atapin et al. (2020)
2020abah	87A-like	1	0.03	Sit (2022)	Sit (2022)
2020abcq	II	2	0.01152	Tonry et al. (2020d)	Payne (2020); Inserra et al. (2023)*
2020abdr	II	1	0.03	Forster et al. (2020d)	Dahiwale & Fremling (2020c)
2020abml	II	1	0.045	Duev (2020a)	Cartier et al. (2020)
2020abou	II	1	0.031	Munoz-Arcancibia et al. (2020a)	Cartier et al. (2020)
2020absk	II	1	0.01889	Duev (2020b)	Perley (2020c)
2020absz	II	1	0.021298	Duev (2020b)	Pessi et al. (2020a)
2020abtf	II	1	0.014	Fremling (2020)	Pessi et al. (2020b)
2020acat	IIb	4	0.007932	Tonry et al. (2020e)	Medler et al. (2022)
2020aceh	IIb	1	0.040788	Munoz-Arcancibia et al. (2020b)	Dahiwale & Fremling (2021c)
2020acsck	IIb	1	0.029	Tonry et al. (2020f)	Gillanders et al. (2021)
2020adnx	IIb	1	0.021001	Srivastav et al. (2021)	Srivastav et al. (2021)
2020aqe	IIb	2	0.012255	Burke et al. (2020)	Burke et al. (2020); Inserra et al. (2023)*
2020bft	IIb	1	0.03	Tonry et al. (2020a)	Smith et al. (2020a)
2020bio	IIb	5	0.009	Itagaki (2020)	Srivastav et al. (2020); Pellegrino et al. (2023)
2020fqv	II	10	0.007	Forster et al. (2020e)	Zhang et al. (2020); Tinyanont et al. (2022)
2020ikq	IIb	1	0.037	Tonry et al. (2020b)	Angus (2020a)
2020itj	IIb	1	0.033	Forster et al. (2020a)	Galbany et al. (2020); Galbany et al. (2025)
2020jfo	II	23	0.005224	Nordin et al. (2020)	Sollerman et al. (2021); Teja et al. (2022); Galbany et al. (2025)
2020mob	IIb	1	0.023	Forster et al. (2020b)	Jha et al. (2020)
2020tjd	IIb	1	0.01	Tonry et al. (2020g)	Angus (2020b)

2020tkc	IIb	1	0.036	Angel et al. (2020)	Dimitriadis et al. (2020)
2021aamk	IIb	1	0.06	Tonry et al. (2021e)	Tucker (2021b)
2021aatd	II	1	0.033	Tonry et al. (2021a)	Wyatt et al. (2021)
2021abmn	II	1	0.04	Tonry et al. (2021b)	Carini et al. (2021a)
2021actu	IIb	1	0.025	Fremling (2021f)	Carini et al. (2021b)
2021adud	IIb	1	0.034	De (2021d)	Figuereo et al. (2022)
2021aevx	IIb	1	0.011771	Fremling (2021g)	Chu et al. (2021e)
2021afdx	IIb	1	0.03	Ragosta et al. (2021)	Ragosta et al. (2021)
2021agle	II	1	0.017	Tonry et al. (2021h)	Pineda et al. (2021)
2021bxu	IIb	1	0.0178	Tonry et al. (2021f)	Desai et al. (2023)
2021esi	IIb	1	0.03	Fremling (2021a)	Angus & Izzo (2021)
2021fsb	IIb	1	0.0535	Chambers et al. (2021a)	Angus (2021)
2021heh	IIb	2	0.026648	Fremling (2021b)	Burke et al. (2021); Graham et al. (2021)
2021hlv	IIb	1	0.021698	Munoz-Arcancibia et al. (2021a)	Dahiwale & Fremling (2021e)
2021lan	IIb	1	0.0225	Tonry et al. (2021g)	Tucker (2021a)
2021M	IIb	1	0.0106	Forster et al. (2021a)	Dahiwale & Fremling (2021b)
2021pat	IIb	1	0.031779	Chambers et al. (2021b)	Huber (2021a)
2021pb	IIb	1	0.03317803	De (2021a)	Dahiwale & Fremling (2021d)
2021pkd	IIb	1	0.03984	Munoz-Arcancibia et al. (2021b)	Chu et al. (2021a)
2021pnp	IIb	1	0.03	Munoz-Arcancibia et al. (2021c)	Rojas-Bravo et al. (2021)
2021rf	IIb	1	0.027172	De (2021b)	Dahiwale & Fremling (2021a)
2021sjt	IIb	1	0.00475	Fremling (2021c)	Siebert et al. (2021a)
2021tbx	IIb	1	0.016503	Forster et al. (2021c)	Chu et al. (2021b)
2021uth	IIb	1	0.025	Munoz-Arcancibia et al. (2021d)	Do (2021)
2021vci	IIb	1	0.022	Chambers et al. (2021c)	Nicholl et al. (2021)
2021vgn	IIb	1	0.032	De (2021c)	Siebert et al. (2021b)
2021wxl	II	1	0.0473	Chambers et al. (2021d)	Csoernyei et al. (2021)
2021wzr	II	1	0.0633	Munoz-Arcancibia et al. (2021e)	Csoernyei et al. (2021)
2021xaz	IIb	1	0.05	Chambers et al. (2021e)	Huber (2021b)
2021xbf	II	1	0.0141	Forster et al. (2021b)	Davis et al. (2021)
2021xyh	II	1	0.035	Chambers et al. (2021f)	Chu et al. (2021c)
2021ybc	IIb	1	0.02925	Munoz-Arcancibia et al. (2021f)	Inserra et al. (2023)*
2021ytk	II	1	0.03	Tonry et al. (2021c)	Deckers et al. (2021)
2021zby	IIb	2	0.025965	Tonry et al. (2021d)	Wang et al. (2023)
2021zet	II	1	0.032	Fremling (2021d)	Bruch et al. (2021a)
2021zgm	II	2	0.013	Fremling (2021e)	Meza et al. (2021); Chu et al. (2021d)
2021zon	IIb	1	0.03	Chambers et al. (2021g)	Huber (2021c)
2022W	IIb	3	0.0265	Tonry et al. (2022d)	Li et al. (2022); Inserra et al. (2023)*
2022aaad	II	1	0.01	Tonry et al. (2022)	Fulton et al. (2022)
2022abua	II	1	0.02687	Jones et al. (2022)	Angus (2022)
2022acrv	II	1	0.028	Tonry et al. (2022j)	Gkini et al. (2022b)
2022acug	II	1	0.012	Tonry et al. (2022)	Pessi et al. (2022)
2022adtt	II	1	0.027	Munoz-Arcancibia et al. (2022c)	Karambelkar et al. (2023)
2022aduz	II	1	0.01	Munoz-Arcancibia et al. (2022d)	Gkini et al. (2022a)
2022adzl	II	1	0.024	Forster et al. (2022)	Tucker (2023a)
2022akf	IIb	1	0.044425	Chambers et al. (2022b)	Huber (2022a)
2022emz	IIb	1	0.015	Tonry et al. (2022e)	Srivastav et al. (2022)
2022fzf	IIb	1	0.03	Chambers et al. (2022a)	Hinds & Perley (2022)
2022hnt	IIb	1	0.0192	Fremling (2022)	Farah et al. (2025)
2022icd	IIb	1	0.056	Tonry et al. (2022c)	Fremling et al. (2022)
2022jpx	IIb	1	0.015	Munoz-Arcancibia et al. (2022a)	Parrag et al. (2022)
2022ngb	IIb	1	0.009	Tonry et al. (2022a)	Izzo et al. (2022)
2022pep	IIb	1	0.046	Tonry et al. (2022b)	Desai (2022)
2022psx	IIb	1	0.019	Munoz-Arcancibia et al. (2022b)	Hinkle (2022)
2022rls	IIb	1	0.016888	Tonry et al. (2022f)	Do (2022)
2022xus	II	1	0.008756	Tonry et al. (2022g)	Huber (2022b)
2022xxq	II	1	0.028	Tonry et al. (2022h)	Huber (2022b)
2022yvw	IIb	2	0.0065	Tonry et al. (2022i)	Zhai et al. (2022); Inserra et al. (2023)*
2023abdg	II	1	0.006	Tonry et al. (2023q)	Terreran et al. (2023a)
2023bec	IIb	1	0.03	Tonry et al. (2023g)	Phan et al. (2023)
2023diq	IIb	1	0.027	Chambers et al. (2023)	Taggart et al. (2023)
2023eaf	IIb	1	0.0304	Munoz-Arcancibia et al. (2023c)	Das et al. (2023)
2023ec	IIb	1	0.03	Tonry et al. (2023f)	Srivastav et al. (2023)
2023fsc	IIb	1	0.02	Fremling (2023a)	Wise et al. (2023)
2023lgx	IIb	1	0.03	Tonry et al. (2023a)	Hinkle (2023)
2023mix	IIb	1	0.011	Tonry et al. (2023b)	Schwab et al. (2023)
2023mjk	IIb	1	0.04	Jones et al. (2023)	Angus (2023)
2023mti	IIb	1	0.051	Tonry et al. (2023c)	Payne (2023)
2023nmh	II	1	0.02	Tonry et al. (2023d)	Tucker (2023b)
2023pbf	II	1	0.011	Tonry et al. (2023e)	Tucker (2023c)

2023rbk	II	1	0.01988	Fremling (2023b)	Taguchi & Maeda (2023)
2023rhj	II	1	0.04	Munoz-Arcibia et al. (2023d)	Byrne et al. (2023)
2023rix	II	1	0.014	Zimmerman et al. (2023)	Terreran et al. (2023b)
2023rmz	II	1	0.032236	Munoz-Arcibia et al. (2023b)	Angus (2024)
2023shg	IIb	1	0.018	Tonry et al. (2023h)	Byrne et al. (2023)
2023tvp	IIb	1	0.019	Tonry et al. (2023i)	Ayala et al. (2023)
2023uvh	IIb	1	0.027	Forster et al. (2023)	Tucker (2023d)
2023wdd	IIb	1	0.024	Tonry et al. (2023j)	Li et al. (2023)
2023wrl	II	1	0.014	Tonry et al. (2023k)	Moore et al. (2023)
2023xic	II	1	0.02	Tonry et al. (2023l)	Gonzalez-Banuelos et al. (2023)
2023xoo	IIb	2	0.0171	Tonry et al. (2023m)	Kopsacheili et al. (2023b); Inserra et al. (2023)*
2023xqo	II	1	0.02	Tonry et al. (2023p)	Kopsacheili et al. (2023a)
2023xvi	IIb	1	0.02	Fremling (2023c)	Hoogendam (2023)
2023ype	II	1	0.019	Tonry et al. (2023n)	Dennefeld et al. (2023)
2023zbj	IIb	1	0.031	Hodgkin et al. (2023)	Murieta et al. (2023)
2023zop	IIb	1	0.02	Tonry et al. (2023o)	Balcon (2023)
2023zps	II	1	0.042	Munoz-Arcibia et al. (2023a)	Csoernyei et al. (2023)
2024ak	IIb	1	0.028545	Fremling (2024)	Sollerman et al. (2024b)
2024ayv	II	1	0.015	Tonry et al. (2024a)	Brivio et al. (2024)
2024btj	II	1	0.007976	Hu et al. (2024)	Dyer et al. (2024)
2024dga	II	1	0.0267	Tonry et al. (2024b)	Pessi & Sollerman (2024)
2024dgy	II	2	0.01	Tonry et al. (2024c)	Inserra et al. (2023)*; Csoernyei et al. (2024a)
2024drv	II	2	0.008132	Tonry et al. (2024d)	Taguchi & Maeda (2024); Leadbeater (2024a)
2024dxh	II	1	0.02	Munoz-Arcibia et al. (2024a)	Csoernyei et al. (2024b)
2024dym	II	1	0.014	Tonry et al. (2024e)	Csoernyei et al. (2024c)
2024egd	II	1	0.031674999	Munoz-Arcibia et al. (2024b)	Sollerman et al. (2024a)
2024ehs	II	2	0.003776	Tonry et al. (2024f)	Li et al. (2024); Leadbeater (2024b)
2024qc	II	1	0.012	Groot & Tranin (2024)	Petrushevska et al. (2024)
ASASSN-14az	IIb	2	0.006731	Davis et al. (2014)	Shivvers et al. (2019); Benetti et al. (2014)
ASASSN-15bd	IIb	1	0.007946	Kiyota et al. (2015)	Shivvers et al. (2019)
ASASSN-15oz	II	9	0.007	Brown et al. (2015)	Hosseinzadeh et al. (2015); Bostroem et al. (2019)
ASASSN-15qz	IIb	2	0.022	Brimacombe et al. (2015)	Smartt et al. (2015); Inserra et al. (2023)*
DES16S1kt	IIb	2	0.068	Challis et al. (2016)	Smartt et al. (2015); Inserra et al. (2023)*
LSQ13bca	IIb	3	0.08	De Cia et al. (2013)	Smartt et al. (2015); Inserra et al. (2023)*
LSQ14hj	IIb	3	0.05	Taddia et al. (2014)	Smartt et al. (2015); Inserra et al. (2023)*
LSQ15rw	IIb	4	0.021	Smith et al. (2015)	Smartt et al. (2015); Inserra et al. (2023)*
OGLE16ekf	IIb	2	0.062	Dimitriadis et al. (2016)	Smartt et al. (2015); Inserra et al. (2023)*
PS1-14od	IIb	3	0.02	Campbell et al. (2014)	Smartt et al. (2015); Inserra et al. (2023)*
PTF09gpn	87A-like	1	0.015	Arcavi et al. (2010)	Taddia et al. (2016)
PTF11dlg	IIb	1	0.062	Gal-Yam et al. (2011)	Schulze et al. (2021)
iPTF13v	IIb	1	0.062		Schulze et al. (2021)
ps15cjr	IIb	3	0.022886	Huber et al. (2015)	Shivvers et al. (2019)

Table B.5. The SNe marked with *** were classified by the Public European Southern Observatory Spectroscopic Survey of Transient Objects (PESSTO; Smartt et al. 2015).

SNe marked with * were obtained from the public data releases of the PESSTO and ePESSTO+ collaborations. Data taken up to 2016 were retrieved from the cumulative PESSTO releases (SSDR1–3; Smartt et al. 2015) available through the ESO Science Archive, with details listed on the PESSTO website (<https://www.pessto.org/index.py?pageId=4>). Those obtained from 2019 onward were retrieved from the ePESSTO+ dynamic release (Inserra et al. 2023).

SNe marked with ^a are available from WISEREP (Yaron & Gal-Yam 2012). The spectra were contributed by Han Lin.